CHARACTERIZATION OF HYDRODYNAMIC FORCES AND INTERFACIAL PHENOMENA IN CELL CULTURE PROCESSES

DISSERTATION

Presented in Partial Fulfillment of the Requirements

For the Degree Doctor of Philosophy in the

Graduate School of The Ohio State University

By

Weiwei Hu, M.S.

*****

The Ohio State University

2007

Dissertation Committee:

Approved By:

Professor Jeffrey J. Chalmers, Adviser

Professor Kurt W. Koelling,

Professor James F. Rathman

_____

Adviser
Graduate Program in Chemical Engineering

ABSTRACT

The maturity of biotechnology as a significant, commercial enterprise has lead to the large scale production of products from a variety of cell types, including bacterial, fungal, mammalian, and microalgae. While both large scale (>10,000 L) mammalian cell culture and microalgae culture are currently used for commercial purposes, there still exist significant engineering challenges. One of these challenges is to quantify, and minimize, the effect of hydrodynamic forces on cells, which is in direct conflict with the ever pressing need to increase gas mass transfer capability and mixing performance of large scale bioreactors to improve productivity.

In this dissertation, a microfluidic channel was applied to quantitatively evaluate the effect of hydrodynamic forces on heterotrophic dinoflagellate *Crypthecodinium cohnii*, a naturally high producer of DHA. In the transient experiments, the lysis of *C. cohnii* cells was not observed even at high energy dissipation rate (EDR) of 5.8×10^{7} W/m^{3}, while a significant sub-lethal effect, the loss of flagellate, was identified at EDR higher than 1.6×10^{7} W/m^{3}. The flagellate can be regenerated approximately 45 minutes after exposure. During the "recovery process", the algae cells began to spin first, and then move in a straight direction. The presence of *C. cohnii* cells in bubble film and foam layer was also verified by microscopic observation. In the long-term experiments,

the microfluidic channel was connected with a small stirred tank bioreactor, which facilitated repeated exposures of cells to high EDR. It was found that the growth of *C. cohnii* cells was not inhibited until an EDR of 5.9×10^{6} W/m^{3} was achieved. This level was significantly higher than that in shaken flask experiments, where the shear stress was claimed to cause a negative effect on dinoflagellate proliferation by numerous published papers. Consequently, the limitation on oxygen mass transfer was identified to be a key issue in shaken flask cultures.

As has been well documented in the literature, bubble rupture typically creates significantly higher hydrodynamic forces than the forces created from impeller agitation. In this dissertation, two approaches were taken to minimize bubble-associate cell damage from gas sparging. The first approach consisted of mass screening surfactants to alleviate cell-bubble attachment. It was found that octyl-, nonyl-, and decyl-maltopyranoside were less toxic to Chinese hamster ovary (CHO) cells among twelve small molecule surfactants tested, and had no negative effect on cell growth in a chemical defined medium until a level around 0.2 times their critical micelle concentration (CMC) was achieved. Trends in the performance of these surfactants were explored based on the chemical structure as well as the dynamic surface tension. Finally, nonyl-maltopyranoside (NM) was identified as the most promising candidate, which can efficiently reduce the cell enrichment in the foam layer to a similar level to Pluronic F-68; a commonly used large molecule protective surfactant. The second approach to minimize bubble-associated cell damage was to develop an optimization strategy for aeration. A novel dual-sparger system was proposed based on theoretical

calculations. These calculations suggest the use of microbubbles of oxygen and large bubbles of air to uncouple oxygen supplement and dissolved carbon dioxide removal, which has the potential to minimize the required aeration rates for mass transfer as well as cell damage by bubble rupture and foam problems in large scale bioreactors.

Dedicated to my wife and my parents

ACKNOWLEDGMENTS

I express my sincere thanks to my advisor, Dr. Jeffrey J. Chalmers, for his intellectual support, guidance, and motivation. His broad view and abundant experience in cell culture area is invaluable to this work. I also appreciate the freedom he granted me to be an independent researcher.

I wish to thank Dr. James F. Rathman and his student, Dr. Poonam Nigam, for their help in my surfactant work. I am also grateful to Paul Green for his technical support on making microfluidic devices.

Part of my work, microalgae cell culture, was in collaboration with the Fermentation Sciences at Martek Biosciences Corporation, Winchester, KY. I thank Dr. Jon Hansen and Mr. Ray Gladue for the tremendous effect they put on my research. Their insightful suggestion made my work in this area easier and fruitful.

I also wish to thank my group members, Dr. Huading Zhang, Dr. Mei Shao, Dr. Xiaodong Tong, Dr. Bhavya Metha, Dr. Mike Mollet, Dr. Yang Zhao, Ruben Godoy, Claudia Berdugo, Ying Xiong, Liying Yang, Rustin Shenkman, and Jianxin Sun for their advices and support. I enjoyed my time with them in Dr. Chalmers' lab.

Finally, I would like to thank my wife, Jun Sun, for her unconditional love and encouragement during the past years, and I also wish to thank my parents and my in-laws for their support.

VITA

November 1, 1977 ……Born – Ningguo, P.R.China

1998 ……B.S. Biochemical Engineering,
East China University of
Science and Technology, China

2001 ……M.S. Biochemical Engineering,
East China University of
Science and Technology, China

2002-2003 ……...University Fellowship, The
Ohio State University

2003 – Present ……....Graduate Research Associate,
The Ohio State University

FIELD OF STUDY

Major Field: Chemical Engineering

Minor Field: Biochemical Engineering, Cell Culture

TABLE OF CONTENTS

LIST OF TABLES

LIST OF FIGURES

CHAPTER ONE

INTRODUCTION

Fermentation and cell culture technology has been widely used to make valuable products that can not be synthesized by chemical methods in an efficient and sustainable way. It covers a broad range of applications, such as pharmaceutical, food additive, energy, industrial catalysis, and environment protection. The types of cells used range from bacteria, fungi, microalgae, plant cells, mammalian cells and even primary, human cells. These cells are either "wild type", mutated, or recombinant cell strains typically optimized for high productivity.

Fish oil is traditionally, and currently, considered an important source of docosahexaenoic acid (DHA). However, in reality, DHA is not produced by fish, but by the marine algae that the fish eat. The challenges of obtaining DHA from fish which include supply variations and contamination by environmental pollutants (which can restrict the application of fish oil in infant formula and pharmaceuticals) has lead to the use of microalgae cell culture in bioreactors to produce uniform, high-quality DHA (Ratledge, 2004). Microalgae cell culture, in actual practice, exhibit significantly more similarity to large scale mammalian cell culture than bacterial or fungal culture.

Therapeutic protein from mammalian cell culture is a fast-growing industry with more than 20-billion annual sales currently. More than one hundred compounds are in

clinical trials. Two thirds of the FDA approved biotechnology products during January 1996 to November 2000 are manufactured using mammalian cells (Chu and Robinson, 2001). In combination of high dosage, chronic usage, and large patient population, it is projected that the demand will increase substantially. Therefore, several processes have to be implemented in stirred tank bioreactors at 10,000L (Varley and Birch, 1999). Careful considerations have to be given with respect to process development and scale-up.

Even though the metabolic activity and regulation of the cells has been extensively studied, which have resulted in a number of fed-batch and perfusion strategies which have been implemented in commercial processes, both microalgae and mammalian cell culture still face a number of engineering challenges. One of the well known challenges is the perceived, and actual, cell damage as a result of hydrodynamic forces in various stages of the cell processing. Until fairly recently, systematically characterization of these forces and the corresponding cell response was not known.

Other than using traditional viscometers or capillary tubes, Gregodiades et al. (2000) constructed a sudden contraction flow channel and simulated it using computational fluid dynamic (CFD) for hydrodynamic forces in terms of energy dissipation rate (EDR). The shear sensitivity of CHO cells attached to microcarriers was tested by pumping them through the channel. Subsequently, Ma et al. (2002) fabricated a gradual converging and diverging microfluidic channel using photolithographic method and determined the sensitivity of mammalian and insect cells to hydrodynamic forces. The geometric characteristics of the channel suggest laminar flow through the whole device, while the generated EDR cover the range generally encountered in bioreactors. Most recently, Mollet et al. (2006) developed an enhanced version of the device where

the photonegative resist was replaced by a 30 gauge stainless steel sheet. The flow microfluidic channel was then cut in the sheet by using Wire Electrical Discharge Machining (WEDM). The effect of hydrodynamic stresses on apoptosis of wild type and bcl-2 transfected CHO cells was studied.

In this study, the hydrodynamic sensitivity of dinoflagellate *Crypthecodinium cohnii*, a naturally high producer of DHA, was examined regarding a range of EDR values. In Chapter 3, a similar microfluidic device at Mollet et al. (2006) was used to quantitatively evaluate the response of *C. cohnii* cells to transient exposure to hydrodynamic forces. The sub-lethal effect as well as the cell-bubble interaction was also studied. In Chapter 4, *C. cohnii* cells were circulated between a small well-controlled bioreactor and the microfluidic device by way of a continuous pumping system in order to assess the cells tolerance to chronic, high levels of EDR. The upper limit of hydrodynamic levels without negative effects on cell growth can be identified to guide industrial operation. In addition, the conflict between the results from this recycle model and the published data using shake flasks was interpreted.

As has been well documented in the literature, bubble ruptures typically generate higher hydrodynamic forces than most of that resulted from impeller agitation, especially in mammalian cell cultures (Ma et al., 2002). For example, the rupture of small bubbles with a diameter of 1 mm will induce hydrodynamic forces at the level of 10^{10} W/m^3 (Boulton-Stone and Blake, 1993), which can cause cell lysis instantly. As was experimentally demonstrated by Trinh et al. (1994), cells can attach to rising bubbles and subsequently lysis when the bubble ruptures. Further, Trinh et al demonstrated that the non-ionic surfactant Pluronic F-68 (PF-68) significantly lowers this cell-bubble

attachment, and subsequent cell damage. Unfortunately, the selection of these protective additives is an empirical process in spite of their important effect on the success of industrial mammalian cell culture. In addition, there is a concern about the effectiveness of PF-68 at high cell concentration (Ma et al., 2004).

A sparged bioreactor is a typical multiphase (gas-liquid-solid) system with various interfaces. The characteristics of the interfacial phenomena associated with a mammalian cell culture, or in this case an algae culture, is significantly beyond any fundamental description. Consequently, in Chapter 5, the results of mass screening of small molecule surfactants is reported in an attempt to find alternatives for PF-68, which can inhibit cell-bubble attachment as well as have no negative effect on Chinese hamster ovary (CHO) cells. This mass screening consisted of toxic/inhibitory effects on the cells as we as effectiveness to prevent cell attachment to bubbles/foam. In Chapter 6, a novel aeration system, which employed dual spargers to uncouple O_2 supplement and CO_2 removal, was proposed for large scale bioreactors. It was compared to traditional one-sparger system regarding required aeration rates based on theoretical calculations of gas-liquid mass transfer, and the effect of bubble size and components on dissolved CO_2 removal was studied.

CHAPTER TWO

LITERATURE REVIEW

2.1 Cell Culture Processes

2.1.1 Microalgae Cell Culture

Although the usage of blue-green algae as food has been recognized for thousands of years (Jensen et al., 2001), the interest in microalgae cell culture is a recent development (only a few decades old). Microalgae is a very diverse group including tens of thousands of species. Only a few strains have been cultivated industrially in large quantities. The application of microalgae cell culture is very broad and promising, which covers the areas of food, cosmetics, pharmaceutics, and CO_2 fixation.

It is well known that microalgae can be used as human nutritional supplement due to their special chemical compositions. Three microalgae species dominate the commercial application in this area: *Chlorella*, *Spirulina*, and *Dunaliella salina*. The general form of the food products from these organisms is dry biomass in terms of powder or compressed tablet. *Chlorella* contains β-1,3-glucan, which can reduce blood lipid and activate the immune system (Spolaore et al., 2006). The reason for using *Spirulina* is its high protein content (up to 70% dry weight) and high digestibility (Soletto et al., 2005). The most important substance in *Dunaliella salina* is β-carotene with a

content up to 14% dry weight (Metting, 1996). In addition, microalgae extracts have already been applied in cosmetic products, such as skin care, hair care, and sun protection. It was found that the extracts of *Arthrospira* and *Chlorella vulgaris* can alleviate skin aging, reduce wrinkles, and support tissue regeneration (Stolz and Obermayer, 2005). Besides dry biomass and crude extracts mentioned above, microalgae cell culture can be also applied to the manufacture of pure molecules with high value. In recent years, a large number of secondary metabolites within microalgae have been reported to have anti-cancer, anti-viral, and anti-bacteria activities (Moore, 1996). However, less progress has been made to bring these products to market.

On the other hand, microalgae cell culture is commercially successful in long-chain polyunsaturated fatty acids (PUFAs) production. PUFAs play important roles in biological membranes and cellular metabolism. They can be classified into four groups, ω-3, ω-6, ω-7, and ω-9, according to the position of the first double bond from the methyl terminal. The biosynthesis of PUFAs is through a series of elongations and desaturations (Yap and Chen, 2001). However, humans lack required Δ12 and Δ15 desaturases, which catalyze the reactions to produce linoleic acid and α-linolenic from oleic acid. In addition, it is still unknown how much α-linolenic can be further transformed to other long-chain PUFAs in humans. Therefore, there is increasing interests to add long-chain PUFAs to nutrients, especially infant formula. Docosahexaenoic acid (DHA) and arachidonic acid (ARA) are two long-chain PUFAs attracting more attention because they are major elements in gray matter of the brain and the retina of the eye,. PUFA's are present in mother's milk and there is clear clinical evidences showing that DHA is essential for the development of infant's visual and neurological functions (Ratledge, 2004). Other health

benefits of DHA, such as preventing cardiovascular diseases, are increasingly recognized (Kang and Leaf, 1996; Horrocks and Yeo, 1999).

Traditionally, oils from fatty fish are considered as good sources for long-chain PUFAs, especially DHA. However there are some disadvantages restricting the application of fish oils into infant formula or as pharmaceuticals, which include potential contamination of environmental pollutants, such as dioxins and heavy metals, inconsistent quality, presence of eicosapentaenoic acid (EPA) that affects the uptake of DHA, and unpleasant smell (Craig-Schmidt et al., 1998). The principal producers of DHA in ocean environments are microalgae, from which fish obtain a majority of their long-chain PUFAs. Therefore, microalgae cell culture is recommended as an alternative to supplying high-quality DHA. Consequently, a number of microalgae species, such as *Crypthecodinium cohnii* and *Schizochytrium*, have been identified as naturally high producers for DHA. Their fatty acids mainly consist of DHA while other long-chain PUFAs including EPA or ARA are negligible.

Current microalgae cell culture technology can be categorized into three systems: open-air ponds, photobioreactors, and heterotrophic fermentors. Open-air pond system is a traditional and simple method. However, only a small amount of photoautrophical microalgae, which are able to grow in highly selective and specialized conditions such as high pH and high salinity, can be successfully cultured in this system without contamination. The enclosed bioreactor systems, which can provide better control and achieve high productivity, are developed to cultivate microalgae. Particularly, photobioreactor and traditional fermentor are utilized to cultivate photoautotrophical and heterotrophical microalgae, respectively. One of the major problems associated with

photobioreactor is scale-up process. It is very difficult to introduce enough light into large scale bioreactor since light can only penetrate a few centimeters into a cloudy broth. Therefore, the most desirable culture system is a fermentor for heterotrophic strains, which eliminate the requirement for light. With such as system, cell densities as high as 50-100 g dry biomass per liter have been reported (Running et al., 1994). It was also reported that the obligate photoautrophic diatom *P. tricornutum* can grow on glucose in the dark when a functional glucose transporter was expressed (Zaslavskaia et al., 2001).

2.1.2 Mammalian Cell Culture

Mammalian cell culture has been widely used to produce therapeutic proteins including hormones, cytokines, enzymes, blood factors, and monoclonal antibodies (Mabs). Mammalian cells have the capability of proper protein folding and post-translational modifications, such as glycosylation. Therefore, they have been chosen to manufacture large, complex, and glycolylated proteins, especially Mabs. The first therapeutic protein from recombinant mammalian cells that obtained market approval was human tissue plasminogen activator (tPA) in 1987. Twenty years later, Mabs represent one of the fastest growing segments of biopharmaceuticals, which have already been commercialized to treat cancer, immune disorders, and infectious diseases. There are 24 Mabs approved to enter USA market by the end of 2004 (Ozturk, 2006). Some blockbuster products had annual sales of more than $1 billion with a demand of several hundred kilograms per year. There are an even larger number of products undergoing clinical development. It was predicted that a surge of therapeutic proteins entering the marketplace will appear in the next two decades (Henry, 2000). In addition, cell therapy

and gene therapy could become new application area of mammalian cell culture technology.

Mammalian cell culture was originally developed for the study of cell functions *in vitro* by academic researchers. Then continuous cell lines, such as Chinese hamster ovary, CHO, baby hamster kidney, BHK, myeloma cells, NS0 and SP2/0, and human embryo kidney, HEK-293, were obtained and approved by regulatory agencies for industrial manufacture. Most of these cell lines can be cultured in suspension culture as opposed to an anchorage-dependent mode, make large scale cultivation achievable in sparged, stirred tank bioreactors.

A typical upstream cell culture process development can be described as following. First, a number of high-producing cell clones are obtained by state-of-the-art transfection, amplification, and selection methods. Then cell culture medium is customized to support the growth of various cell clones. The medium normally contains more than 60 synthetic ingredients with well-defined concentrations, including carbon sources, amino acids, salts, vitamins, lipids, growth factors, and buffers. Because of the disadvantages of batch variation and vulnerability to contamination, serum and other animal components are required to be eliminated from medium formulation. Finally, bioreactor operation parameters are optimized in order to achieve consistent product quality and high protein expression level. Small scale bioreactors are used to determine acceptable range of pH, DO, temperature, and inoculation density. Then the cell culture process is scaled-up to production levels of 20,000 L, or greater. Overall, the improvement of host cell line engineering, media optimization, and bioreactor operation

in last two decades resulted in a dramatic increase of product titer to the range of grams per liter (Wurm, 2004).

2.2 Large Scale Cell Culture

The market of several therapeutic proteins has already exceeded 100 kg per year because of high dosage and multiple indications, which requires efficient manufacture processes in large-scale stirred tank bioreactors of 1,000 to 20,000 L. For example, one 12,000 L bioreactor using a fed-batch process can manufacture 30 kgs of proteins annually based on the average productivity of 0.5 g/L and purification yield of 50% (Molowa et al., 2002). It was estimated that the manufacturing capability for mammalian cell culture was only half of the demand in 2004, which extremely restricted delivering sufficient amounts of medicines into the market. One specific example is Enbrel® (Molowa et al., 2002). As a result, contract manufacture provides an alternative to alleviate the problem of supply shortage as well as reduce huge and risky initial capital investment. The average cost of goods for Mabs from mammalian cells is more than 200 USD per gram, which is more than 10-fold higher than that of small molecule medicines by chemical synthesis (Molowa et al., 2002). It can be predicted that the maturing of mammalian cell culture industry as well as the pressure to increase productivity and reduce cost will inevitably lead to the need to obtain higher product concentrations, which require higher cell concentrations with the corresponding nutrient demands.

To some extend, such economic pressure already exist in the DHA market since, for one reason, DHA is currently mainly employed as a food ingredient, not a life saving

drug. This economic pressure is manifested in a number of ways, such as making the use of very large scale fermentors desirable.

2.2.1 Scale-Up

Intensive studies have been conducted to improve large scale cell culture process for maximal specific and volumetric productivity. Ideally, the goal of the scale-up process is to preserve the same "microenvironment" for cells as the process is scaled up. However, there is no universal guideline on how to scale-up a cell culture processes. It results from the complexity of three-phase bioreactor systems and the unknown behavior of fluid flow in turbulence regime as well as incomplete understanding of how a cell interacts with its environment. Given the limitations of time and budget, scale-up is as much an art as a science. With improved understanding of system characteristics, this scenario could be changed in the future.

The parameters in cell culture processes can be divided into two groups: volume-independent parameters and volume-dependent parameters. The operating ranges of pH, dissolved oxygen, dissolved carbon dioxide, and temperature do not change with scale. However, working volume, feed volume, impeller speed, and aeration rates do change during scale up. From the perspective of time length, the characteristic time of mixing, circulation, and potentially mass transfer increase in large scale bioreactors. However, the characteristic time of oxygen uptake and other biological reactions are constant. Since large characteristic time represents a slow process, the mixing and mass transfer is more likely to be limited steps at large scale. Empirical or semi-empirical approaches for scale-up are compared as below.

1) Geometric similarity: To duplicate the mixing patterns at small scale, the bioreactors are generally scaled-up based on geometric similarity. The important geometric parameters are the ratio of liquid height/vessel diameter (H/T), impeller diameter/vessel diameter (D/T), and impeller clearance/vessel diameter (C/T). However, not many companies actually own geometrically similar bioreactors from laboratory to production facilities (Einsele, 1978). Some of large-scale bioreactors for mammalian cell culture are retrofitted microbial fermentors. Therefore, the effect of bioreactor geometry on process characteristics should be investigated.

The range of aspect ratio (H/T) is from 1:1 to 3:1. The aspect ratio of bench bioreactor is normally in the lower end of this range, 1:1 to 1.5:1. At large scale bioreactor, this ratio could increase to 2:1 or more, which can improve the usage of aerated gas and reduce operation cost. Higher D/T ratio also shows advantages at the commercial scale, such as energy efficiency. By using a larger impeller, the gas handling capacity is increased. The gas dispersion is also improved because mammalian cell cultures are conducted in the impeller flooding regime with low agitation speed. On the other hand, the height of the bioreactor increases inevitably during scale-up process. Therefore, it is necessary to increase the number of impellers in large scale bioreactors, which may bring out the problem of fluid compartmentalization and subsequent inefficiency of mixing. In addition, different types of impeller such as Rushton turbine and Hydrofoil impeller could be used at large bioreactor to fulfill various tasks simultaneously.

2) Equal volumetric mass transfer coefficient: Oxygen has low solubility in medium, which should be consistently replenished. The oxygen transfer capacity of large scale bioreactors should match the oxygen uptake rate of cells, especially at high density.

There are abundant empirical correlations regarding the calculation of overall volumetric mass transfer coefficient (k_La) from power input per volume (P/V) and superficial gas velocity (Us). k_La also depends on the properties of the medium, such as surfactants, viscosity, and antifoam usage (Dorresteijn et al., 1994). It has been recommended to use k_La and gas flow rate (vessel volumes per minute, vvm) as scale up criteria (Oldshue, 1983; Bailey and Ollis, 1986). However, most of published empirical equations only apply for microbial fermentation systems, which used high aeration rate and agitation speeds. In mammalian cell culture, the information about k_La is still limited, especially for large scale bioreactors.

3) Equal impeller tip speed: In stirred tank bioreactor, there is a concern about the sensitivity of cells to the shear generated by the impeller. On the other hand, enough mixing has to be provided to ensure sufficient homogeneity. Therefore, the impeller tip speed (U_T) has been chosen as a scale up criteria. The typical values of U_T for filamentous microorganism and mammalian cell are around 5 m/s (Wang et al., 1979) and 2 m/s (Chalmers, 2000), respectively.

4) Equal energy dissipation rate (EDR): The power input through the shaft and bubbles as well as how it is dissipated in surrounding fluid has a great impact on mixing performance and hydrodynamic forces distribution in bioreactor system. Therefore, energy dissipate rate (P/V) is recommended as a criterion for scale-up processes. The ungassed power input is determined by fluid density (ρ), impeller speed (N), impeller

type, and impeller diameter (D). The power input through gas aeration is proportional to superficial gas velocity (Us). Under aeration conditions, the power input from agitation decreases because of the formation of gas-filled cavities behind the blades of impellers. The ratio of gassed to ungassed power consumption (P_g/P) could be 50% or lower when Rushton turbines are used (Warmoeskerken, 1986). Due to the complexity of multi-phases cell culture system, the accurate prediction of gassed power is very difficult. In addition, multiple impellers are normally used in large scale bioreactor. The total consumed power is related on the interaction among impellers through liquid fluid flow.

It is obvious that the scale-up criteria mentioned above can not be satisfied simultaneously. Oldshue (1966) and Amanullah et al. (2004) analyzed the relationships among different criteria while maintaining geometrical similarity. Scale up according to constant EDR results in U_T and k_La. Scale up at constant U_T causes low EDR and k_La. The criterion of equal k_La is often used with equal vvm or equal Us, which requires high U_T. Therefore, the choice of scale-up rules should consider the potential responses of cells to the critical transport property. For example, equal EDR or U_T may be chosen if the shear sensitivity of cells is an issue, such as in mammalian cell culture case. Scale up at equal k_La may be applied if the oxygen transfer is a limited factor, such as in microbial fermentation case.

Finally, it is necessary to mention that the hydrostatic pressure presents another concern in large scale bioreactor. As the liquid height increases, the hydrostatic pressure will change accordingly. The cells at the bottom of large bioreactor will experience high pressure. Fortunately, it was found that cell growth and product formation hasn't been compromised under pressure up to 0.9 MPa (Takagi et al., 1995). However, the effect of

hydrostatic pressure on mass transfer performance of gas bubbles should be considered because the gas solubility and bubble sizes are changed.

2.2.2 Scale-Down

The rate-controlling mechanism in large-scale bioreactors can be identified according to regime analysis. Particularly, the characteristic times of physical transport phenomena including mixing, oxygen transfer, and gas resident time are expected to increase during scale-up processes, which indicates a slow mechanism. For example, the ideal mixing can be easily achieved in laboratory scale bioreactors, while it is non-realistic to have the same mixing performance in industrial scale vessels. The mixing time will inevitably increase from several seconds to several minutes during scale-up. Especially for shear sensitive species such as mammalian cells, the maximum mixing intensity is also limited by the hydrodynamic forces from the impeller. Therefore, it results in the inhomogeneous distribution of substance in large scale bioreactors, such as pH, DO, and nutrients (Tramper, 1995; Nienow, et al., 1996). The cells will experience fluctuating environmental conditions when they move along with fluid flow.

A scale-down model using laboratory bioreactors is commonly used to replicate the characteristics of production vessels in order to obtain optimized operation strategy. Several experimental methods have been developed to simulate the substance gradients by using two-compartment system, which consists of two stirred tank reactors (STR+STR) or one STR linked to one plug flow reactor (STR+PFR) (Oosterhuis et al, 1985; Larsson et al., 1985). Basically, one reactor has ideal conditions for cells. The other one has a harsh environment, which may occurred in certain region of large scale

bioreactor due to insufficient mixing, such as high pH, low DO, and high glucose concentration. The cells in both bioreactors can be exchanged by a peristaltic pump. The circulation time distribution (CTD) of scale-down models, which is characterized by mean circulation time and standard deviation, should match that in production level because it presents the frequency and probability of the cells circulating through different environment conditions (van Barneveldt et al., 1987).

Most published papers regarding scale down model focused on microorganism systems. Fed-batch technique is commonly applied to microbial fermentation. High glucose concentration (around 500~600 g/L) is used as feed solution, which will result in a substrate gradient in large scale bioreactor because of insufficient mixing relative to biological reaction. Larsson et al. (1996) measured the glucose concentration in a $30m^3$ bioreactor under two feed positions. When the glucose solution was added in the top stagnant zone, the variation between top and bottom of reactor is about 20~60mg/L. When the glucose was added close to the impeller, the variation between top and bottom is only around 10~30 mg/L. Neubauer et al. (1995) investigated the metabolic changes of *Escherichia coli* under glucose fluctuation using a STR+PFR model. Intracellular guanosine 3'-diphosphate 5'-diphosphate (ppGpp) concentration was selected as a marker since it increased quickly and significantly during glucose starvation. It was found that the synthesis of ppGpp increased when cells went through the PFR containing less glucose. However, the full stringent response was not induced by repeated short-time starvation, which was reflected by a slight change of biomass yield and growth rate.

Scale-down model was also used to study the effect of oxygen gradient. Larsson and Enfors (1993) used a system consisting of an ideally mixed and aerated STR and an

insufficiently mixed PFR without aeration. *E. coli* ATCC 15224 went though repeated aerobic-anaerobic fluctuation. The cell metabolism, represented by hydrogen production, was changed under oscillating oxygen concentrations. The formation of hydrogen was dependent on the residence time of cells at anaerobic condition. STR+STR model can also be used (Byun et al. 1994). Two STRs were aerated by oxygen and nitrogen to simulate aerobic and anaerobic conditions, respectively. It was shown that the circulation between bioreactors has a clear effect on *Enterobacter aerogenes* growth and metabolism.

Finally, several investigations with respect to variation of pH in large scale bioreactors have been conducted in recent years. The industrial pH control is fulfilled by pulse injection of concentrated acid or base solution to broth surface depending on the deference between pH probe data and set point. Amanullah et al. (2001) used *Bacillus subtilis* culture as a model to study the effect to pH fluctuations. STR and PFR mimicked the low pH region in the bulk and high pH zone near the addition point, respectively. 5 M sodium hydroxide was added via a "mixing bulk" located between STR and PFR. It was shown that product formation was affected by the residence times of cells in the PFR, more than 1 minute, even though biomass concentration remained unchanged. Osman et al. (2002) performed a study of pH perturbation in GS-NS0 cell culture using a STR+STR model. The magnitude, frequency, and total number of perturbations were investigated. It was found that the increase of perturbation (pH 8.0) number decreased the viable cell number. The decrease in perturbation (pH 9.0) frequency from 6 minutes to 60 minutes per time alleviated cell death significantly (28.3% vs.3.4%).

2.2.3 Computational Fluid Dynamics (CFD)

CFD is becoming a very powerful tool for process design. In order to understand the complex phenomena in bioreactors, such as turbulent flow fields, CFD is used to virtually visualize and quantitatively analyze flow motion other than difficult measurement using laser dropper velocimetry (LDV) and particle image velocimetry (PIV). Consequently, the critical parameters, such as mixing, shear stresses, and mass transfer coefficient, can be estimated and evaluated, which can lower the risks associated with scale-up processes. CFD can also be integrated with cell physiology for a more precise forecasting of the impact of scale-up considering the close interaction between fluid flow and the biological reactions.

Basically, a series of conservation or transport equations are used in CFD numerical simulation. For instant, the continuity equations ensure conservation of mass. Navier-Stokes equations describe the conservation of momentum transported by convection, diffusion, and other source terms. Heat transfer can be expressed in terms of conservation equation of total enthalpy. Turbulence equations are used in order to model Reynolds stresses. Standard k-ε model is a robust two-equation eddy viscosity model, which can be applied to a wide range of turbulent flow. k and ε represent the kinetic energy of turbulence and the rate of dissipation of turbulence, respectively. Based on Boussinesq hypothesis, the Reynold stresses can be expressed in a term of mean velocity gradients. Subsequently, k-ε model has been modified for superior performance under certain circumstances. Chen-Kim k-ε model is good at complex elliptic turbulent flow and RNG k-ε model is suitable for turbulent flows with regions of high strain. In addition, Reynolds stress model (RSM) and large eddy simulation (LES) model are two turbulence

models without using Boussinesq hypothesis. They can improve accuracy of simulation with the requirement of large computational resources and long calculation time. Therefore, the selection of turbulence models has a great impact on simulation results.

One important application of CFD in stirred tank bioreactor is to evaluate mixing performance. CFD data can be used to compute the power number and flow number of an impeller as well as assess mixing time by simulation of tracer experiments. Bujalshi et al. (2002) studied the effect of computational parameters and the addition position of a tracer on the mixing time from simulation. Sliding mesh approach, in which the grid surrounding a Rushton turbine physically moves during the solution, was applied to model the flow field. They found that the addition point of the tracer has a great impact on CFD predictions. The accuracy of simulation was improved when the tracer was added at the points close to sliding mesh surface.

Davidson et al. (2003) investigated the CTD of bioreactors using FLUENT software, a CFD package. The CTD is a critical parameter to interpret cellular response to inhomogeneous conditions in large scale bioreactors. It was found that CFD results using standard k-ε model can qualitatively capture the nature of experimentally determined CTD. In addition, CFD simulation pointed out the limitation of current methods for processing experimental signals. Jaworshi et al. (2001) used CFD simulation with standard k-ε model to evaluate the performance of 6-bladed 45° pitch blade turbine (PBT) impellers and compared it with LDV measurement. The effect of impeller size, location, and pumping direction on flow patterns was studied. There was a close agreement between CFD and LDV results regarding mean velocity components. Finally, the mixing and hydrodynamic environment of a novel bioreactor for tissue engineering

comprised of walls with sinusoid-wave structures was also investigated by CFD simulation and compared to conventional spinner flasks (Bilgen et al., 2005). Improved mixing and decreased shear stresses was found in the novel bioreactor.

On the other hand, CFD tools have been used for studying mass transfer characteristic in bioreactors. Eulerian approach is typically applied to model two-phase (gas/liquid) flow in sparged stirred tank, which treat the dispersed phase (bubbles) as a continuum. Besides continuity and momentum equations, drag forces and virtual mass force of bubbles are also taken into account. Dhanasekharan et al. (2005) developed a generalized approach to model oxygen transfer in an air-lift bioreactor, which can be applied to stirred tanks. Bubble breakup and coalescence is also considered in order to obtain a distribution of bubble size in a population balance model. The gas hold-up and volumetric mass transfer coefficient from CFD simulation is comparable to experimental data. The variation is due to difficulties in simulating the bubble number density distribution accurately. Reuss et al. (2000) have used CFD to simulate the performance of the stirred tank and impellers used by Bombac et al. (1998), who measured the local gas hold-up by conductivity sensors. It was shown that the simulated local gas hold-up as well as fluid flow velocity in impeller region can reasonably agree with measured data. The variation was probably caused by the prediction of bubble sizes. Schmalzriedt et al. (2003) also simulated the distribution of mass transfer coefficient and dissolved oxygen concentration in a multiple-impeller system consisting of both Rushton turbine and pitched blade impellers. The $k_L a$ value from simulation was in the same range as that from empirical equations.

2.3 Hydrodynamic Forces

2.3.1 Overview of Hydrodynamic Forces in Bioreactors

It is well known that the bubble rupture at a liquid interface is damaging to cells. A thin liquid film forms when a bubble approaches the interface, which continues to drain until breakage. When the film breaks, a toroidal rim develops and expands to the edge of the bubble cavity. Then the liquid close to the bottom wall of bubble cavity is accelerated in a convergent way resulting in two opposite jets. The hydrodynamic force of the bubble rupture process has been evaluated by computer simulation, which is strongly related to bubble size. It could be high enough to kill mammalian cells (Boulton-Stone and Blake, 1993; Garcia-Briones et al. 1994). Trinh et al. (1994) demonstrated the low viability of cells in collected upward jets from bubble rupture.

On the other hand, mechanical agitation inevitably results in strong fluctuations in the fluid velocity due to the moving impeller blades and the trailing vortices. The distribution of hydrodynamic forces in bioreactor is heterotrophic with the highest value in the impeller discharge stream. For example, 43.5% and 70.5% of total mechanical power input is dissipated in the impeller discharge region for Rushton turbine (radial flow impeller) and pitched blade turbine (axial flow impeller), respectively, calculated by experimental 2-D velocity data using Laser Dropper Anomometer (LDA) (Zhou and Kresta, 1996a). Mollet et al. (2004) used a three-dimensional particle tracking velocimetry (PTV) system to obtain full-field velocity maps of a bioreactor. They reported 27.8% total energy is dissipated in 5.74% of the total liquid volume (1.6L) for a Rushton turbine.

According to the most commonly applied Kolmogorov microscale, the minimal length scale of eddies, η_{min}, is determined by the maximum turbulence energy dissipation rate, ε_{max}, if isotropic turbulence is assumed.

$$\eta_{\min} = \left(\frac{\nu^3}{\varepsilon_{\max}} \right)^{1/4} \tag{2.1}$$

where ν is kinematic viscosity (m^2/s). It has been proposed that the cells are likely to be damaged if the micro-eddy length is similar to or smaller than cell size (Aloi and Cherry, 1996). However, it is difficult to identify the value of ε_{max}. Zhou and Kresta (1996b) investigated the effect of tank geometry and impellers on ε_{max}. They found that impeller diameter and off-bottom clearance had significant impact on $\varepsilon_{max,}$ while the number of baffles did not. ε_{max} was the highest when using Rushton turbine impeller, which has the highest power number. The ε_{max} is normally one or two orders of magnitude higher than average energy dissipation rate (ε_{avg}). According to experimental data (Zhou and Kresta, 1996b), a non-dimensional constant for a giving impeller, E, is defined for the theoretical calculation of ε_{max} (Mollet et al. 2004).

$$E = \frac{\varepsilon_{\max}}{N^3 D^2} \tag{2.2}$$

where D is the impeller diameter and N is the impeller rotation speed (s^{-1}).

Whether mechanical agitation without sparging can be harmful to suspended cells is still not clear. Oh et al. (1989 & 1992) investigated the effect of agitation ranging from 100 to 450 rpm on three hybridoma cell lines. They used surface aeration to avoid bubble entrainment and maintained oxygen concentration greater than 20% of air saturation. It was found that cell growth, viability, and metabolic activity including glucose

consumption, lactate production, and antibody production was similar under different agitation speeds. In a separate experiment by Kunas and Papoutsakis (1990), the agitation up to 600 rpm without bubble rupture also had no significant effect on cell growth. On the other hand, the industry still has a concern regarding cell damage due to agitation-induced hydrodynamic forces, especially at large-scale bioreactor. Li, et al. (2006) reported lower cell density and viability observed at high agitation speed of 450 and 550 rpm in 2L Applikon bioreactor, which represents hydrodynamic force conditions at 2000L commercial scale. Even though the sparging aeration was also applied in their study, the author believed the mechanical agitation played a major role in cell damage since the aeration rate was smaller at high agitation speed.

2.3.2 Sub-Lethal Effect of Hydrodynamic Forces

The sub-lethal effect of hydrodynamic forces on cells should get more attention since it is difficult to be detected and may cause serious problems in long-term. It includes the change of intracellular metabolism activity in a variety of ways, such as cell cycle, respiration, and gene/protein expression. For example, calcium is an important intracellular messenger, which has an effect on signal transduction, mitochondrial activity, and cytoskeletal alteration. Aloi and Cherry (1996) studied the response of Sf-9 cells under elevated agitation speed for four hours by a 6 bladed Rushton turbine. A significant increase of intracellular calcium concentration was found. The time dependency of calcium response was also observed, which was due to the slow breakdown of cellular functions. Bao et al. (1998) have studied the effect of shear up to 16 dyn/cm^2 on gene expression in human endothelial cells. Cell monolayer on glass slides was subjected to

well-defined laminar flow for 4 hours in a parallel-plate flow chamber. Platelet-derived growth factor A (PDGF-A) and monocyte chemoattractant protein-1 (MCP-1) mRNA levels were increased 3- and 2-fold at step flow after 1.5 hours, respectively. PDGF-A and MCP-1 expression were increased 6- and 7-fold at impulse flow after 1.5 hours, which were sustained for at least 4 hours. MCP-1 is a potent chemotactic agent for monocytes and PDGF-A is a potent mitogen and chemotactic agent for smooth muscle cells. Both of them are believed to participate in the early events of atherosclerosis. Therefore not only the magnitude but also the history of hydrodynamic forces has great impacts on gene expression.

Mcdowell and Papoutsakis (1998) studied the effect of agitation intensity on gene expression of HL60 cells. They found that a step increase of agitation rate from 80 rpm to 300~400 rpm at the middle of a 5-day cultivation increased the CD13 receptor surface content and CD13 mRNA levels in a dose-dependent manner. Carswell and Papoutsakis (2000) investigated the hydrodynamic forces on human primary T cell and transformed TALL103/2 cell cultivation. They found that exposure to agitation up to 300 rpm with 80 ml/min sparger aeration significantly increased the rate of down-regulation of the interleukin-2 receptor (IL-2R). Agitation had no significant effect on cell metabolism or levels of cellular apoptosis in the cultures. However, the transformed TALL 103/2 cell line was found to be extremely sensitive to agitation.

The relationship between agitation and the permeability of cell membrane has been demonstrated by the evidence that the leakage of fluorescein diacetate, a positively charged dye, from hybridoma cells increased with the intensity of agitation (Al-Rubeai et al. 1993). In addition, the number of surface antigen receptors embedded in cell

membrane decreased by agitation. The change can be alleviated by the addition of Pluronic F-68 (PF-68). Keane et al. (2002) have studied the effect of shear stress on the expression of a recombinant protein by CHO cells. The anchorage-dependent CHO cells were cultured on the bottom of a well-defined chamber for more than 50 hours. The flow above the cells was adjusted to provide different shear stress ranging from 0.005 to 0.8 N/m^2. It has been found the production of human growth hormone (hGH) ceased when the shear stress was above 0.10 N/ m^2 without the presence of PF-68. Even with 0.2% (w/v) PF-68, the specific hGH production rate was also decreased with the increase of shear stress. The glucose uptake rate increased as well as lactate productivity decrease, which revealed a change of cell metabolism activity.

Senger and Karim (2003) studied the effect of shear stress on the glycosylation of recombinant tissue-type plasminogen activator protein (r-tPA) produced by CHO cell suspension cultured in a 3 L bioreactor. The shear stress, characterized by the impeller Reynold's number, was manipulated by changing the impeller agitation speed. They reported that shear stress induced an alteration of cellular homeostasis in terms of an increase in intracellular synthesis without cell division. The maximum r-tPA production was achieved at moderate shear stress. The fraction of type II r-tPA glycoform production increased at a high shear condition, which resulted in extensive cell death. Wu et al. (2002) have studied the effect of hydrodynamic forces on virus vector expression for gene therapy by changing agitation rate from 70 rpm to 200 rpm in microcarrier cultures for more than 100 hours. It has been found that the hydrodynamic forces increased the maximum specific retrovirus titer in PA317-RCM1 cells but lower the achievable specific adenovirus titer in 293 cells.

2.4 Interfacial Phenomena in Bioreactors

2.4.1 Gas-Liquid Mass Transfer

Heterotrophic cells require O_2 for survival and growth. Because the solubility of O_2 in medium is very low, continuous replenishment of O_2 by aeration is necessary. In bioreactors, various methods are used to aerate cultures including surface, membrane, and sparging aeration. Membrane aeration system is relatively complex and not scalable for commercial applications (more than 500L). Sparging aeration is simple, efficient, and easy to scale up; consequently, it is widely used for oxygenation at large scales. Another important purpose of aeration is to remove CO_2 from culture medium. CO_2 is a major by-product when animal cells consume O_2. In sparged bioreactors, the dissolved CO_2 can transfer from liquid medium to rising bubbles, and then leave culture system through exit gas.

Most of previous research regarding aeration strategy has focused on increasing O_2 transfer rate to achieve high cell density culture (Honda-Corrigan, 1989; Zhang, 1993). However, recent studies have shown that high dissolved CO_2 concentrations have negative effects on cell growth, decrease productivity, and alter product quality, especially for mammalian cell culture. Kimura and Miller (1996) reported a decrease in specific growth rate of the MT2-1-8 CHO cell line in a dose-dependent way when CO_2 partial pressure (pCO_2), a common way to represent dissolved CO_2 level, was elevated from 140 mmHg to 250 mmHg. The specific tPA production rate was inhibited, while the glycosylation of tPA did not change (Kimura and Miller, 1997).

Two mechanisms are proposed to interpret the effect of elevated dissolved CO_2. First, carbon dioxide as a non-polar molecule can diffuse across the cell membrane and alter cellular metabolism by affecting intracellular pH even if the pH of growth medium is controlled (Albert et al., 1989). Second, elevated dissolved CO_2 results in an increase of hydrogen and bicarbonate ion concentration. The addition of base to control pH also leaves cations in the medium. As a result, osmolality of the medium will rise, which has already shown negative effects on cell growth even though the specific productivity was enhanced in some cases (Ozturk and Palsson, 1991). Therefore, a number of studies have been conducted to decouple the effect of osmolality with dissolved CO_2.

deZengotita et al.(1998) found that elevated osmalality induced apoptosis of hybridoma cells and elevated dissolved CO_2 inhibited glycolysis of cells. Glutamine metabolism was not affected by elevated dissolved CO_2, but by osmalality. It has been shown that cell-surface polysialic acid (PSA) content, a parameter reflecting the degree of protein glycosylation, decreased with the increase of bicarbonate concentration and osmolality, and can be alleviated by lowering the pH or partially removing sodium chloride from the medium (Zanghi et al., 1999). In addition, osmoprotectant, such as glycine betaine and L-proline, can partially offset the changes in PSA content (Schmelzer and Miller, 2002). Zhu et al. (2005) reported the adverse effect of elevated osmolality (400-450 mOsm/kg) was substantially amplified at high dissolved CO_2 conditions (140-160 mmHg) in bench-scale bioreactors culturing CHO cells for an antibody-fusion protein. It resulted in 20% and 10% decrease in viable cell density and viability, respectively,

Unfortunately, the increase of the dissolved CO_2 level was often observed in large-scale bioreactors. Garnier, et al. (1996) estimated the dissolved CO_2 in a 150L bioreactor can reach 0.18 atm (~140 mmHg) on the seventh day of cultivation. It also showed that the dissolved CO_2 level was 70 mm Hg and 170 mm Hg at bench scale of 1.5 L and pilot plant scale of 1000 L, respectively (Mostafa and Gu, 2003). Zhu et al. (2005) reported the highest level of dissolved CO_2 (120~150 mmHg) in production-scale bioreactors. Theoretically, high aeration rates can increase both mass transfer capability of O_2 and CO_2. However, they are strictly limited by the subsequent foaming problems and bubble-associated cell damage. Therefore, the aeration strategy including sparger design should be carefully selected.

The selection of spargers for cell culture processes should not only meet the mass transfer requirement but also provide the best GMP operation. The spargers should be easily cleanable, steam sterilizable, and free draining. Point, ring, and frit spargers are three types commonly used in bioreactor. Point sparger is the simplest one with a single nozzle. Ring spargers are made of a tubular ring with air nozzles drilled at the bottom. Frit sparger utilizes porous material such as sintered glass or stainless steel to create microbubbles in the bioreactor. Point sparger is the best from GMP perspective, while frit sparger is the worst since it is very difficult to clean porous elements. However, point sparger generally results in large bubble, which may be not sufficient for oxygen mass transfer. Compared to point spargers, ring spargers typically do not improve the mass transfer significantly but does increase the difficulty in cleaning. When frit spargers are applied, the oxygen supplement and dCO_2 stripping should be carefully balanced.

Another important aspect related to sparger selection is the detrimental effect of sparged bubbles on cells.

2.4.2 Cell-Bubble Interaction

Extensive studies have been performed to investigate the mechanisms of bubble-associated damage (Chalmers and Bavarian, 1991a and 1991b). The bubble disengagement region at the liquid surface has been identified as the major cell damage area in most studies (Chisti, 1993 and 2000). Thermodynamically, mammalian cells have a tendency to attach to rising bubbles, and maintain attachment when bubbles arrive at liquid surface (Chattopadhyay, et al., 1995a). Subsequently, the large hydrodynamic forces associated with bubble rupture can damage cells (Trinh et al., 1994). The maximum EDRs resulting from bubble rupture increase with decreasing bubble size (Boulton-Stone and Blake, 1993; Garcia-Briones et al. 1994). For instance, the rupture of small bubbles, on the order of 2 mm in diameter, can result in a maximum EDR around 10^7 W/m^3, which is in the range reported to damage suspended mammalian cells (Ma et al., 2002).

In order to alleviate bubble-associated cell damage, surfactants (surface-active agents) are normally added into culture medium (Chattopadhyay et al., 1995b; Wu, 1995). Surfactants are such substances that have a tendency to migrate onto the interfacial faces and reduce the surface tension. Normally, they have both hydrophobic and hydrophilic parts. The water-soluble surfactants can be divided into four groups depending on their hydrophilic properties: anionic, cationic, Zwitterionic (both anionic and cationic), and non-ionic. Currently, the most widely used protective surfactant in cell culture systems is

PF-68, a nonionic surfactant with a tri-block structure of polyoxyethylenen (POE) and polyoxypropylene (POP) and molecule weight around 8400. Even though various explanations for its protective mechanisms have been proposed, there is no final agreement. Basically the suggested mechanisms can be classified into two groups: biological and physical mechanism. Biological mechanisms focus on the interaction between the surfactants and the cell membrane. PF-68 has been proven to reduce the fluidity of the cell plasma membrane (Ramirez and Mutharasan, 1990) and the hydrophobic property of the cell surface (Wu, 1996). On the other hand, physical mechanisms focus on the effect of the additives on the fluid environment surrounding the cells. It has shown that the surfactants prevent cell adhesion to bubbles by decreasing vapor-liquid interfacial tensions (Chattopadhyay, et al., 1995a). Michaels et al. (1995) examined the induction time (the time required for cell-to-bubble attachment) for the various additives. It was found that PF-68 can extend the induction time to more than 5 second, while it was less than 0.5 second without any additive. Ma et al. (2004) found that the enrichment factor, the ratio of cell concentration in the foam layer to that in the bulk, was around 0.5 at 3 g/L PF-68, while it is more than 10 at 0.001 g/L PF-68.

A hypothetical killing volume associate with each bubble, V_d, has been proposed to correlate the cell death rate with aeration (Tramper et al. 1987).

$$k_d = \frac{QV_d}{V_b V_r} \tag{2.3}$$

where Q is the gas flow rate; V_r is the reactor volume; V_b is the bubble volume; k_d is the first order death rate. Meier et al. (1999) proposed another equation including swept out volume of a rising bubble, $V_{d,\,\mathrm{rise}}$, to explain the rising-dependent killing volume.

$$\frac{k_d V_d}{Q} = \frac{V_d}{V_r} + \frac{V_{d,risie}}{V_r} \qquad (2.4)$$

They found that the cell attachment to rising bubbles played an important role in cell damage for tall reactors without protective additives. When PF-68 and methyl cellulose are present, the cell attachment becomes negligible for large bubble with diameter more than 0.5mm, while it is still significant for microbubbles with diameter in the range of 100 μm. This model is able to unify the conflicted cell death data in the literatures.

2.4.3 Foam

In sparged bioreactors, the foam layer almost inevitably forms because of the present of abundant surface-active substances in the medium, especially at the end of culture. The foam emerges when bubbles arrive at the liquid surface faster than bubbles rupture. The accumulation of bubbles at the surface leads to a honeycomb structure where a large number of bubbles are coexisting separated by very thin liquid lamellas. Foams can be classified into dry foams and wet foams by liquid contents, or polyhedral foams and spherical foams by bubble shapes. It is important to realize that foam production is a vicious circle in cell culture process. Small amount of foam may cause cell lysis and release cell constituents into the medium, which will induce even greater foam. The detrimental effects caused by foaming in bioreactors are listed as following: 1) Blockage of exhaust filters. 2) Pressure build-up. 3) Ease of contamination. 4) Reduction in working volume and time, and 5) Trapping cells and proteins into the foam layer (Fazilet, 1998).

The foam liquid present in the films between two adjacent polyhedral bubbles and Plateau border channels where neighboring films meet. The foam level and stability are critically determined by the drainage kinetics of the foam liquid. The liquid in the films flows to Plateau border channels due to the capillary pressure. Then the liquid flows downward and out of the foam driven by gravity through the interconnected network formed by Plateau border channels. When the thickness of a bubble film is less than 100 nm, the repulsive force will arise which is referred to as the disjoining pressure. If the disjoining pressure decreases when the film keeps thinning, rupture of a film will occur since the mechanical and thermal disturbances grow in a boundless way. The factors that change liquid drainage or disjoining pressure, such as viscosity and ionic strength, will influence the foam properties. The cells entrapped in the foam may return to bulk medium undamaged along with the liquid drainage.

In cell culture processes, fresh bubbles are continuously introduced into liquid medium for aeration and finally reach the foam/liquid interface. It was found that the bubbles pulsated with high frequency, other than immediate stop, which can bounce away from free surface before entering a foam layer (Krzan, et al. 2003). At the bottom of foam layer, the bubbles are close to spherical shape with a gas volume faction of 0.74. As the bubbles move up within the foam layer, the gas volume fraction of the upper portions of the foam becomes larger. Based on a one-dimensional drift-flux model for gravity driven flow without wall shear, Pilon and Viskanta (2004) reported the onset of foaming occurs at gas volume faction of 0.85 for non-coalescent bubbles. Most of the drainage happens within a very short distance from the bottom (Bhakta and Ruckenstein, 1996). In addition, they showed that there is an upper limit of superficial gas velocity, within which the

steady state foam height can be reached. Pilon et al. (2002) investigated transient thickness of pneumatic foams. It was also found that a steady-state foam thickness with little variation can be quickly reached under low superficial gas velocities. With the increase of gas velocity, the oscillation of foam thickness became significant due to small liquid droplets with high speed or pressure waves generated by bubble bursting. Koehler et al. (2004a) pointed out that the exterior channels which contact surrounding walls may play an important role in liquid drainage in narrow containers. They also used a confocal microscope to study the velocity field in individual Plateau borders and nodes by tracking the motion of tracer particles (Koehler et al., 2004b). The surface viscosity was calculated according to velocity profile, which was consistent with values in the literature.

Unwanted foaming can be partially reduced by mechanical foam breakers or addition of chemical antifoams. Typical antifoams consist of either pure oil (silicone oils, fatty acids, alkyl amines) or the mixture of hydrophobic particles (silica, Al_2O_3, polypropylene) and oil. As fast antifoams, the oil globules can easily enter foam film and form oil bridges. Then the globule is stretched in a radial direction because of capillary pressure, which results in a very thin and unstable oil film. Finally the entire foam lamella is destroyed when this oil film ruptured. This process is referred to as the "bridging-stretching mechanism" (Denkov, et al. 1999).

On the other hand, a "bridging-dewetting" mechanism is proposed to explain antifoam function of hydrophobic particles (Frye and Berg, 1989). A "solid-bridge" is formed when particle are presents in foam film. Due to its hydrophobic property (contact angle > 90º), the particle is dewetted by liquid, which induces foam film rupture. For slow antifoams, it takes much longer time for oily globules to enter adjacent foam films.

Therefore, the entry barrier has a significant effect on antifoam activity. It has been found that negative "entry coefficient", EO, results in inefficient antifoam activity since the oil drop would remain inside the aqueous phase other than forming bridges:

$$EO = \sigma_{AW} + \sigma_{OW} - \sigma_{OA} \tag{2.5}$$

where $\sigma_{AW,}$ $\sigma_{OW,}$ and σ_{OA} represents interfacial tension between air-water, oil water, and oil-air, respectively. Another important function of hydrophobic solid particles in antifoams is lowering the entry barrier and facilitating the drop entry, explained as "pin effect". Besides two mechanisms mentioned above, some antifoam can lower the surface viscosity and elasticity or bulk viscosity, which enhance the liquid drainage.

2.4.4 Protein Adsorption

Protein adsorption and degradation is usually observed when proteins experience a hydrophobic surface, such as air-liquid interface. When marginally stable protein molecules approach a hydrophobic surface, they unfold to expose their hydrophobic amino acids to the surface, which are normally buried inside globular regions. Protein adsorption at gas-liquid interface results in inevitable change of secondary and tertiary structure. The structurally-perturbed protein molecules may be released into bulk solution directly. They also can form aggregates by hydrophobic interactions, which is often irreversible. To a certain extent, the aggregation returns back to the bulk liquid forming amorphous precipitate or fibrils. The formation of non-native protein aggregation also depends on the environments, such as temperature, pH, and ionic strength (Chi, et al., 2003). It was also found that the level of nonnative intermolecular β-sheet structures

increased in protein aggregates (Dong, et al., 1995). A small amount of irreversible therapeutic protein aggregates are not acceptable since they have negative impact on pharmacokinetics and safety due to immunogenicity (Braun, et al., 1997).

From a thermodynamic perspective, the decrease of the entropy of the water molecules orderly surrounding hydrophobic protein domains is the driving force for adsorption. Therefore, the amino acid compositions of protein and its structure have a great influence on adsorption process. According to their degree of hydrophobicity and flexibility, the proteins can be classified as "soft" or "hard". Flexible soft protein, which has high percentage of hydrophobic amino acids, can quickly migrate and cover the air-water interface by forming a monolayer within several minutes. However, it takes longer time for hard protein, which is more hydrophilic, to obtain the same coverage of surface. Maa and Hsu (1996) found the aggregation of recombinant rhGH and recombinant human deoxyribonuclease (rhDNase) was not affected by high shear. However, the presence of the gas-liquid interface induced rhGH to form non-covalent aggregates, which had no significant effect on rhDNase (Maa and Hsu, 1997). rhGH was found to be more surface active than rhDNase. Middelberg et al. (2000) compared two poly-peptides with different hydrophobicities. They found that hydrophobic Lac21 peptide formed a monolayer at an octane-water interface more quickly in comparison to its tetrameric counterpart, Lac18. Besides gas-liquid interfaces, the ice-water interface also contributes to protein denaturation during freezing-thawing (Chang et al., 1996). Protein aggregation was found in ultrafiltration and sterile filtration, which may form gel-like deposit and foul the membranes (Maruyama, et al., 2001; Maa and Hsu, 1998).

Surfactants can be applied to prevent physical denaturation of proteins during downstream, formulation, and fill-finish process. Several mechanisms are proposed to explain the effect of surfactants (Roth et al., 2000; Green et al., 2000; Norde and Giacomelli, 2000). For example, surfactants can lower the surface tension, which deceases driving force for protein adsorption. Surfactants may displace protein at interface, which reduces equilibrium protein adsorption. The physical damage is also alleviated for adsorbed proteins since the surface tension decreases with the presence of surfactants. It was found that nonionic surfactants, such as PF-68, Brij 35, and Tween 80, can prevent the interfacially induced aggregation of rhGH (Katakam, et al., 1995). Maa and Hsu (1997) demonstrated that Tween 20 reduced the soluble aggregation of rhGH in the foam. Tween-20 surfactants can significantly reduce the formation of insoluble rhGH aggregates during spray-drying process (Maa, et al., 1998). Consistently, Zhang and Ferrari (1997) showed that Tween 20 reduce albumin adsorption onto silicon surfaces. A small amount of Tween 80 can alleviate denaturation of interleukin-1 receptor antagonist at the ice-water interface during freeze-drying (Chang et al., 1996).

On the other hand, the direct interaction between surfactants and protein molecules also contributes to their protecting effect in some cases. The surface tension of protein-surfactant system may increase in comparison to pure protein solution since surfactants can bind to hydrophobic domains of the protein, which make it less surface-active. The solubility of protein-surfactant complex increases because it is more hydrophilic. Therefore, surfactant can effectively prevent insoluble aggregates (Kreilgaard, et al., 1999). In addition, the binding of surfactant to protein may increase the energy barrier of unfolding from thermodynamic perspective (Bam et al., 1998).

Arakawa and Kita (2000) found that Tween 80 can alleviate thermally-induced aggregation of bovine serum albumin without involvement of any surface.

CHAPTER THREE

THE SENSITIVITY OF DINOFLAGELLATE *CRYPTHECODINIUM COHNII* TO TRANSIENT HYDRODYNAMIC FORCES

The content of this chapter has been prepared for publication: Hu W, Gladue R*, Hansen J*, Wojnar C*, Chalmers JJ, The effect of acute hydrodynamic forces on dinoflagellate *Crythecodinium cohnii*

* Fermentation Sciences, Martek Biosciences Corporation, 555 Rolling Hills Lane, Winchester, KY 40391

3.1 SUMMARY

The increased interest in the benefits of fish oils for human health has resulted in commercial development of dinoflagellate *Crypthecodinium cohnii* for production of docosahexaenoic acid (DHA). The nearly commodity level market demand for DHA requires highly efficient, very large scale cultures of *C. cohnii* cells. While the effect of hydrodynamic forces on dinoflagellates has been investigated for several decades, the majority of previous work focused on the negative effects of oceanic turbulence on the population growth of environmentally important dinoflagellate. In contrast, significantly

less is know on the effect of hydrodynamic forces encountered by algae in bioprocesses. Unlike other studies conducted on microalgae, this study employed a microfluidic channel to evaluate the effect of transient hydrodynamic forces on *C. cohnii* cells, which focused on a much higher hydrodynamic level encountered in bioreactors than that in the ocean. It was found that *C. cohnii* cells can sustain the energy dissipation rate of 5.8×10^{7} W/m^3 without be lyzed. On the other hand, an obvious sub-lethal effect, the loss of flagellate, was observed at a lower level of 1.6×10^{7} W/m^3. Finally the cell-bubble interaction and the effect of bubble rupture were also explored in order to simulate the conditions of sparged bioreactors.

3.2 INTRODUCTION

Dinoflagellate represents an important phytoplankton group in the ocean environment. It has two dissimilar flagella, longitudinal and transversal, which act as steering and propelling devices, respectively. Dinoflagellate contain most common organelles, such as endoplasmic reticulum and mitochondria, along with unique nucleus, which distinguishes them from the nucleoid region of prokaryotes and the true nuclei of eukaryotes (Raikov, 1995).

Oceanic turbulence has been recognized as a crucial factor influencing dinoflagellate activities. Turbulence, with length scales from millimeter to several meters, is essentially generated by vigorous water motion, augmented with the help of strong winds. The energy dissipation rate (EDR) can vary over eight orders of magnitude with the highest value around 10^{-2} $m^2 \cdot s^{-3}$ in breaking waves and the lowest value around 10^{-10} $m^2 \cdot s^{-3}$ in stratified interior of the oceans (Terray et al. 1996; Gargett 1997).

There exists sufficient evidence that dinoflagellate blooms, such as red tide, have high probability of occurring during calm sea environments. For example, Pollingher and Zemel (1981) conducted field observations in Lake Kinneret (Israel) and found a negative relationship between the appearance of *Peridinium* bloom and the magnitude and duration of wind and waves. Therefore, dinoflagellate is generally considered a turbulence-sensitive specie compared to diatoms and cyanphytes, which has been clearly illustrated in classical Margalef Mandala (Margalef, 1978).

In order to verify this observation, laboratory experiments were conducted to reproduce oceanic hydrodynamic forces in small-scale apparatus in order to study their effects on monocultures of dinoflagellate. One of the simplest methods is using shake flasks. Pollingher and Zemel (1981) reported that shaking during the dark period had a strong negative effect on cell growth of freshwater dinoflagellate *Peridinium cinctum* f. *westii* (Lemm.) Lefèvre. It was suggested that it is related to the pre-mitotic and mitotic stages of cell division, and the cells resumed their growth after cessation of shaking.

However, hydrodynamic forces in shake flasks are complicated, depending on the shaking speed, shaking orbit, and loading volume. Most recently, Zirbel et al. (2000) used digital particle imaging velocimetry (DPIV) to measure the fluid motion in flasks shaken at an orbit of 2.54 cm and rates of 40 to 120 rpm. The loading volume was 60 ml in 125 ml Pyrex flasks. DPIV data implied shear stress was no doubt inhomogeneous distributed in shake flasks with high values occurring close to the wall. They found that shaking even at 75 rpm, which corresponded to wall shear stress of 0.0025 to 0.0035 $N \cdot m^{-2}$, still inhibited the cell growth of dinoflagellate *Ceratocorys horrida*. The *C. horrida*

morphological changes, reversible shortening of spines, even happened at 45 rpm corresponding to wall shear stress of 0.000174 $N \cdot m^{-2}$.

On the other hand, couette devices have been largely applied to evaluate the sensitivity of various cells to hydrodynamic stress because it can generate a constant, homogeneous, and well-defined laminar flow (Joshi, et al., 1996). Thomas and Gibson (1990a, 1990b, and 1992) used a glass Couette to study the effect of quantified hydrodynamic forces on *Lingulodinium polyedrum*, *Gymnodinium sanguineum* Hirasaka, *Prorocentrum micans*. The thresholds of energy dissipation rate to inhibit *L. polyedrum* growth in terms of cell division and cell size was 2×10^{-5} $m^2 \cdot s^{-3}$, while *G. sanguineum* and *P. micans* had lower and higher thresholds, respectively. Thomas et al. (1995) investigated the physiological mechanisms behind the inhibition of *Gonyaulax polyedra* growth using a Couette device and a phytoplankton wheel. It has shown that photosynthesis was less shear-sensitive than growth. Intracellular pigment content increased even though the cell division was inhibited. Juhl, et al. (2000 and 2002) fabricated a novel Couette without dead space at the bottom to study the effect of environmental conditions and physiological state of the cells on shear sensitivity of red-tide causing dinoflagellate *L. polyedrum*. Late hour of the dark phase was the moment the cells had high sensitivity, which was also affected by illumination intensity and the stage of exponential phase.

More interestingly, several investigators have used the oscillating grid method, which employed the movement of a control rod immersed into a water tank to generate turbulent vortices. Sullivan and Swift (2003a) applied Acoustic Doppler Velocimeter (ADV) technology to determine the EDR at five positions in a seawater tank under two

oscillating speeds of rods. They tested ten species of autotrophic dinoflagellates, which showed quite different responses. The high turbulence around 10^{-4} $m^2 \cdot s^{-3}$ benefits the growth of *L. polyedrum* (Stein) Dodge, *Gymnodinium catenatum* Graham, and *Alexandrium fundyense* Balech. However, cell size characterized by cross-sectional area was not changed dramatically for most of the tested species except *L. polyedrum* and *Ceratium fusus*. Furthermore, they also found that the growth rate of *L. polyedrum* Balech increased linearly as a function of the logarithmic increase in EDR until reaching a threshold of 10^{-3} $m^2 \cdot s^{-3}$ while *Alexandrium catenella* (Wheedon and Kofoid) had a opposite response (Sullivan et al., 2003b). Both of them maintained reasonable growth rates even at high turbulence of 10^{-3} $m^2 \cdot s^{-3}$.

Besides their importance in the ocean environment, dinoflagellate are gaining attention for industrial applications. *Crypthecodinium cohnii*, a chloroplastless heterotrophic marine dinoflagellate, can be used to produce triacylglycerol oil containing high percentage of docosahexaenoic acid (DHA). DHA is essential for the development of infant's visual and neurological functions. It is present in mother's milk, and the World Health Organization (WHO) recommends adding it to infant formula. Compared to traditional sources from fish, *C. cohnii* cell culture provides a better way to manufacture high quality DHA without environmental man-made pollutants such as dioxins and other polyunsaturated fatty acid such as eicosapentaenoic acid (EPA), which can affect the uptake of DHA (Craig-Schmidt et al., 1998). de Swaaf, et al. (1999, 2003a, and 2003b) systematically investigated high-density fed-batch cultivation of *C. cohnii* for DHA production in 2 L bioreactors, and obtained volumetric productivities of 53 mg l^{-1} h^{-1}.

The objective of this work was to evaluate the shear sensitivity of the industrial important microalgae, *C. cohnii,* using an improved microfluidic device, which has been applied in the study of mammalian and insect cells. Rheology properties of the cell suspension were considered in computational fluid dynamic (CFD) simulation and energy dissipation rate (EDR) calculation. The lethal and sub-lethal effects of high hydrodynamic force on *C. cohnii* cells were examined, which was correlated to bioreactor conditions. Finally, the interaction between *C. cohnii* cells and bubbles was also investigated in order to assess the potential detrimental effect of bubble rupture and foam layer.

3.3 MATERIALS AND METHODS

3.3.1 Microfluidic Device

In this study, an improved flow contraction device, consisting of a microfluidic channel made of 30 gauge stainless steel and cut by wire discharge machining. The new machining technique resulted in a perfectly vertical and smooth channel wall verified by microscope observation (Figure 3.1a). Figure 3.1b is a 3-D drawing of the narrow neck of the channel sandwiched by sealing blocks, where five virtual cross-sectional plates represent the positions the hydrodynamic forces were calculated. Plate #3 is the narrowest part of the channel which has a width of 220 μm. The flow direction is from left to right along with X axis.

3.3.2 CFD Simulation

The fluid flow within the microfluidic channel was simulated using a CFD package, FLUENT (FLUENT Inc., Lebanon, NH) using a similar grid pattern as Ma et al. (2002). The actual dimensions of the channel were measured microscopically in order to eliminate any derivation obtained during fabrication. Even though the cross-section of channel is rectangle, 3-D simulation of the whole channel was performed to account for any unsymmetrical flows. The total number of nodes was around 600,000 with the finest grid of 5μm located at the constriction region around plate #3. In addition, rheology behavior of cell suspension was considered in CFD simulation and also calculation of EDR. EDR is a scalar quantity to characterize hydrodynamic conditions, which is defined as the double dot product of shear stress and velocity gradient.

3.3.3 Dinoflagellate

C. Cohnii (ATCC 30772) is a commercially available strain, which was originally cultured in chemical-defined ATCC medium 460 and then transferred to complex medium consisting of 20g/L glucose (Sigma, St. Louis, MO), 5g/L yeast extract (Fisher Scientific, Hampton, NH), and 12.5g/L sea salt (Sigma, St. Louis, MO). The effects of these medium components on cell growth have already been investigated by de Swaaf et al. (1999). The medium components were filter-sterilized using a 0.2 μm membrane filter (Corning Life Sciences, Corning, NY) in order to avoid white precipitates after autoclave at 121ºC. The initial pH was adjusted to 6.5. *C. Cohnii* cells were grown statically in 50 ml of medium in 250 ml Erlenmyer flasks at room temperature (around 23ºC) for maintenance. The static cultures were sub-cultured every four days at a ratio of 1:20. The

cell diameter was within the range 3~30μm with the median value around 13 μm, measured by Coulter Multisizer II (Beckman Coulter, CA).

There are two forms of *C. cohnii* cells during one cell cycle: swimming cells and cysts (Kwok and Wong, 2003). When cells move from G1 phase to S phase, the deflagellation is initiated and the swimming cells become cysts. After M phase, the daughter cells regain flagella and begin to swim. Since the cells can have multiple fissions, 1, 2, 4, or 8 cells can theoretically originate from one cyst (de Swaaf, 2003). The cell concentrations were determined by hemocytomer counting. 0.1% (w/v) SDS solution was added with a ratio of 1:10 (v/v) into the samples to get rid of movement of swimming cells. Mathematically, the motility is represented by

$$Motility = \frac{N_{total} - N_{nonmotile}}{N_{total}} \times 100\% \qquad (3.1)$$

where N_{total} is the number of total cells after adding SDS solution; $N_{nonmotile}$ is the number of totally nonmotile cells before adding SDS solution, which does not account for cells that can only spin or move very slowly.

3.3.4 Cell Damage Study

C. Cohnii cells were harvested after a two-day, static cultivation, and subsequently loaded into a syringe after gentle mixing. The cell concentration and motility was determined. Then the cell suspension (~50ml) was forced through the flow contraction device using a syringe pump (Model PHD 2000, Harvard Apparatus, Dover, MA). The first 10ml was not collected and the rest of the effluent can be reloaded into the syringe for multiple passages. The effluent after each pass was sampled for lactate

dehydrogenase (LDH) assay using CytoTox96 kit (Promega, WI) and cell number counting. The flow rates were varied in the range of 10 to 90 ml/min with 20 ml/min increments. The flow remained in laminar region for all applied flow rates even at substantially high Reynolds number thanks to the specific channel structure (McQueen and Bailey, 1989). Rheological properties of cell suspension were measured using an ARES Rheometer (TA Instruments, New Castle, DE).

3.3.5 Cell-Bubble Interaction Experiments

To view the cell attachment in bubble film, the contracted part of a normal pipette tip (1ml) was sealed with a 26 gauge needle. The tip was subsequently overfilled with *C. cohnii* cell suspension from static culture. Bubbles were introduced through the needle at the bottom. A SCIMAX CCD digital camera (MVIA, Monaca, PA) with infinity lens (ISCO Precision Optics GMBH, Germany) was used to capture the image of single bubble or foam at the top of over-filled pipette tip. Bovine Serum Albumin (BSA) was added in order to obtain stable foam layer. Pluronic F-68 was also examined for its preventing effect on cell-bubble attachment.

A bubble collector developed by Ma et al. (2004) was applied to quantitatively study the entrapment of *C. cohnii* cells into foam layer and their drainage kinetics. This device can separate foam formation with bubble rupture. Different spargers were used including a sintered glass (ACE glass, Vineland, NJ) and a 30 gauge needle in order to obtain various bubble sizes. The gas flow rate was controlled at 2.5 ml/min, which can ensure not only sufficient mixing but also plug flow of foam layer at the top. The cell suspension of 3.2×10^6 cells/ml containing 1.5 g/L BSA was used in this part.

3.4 RESULTS

3.4.1 CFD Simulation

EDR is a parameter strongly depending on the rheology properties of fluid. However, it has been reported that *C. cohnii* cells can excrete extracellular polysaccharide which will change the rheology behavior of broth significantly (de Swaaf et al., 2001). In this study, *C. cohnii* cell suspension after two-day cultivation was found to exhibit only a minor shear thinning, which may result from relatively low cell concentration. A Carreau model was used to describe the relationship between shear rate (γ) and viscosity (μ), which was input into FLUENT simulation.

$$\mu = 1.6 + 16.4 \times \left[1 + (0.3\gamma)^2\right]^{-4} \quad cPa \tag{3.2}$$

From the velocity vector output from the CFD code, the EDR (ε) at each node can be calculated by the following equation:

$$\varepsilon = \tau : \nabla U = \begin{bmatrix} 2\mu_{xx}\frac{\partial U_x}{\partial x} & \mu_{yx}\left(\frac{\partial U_y}{\partial x} + \frac{\partial U_x}{\partial y}\right) & \mu_{zx}\left(\frac{\partial U_z}{\partial x} + \frac{\partial U_x}{\partial z}\right) \\ \mu_{xy}\left(\frac{\partial U_x}{\partial y} + \frac{\partial U_y}{\partial x}\right) & 2\mu_{yy}\frac{\partial U_y}{\partial y} & \mu_{zy}\left(\frac{\partial U_z}{\partial y} + \frac{\partial U_y}{\partial z}\right) \\ \mu_{xz}\left(\frac{\partial U_x}{\partial z} + \frac{\partial U_z}{\partial x}\right) & \mu_{yz}\left(\frac{\partial U_y}{\partial z} + \frac{\partial U_z}{\partial y}\right) & 2\mu_{zz}\frac{\partial U_z}{\partial z} \end{bmatrix} : \begin{bmatrix} \frac{\partial U_x}{\partial x} & \frac{\partial U_y}{\partial x} & \frac{\partial U_z}{\partial x} \\ \frac{\partial U_x}{\partial y} & \frac{\partial U_y}{\partial y} & \frac{\partial U_z}{\partial y} \\ \frac{\partial U_x}{\partial z} & \frac{\partial U_y}{\partial z} & \frac{\partial U_z}{\partial z} \end{bmatrix} \tag{3.3}$$

The viscosity (μ) in shear tensor matrix (τ) was calculated based on corresponding shear rate (γ) according to equation 3.2. Since the velocity gradients in the channel are generally high, the apparent viscosity is close to the constant value, 1.6cPa. Therefore, the effect of non-Newtonian rheology was not significant in this case. However, at higher

values of non-Newtonian visocity, shear thinning properties of the broth can have a significantly higher effect in the high shear rate range.

How to use a single value to represent hydrodynamic conditions is challenging since the EDR in the microfluidic channel is inhomogeneously distributed. In addition, it is obvious that the fluid velocity is larger in the center of the channel and smaller at the walls. Correspondingly, given an equally distributed cell suspension, a majority of the cells will pass through the center, where the EDR is lower, compared to the wall region. Therefore, this study weighted the EDR at five virtual cross-sections by the flow rates. Each cross-section is equally divided into 1600 sub-sections. The percentage of volume flow rate across each sub-section to the total flow rate was used as a weighting function for the corresponding local EDR. The results are listed at Table 1. As expected, the EDRs after weighting were lower than the values from other methods such as particle tracking technique (Mollet et al., 2006), even though they used a viscosity of 1 cPa. As has been discussed previously (Ma et al., 2002), the maximum EDR values in the microfluidic channel change dramatically with the flow rates. In this study, the maximum EDR occurred at cross section number 2, before the narrowest part of the channel, which was varied by two orders of magnitude in our experiments. In addition, the EDR at different positions under certain flow rate was compared in Table 3.1, which also varied by 5 to 10 fold.

3.4.2 Cell Damage and Sub-lethal Effect

Cell suspensions from static culture with a concentration of 3.5×10^6 cells/ml and a motility of 87% were used. LDH assay has been widely used to assess the lysis of

mammalian and insect cell. There is no available information regarding its application on *C. cohnii* cells. A preliminary experiment demonstrated that there was a linear relationship between LDH absorbance and cell concentration (Figure 3.2). Both LDH results and visual counting indicates that no significant cell lysis occurred for all flow rates tested (data not shown). However, a significant loss of motility was observed when flow rate was more than 50 ml/min flow rates (Table 3.2), corresponding to a maximum EDR of 1.6×10^{7} W/m^{3}.

Visual observations using phase-contrast microscopy suggested that this drop in mobility was the result of the actual physical loss of longitudinal flagellum, not the loss of moving ability of attached flagellum. The damage on transverse flagellum was not clear since it is normally embedded into grooves. It may be also injured if the cells can not move at all. In addition, it was observed that a significant number of the cells subjected to the 50 ml/min conditions could only spin slowly in one direction, as opposed to the typical forward swimming normally observed. This was the first time that such behavior was observed. It implies that transverse flagellum may be intact and still functional while the longitudinal flagellum was excised. Equally interesting, the motility recovered, typically 30 minutes after exposure (Figure 3.3). The velocity of cell movement did not recover until after 45 minutes. During the "recovery process", the algae cells always began to spin first, and then move in a straight direction. For example, more than half of the cells can only spin even though the motility was fully recovered after 30 minutes (Figure 3.3). Visual observations confirmed the reappearance of flagella with this resumption of motion. A picture of *C. cohnni* cell with flagella is presented in Figure 3.3. The length of flagellate was around 20 μm with the width less than 1 μm.

3.4.3 Qualitative Study of Cell-Bubble Attachment

Figure 3.4 is a photo of *C. cohnni* cells attached to a bubble at the top of an over-filled pipette tip. Cells appear as small white dots in the bubble film. Cell attachment can be observed even though most of cells can swim (motility>85%). In addition, the entrapment of *C. cohnni* cells into the foam layer was also observed. The cells presented in the liquid film between two adjacent bubbles (Figure 3.5a). It was also found that there were cell clumps presented in the nodes of the foam, where multiple Plateau border channels meet (Figure 3.5b). It seems that motile *C. cohnii* cells moved toward the same points from different channels along with liquid drainage, where they can not dissipate quickly. PF-68 has been widely used as an additive to prevent bubble-cell attachment in mammalian cell culture. In this study, it was demonstrated that PF-68 can reduce the appearance of *C. cohnni* cells in bubble film (Figure 3.6a). However, it can not prevent the cells presenting in foam liquid between two bubbles (Figure 3.6b).

3.4.4 Quantitative Study of Cell-Bubble Attachment

In order to clarify the effect of bubble rupture on *C. cohnii* cells, the foam liquid was collected for motility analysis (Figure 3.7). Fraction A to D represented the collected foam liquid for every 5 ml pumped air in a sequence. It was found the rupture of small bubbles resulted in the loss of motility in approximately 20% of the cells, while the rupture of larger bubbles only resulted in a 4% decrease (Table 3.3). In addition, there was no significant different among different fractions. It is difficult to quantitatively measure the size of bubbles when they ruptured in a collection tube. It was estimated that

the bubble size from sintered glass sparger was around 1 mm and that from 30 gauge needle is around 5 mm. Therefore, the rupture of bubbles will generate a maximum EDR of 1×10^{10} W/m^3 and 1×10^{5} W/m^3, respectively (Boulton-Stone and Blake, 1993). The effect of bubble rupture on the loss of motility is consistent with the results from microfluidic channel experiments. The motility of cells in the bulk was not changed, which implied there was no significant difference between the tendency of motile cells and immotile cells to attach to rising bubbles.

In addition, it was found that *C. cohnii* cells were enriched in the foam layer generated by sintered glass sparger (Table 3.4). The cells were more concentrated on the top layer of the foam (Fraction D), which implied that the motile *C. cohnii* cells did not drain efficient along with liquid out of foam layer through Plateau border channels. It may result from the appearance of cell clumps in the nodes (Figure 3.5b). However, the cell enrichment was not significant for the large bubble foam from 30 gauge needle.

3.5 DISCUSSION

The sensitivity of the dinoflagellate, *C. cohnii*, was examined in a well-defined microfluidic device. The hydrodynamic conditions have been quantitatively studied by CFD simulations, which can help us relate it to the response of cells. Unlike previous studies of microalgae in the ocean environment, higher ranges of EDR were tested which covered the most conditions encounter in bioreactors. It was found that *C. cohnii* was more difficult to lyzed in comparison to mammalian cells. While mammalian cells do not have a cell wall, *C. cohnii* cells have amphiesma (surrounding walls) that contains several cellulosic plates, 15-20 nm in thickness, as well as four to five other membranes

(Kwok and Wong, 2003). Consistently, Barbosa, et al. (2003) found that cell wall-lacking mutant of *Chlamydomonas reinhardtii* are more sensitive to high shear in the sparger zone.

A clear sub-lethal effect of hydrodynamic forces on *C. cohnii* cells, the loss of flagella, was observed. The ecological importance of this cell response can be explained as follows. Dinoflagellate normally floats on the surface of calm sea (Broekhuizen 1999). When they surfer from strong winds or breaking waves, the deflagellation activity was initiated, which can help them escape from the dangerous area by sedimentation to deep sea. They can come back to the surface again since the flagella can be regenerated in a short time. The motility of dinoflagellate has been hypothesized as an important reason why this specie can survive for millions of years in a severe competition with other phytoplankton.

The loss of flagella was also observed when dinoflagellate *Chlamydomonas* suffered high hydrodynamic stress in a homogenizer (Cheshire and Keller, 1991). It was not clear that the loss of flagella is a proactive biological response of cell to harsh environments or a passive physical break-off. Other environment stresses such as pH shock caused dinoflagellate to shed their flagella (Quarmby et al., 1992). More recently, Zirbel et al. (2002) found the spines of marine dinoflagellate *Ceratocorys horrida* shortened or disappeared in a shaken flask culture compared to still conditions. The scanning electron microscopy pictures showed no evidence of fracture plane. However, the hydrodynamic forces in the shaken flask were much lower than the level to induce deflagellation determined in this study. There are possible other factors involved in shake flask study, which was discussed in Chpater Four. The flagellate or spines can regenerate

when hydrodynamic stress was removed. The recovery process can be manipulated by extracellular Ca^{2+} levels. It took about 50 minutes for *Chlamydomonas* to outgrow its flagella to original full length (Cheshire and Keller, 1991).

In addition, the loss of motility can be used as a marker to assess the hydrodynamic conditions in complex systems. Chen et al. (2003) proposed the use of dinoflagellate bioluminescence as a novel tool to study hydrodynamic forces in bioreactors. It was based on the fact that bioluminescence of some dinoflagellate species can be triggered by flow stimuli. The luminescent response of *Lingulodinium polyedrum* cells started at a shear stress of 0.1-0.3 N/m^2 with the maximum at 1-2 N/ m^2, corresponding to 10^5 W/m^3 (Latz and Rohr, 1999). One significant difference is the size of *C. cohnii* cells is considerable smaller than that of most dinoflagellates with bioluminescence (40-900 μm). The deflagellation was triggered by a higher level of EDR.

Finally, the interactions between bubbles and *C. cohnii* cells were also studied. It provides meaningful information for industrial operation. For example, the bubble size should be carefully considered since the rupture of small bubbles resulted in the sub-lethal effect on cells as well as high cell enrichment in the foam. The use of antifoam may be helpful since it is relative difficult for motile *C. cohnii* cells to escape from the foam layer. Our visualization experiments suggested using PF-68 for alleviating bubble-associated cell damage. However, the overall impact of PF-68 on manufacture processes still needs to be evaluated. Camacho et al. (2001) reported that carboxymethyl cellulose, another polymer surfactant as PF-68, can protect microalgae *Phaeodactylum tricornutum* against hydrodynamic stress in photobioreactors.

3.6 CONCLUSIONS

A novel microfluidic device was used for the investigation of dinoflalgellate's response to hydrodynamic stress. It was found that dinoflagellate *C. cohnii* cells are robust compared to mammalian cells. However, a clear sub-lethal effect of hydrodynamic forces, the loss of flagella, was observed. Furthermore, a possible mechanism underneath this effect was tentatively given. In addition, the cell-bubble attachment and the entrapment of cells into the foam layer were identified. In the future, a long-term effect of hydrodynamic forces on *C. cohnii* cells will be performed.

Virtual cross-section plate	Flow rate (ml/min)				
	10	30	50	70	90
1	1.17×10^{5}	1.12×10^{6}	3.04×10^{6}	6.07×10^{6}	1.13×10^{7}
2	6.38×10^{5}	5.88×10^{6}	1.63×10^{7}	3.25×10^{7}	5.82×10^{7}
3	5.36×10^{5}	4.61×10^{6}	1.35×10^{7}	2.62×10^{7}	4.27×10^{7}
4	4.72×10^{4}	1.12×10^{6}	1.47×10^{6}	3.59×10^{6}	1.04×10^{7}
5	4.58×10^{4}	6.42×10^{5}	1.28×10^{6}	3.08×10^{6}	1.20×10^{7}

Table 3.1 Volumetric flow rate weighted median EDR at different cross-sections (as in Figure 3.1, units W/m^3)

	10 ml/min	30 ml/min	50 ml/min	70 ml/min	90 ml/min
None	87±2 %	87±2 %	87±2 %	87±2 %	87±2 %
Once	88±1%	86±2 %	70±5 %	52±2 %	24±10 %
Twice	87±1 %	83±1 %	67±4 %	35±3 %	6±1 %
Three times	85±1 %	83±1 %	62±1 %	22±8 %	2±0.5 %

Table 3.2 Change of *C. cohnii* motility after pumped through the microfluidic channel

	Initial	Fraction A	Fraction B	Fraction C	Fraction D
Sintered glass sparger	88±4 %	71±2 %	68±1 %	67±5 %	70±2 %
30 gauge needle	84±1 %	79±3 %	80±1 %	79±2 %	80±3 %

Table 3.3 The change of motility in collection tube (as in Figure 3.7)

	Fraction A	Fraction B	Fraction C	Fraction D
Sintered glass sparger	1.37±0.10	1.45±0.15	1.53±0.08	1.80±0.14
30 gauge needle	0.95±0.03	0.99±0.11	0.96±0.03	1.10±0.05

Table 3.4 The cell enrichment in the foam layer

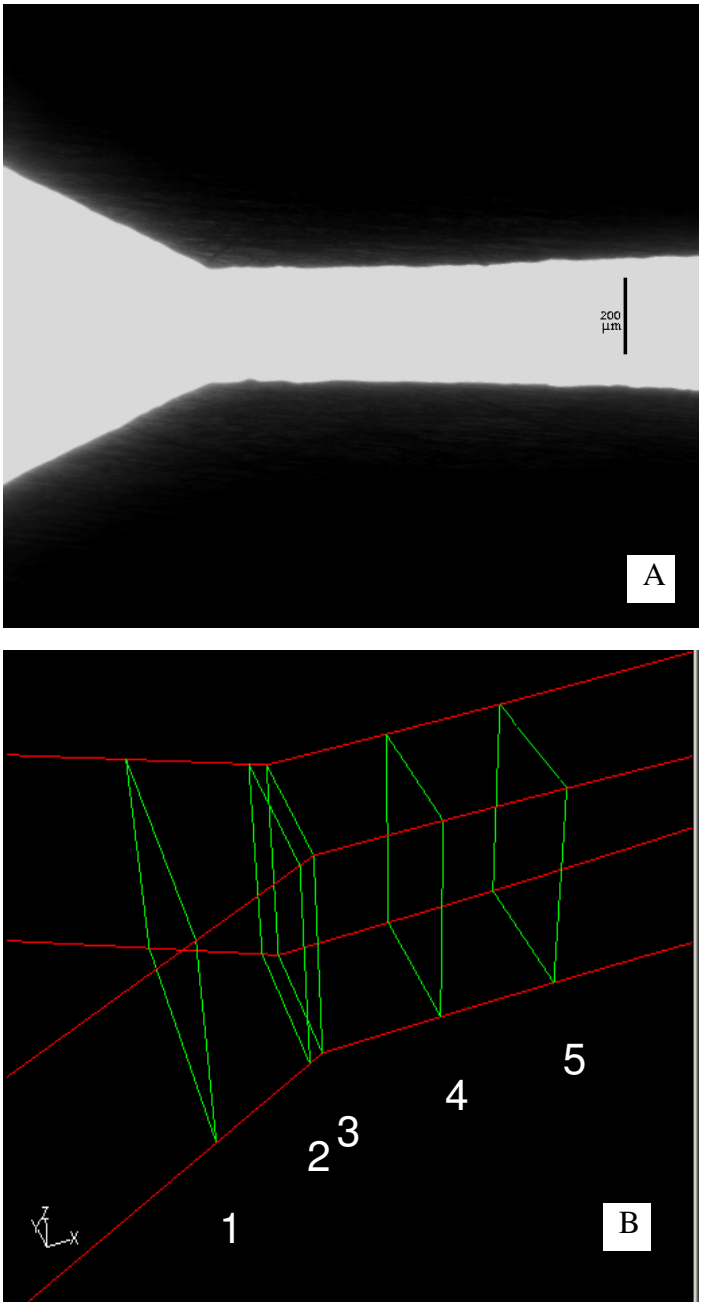

Figure 3.1. Outline of the microfluidic channel. A) Microscopic picture; B) 3-D drawing. #1-5 represent virtual cross-sections for EDR calculation.

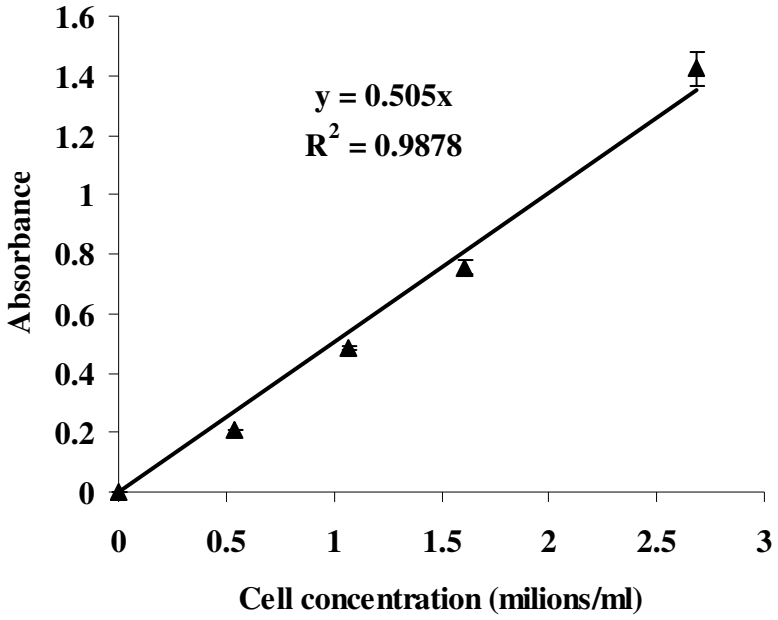

Figure 3.2. The relationship between LDH absorbance and *C. cohnii* cell concentration;

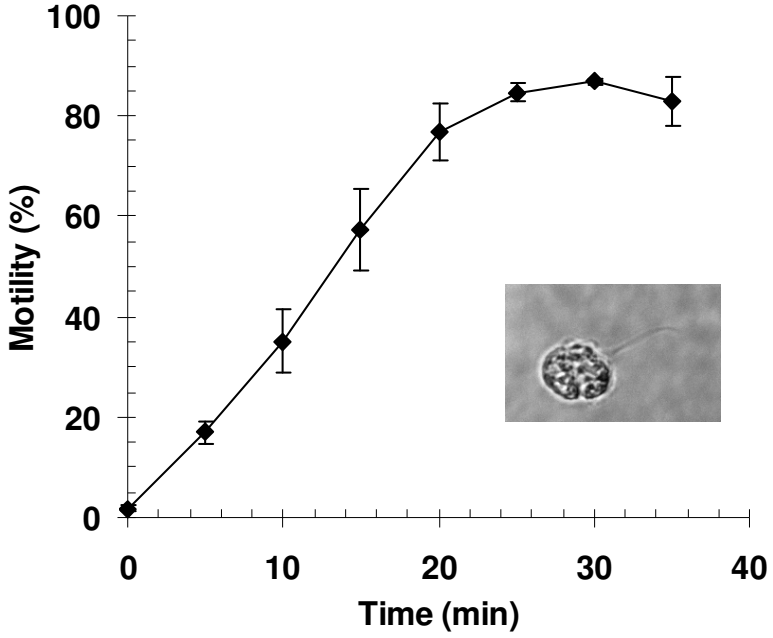

Figure 3.3. The recovery of the motility of *C. cohnii* cells. The small picture is an image of one *C. cohnii* cell with flagella.

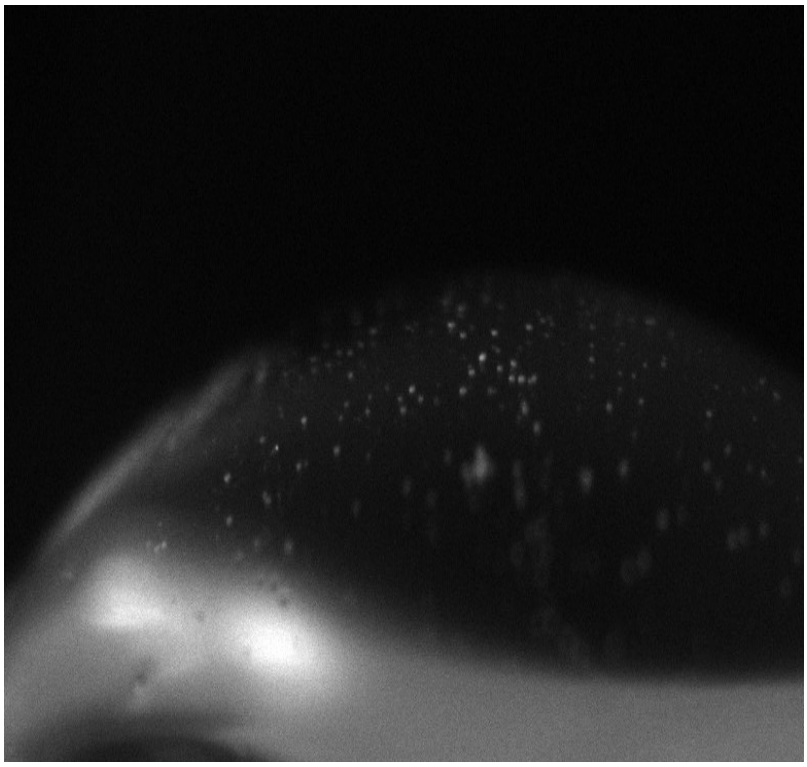

Figure 3.4. Photograph of *C. cohnii* cells resting on bubble film

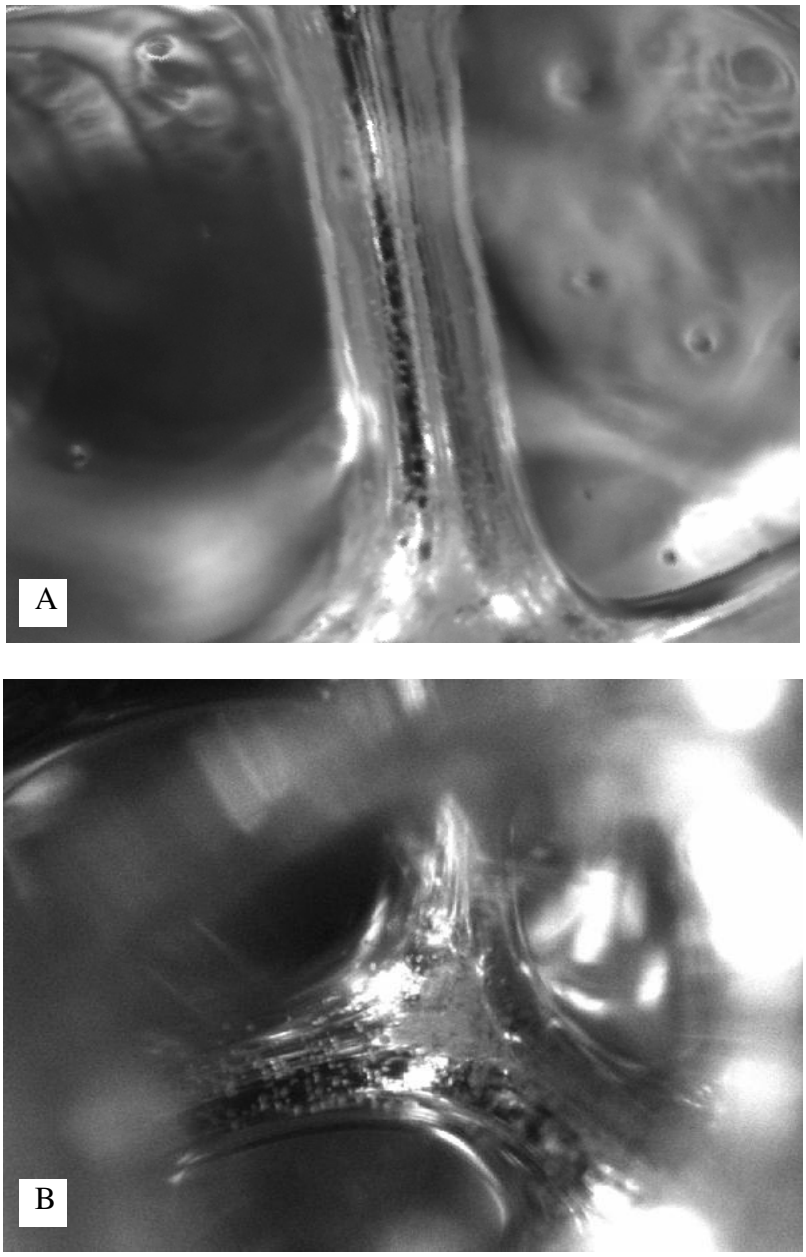

Figure 3.5. The entrapment of *C. cohnii* cells in the foam A) film between two adjacent bubbles; B) node where Plateau border channels meet

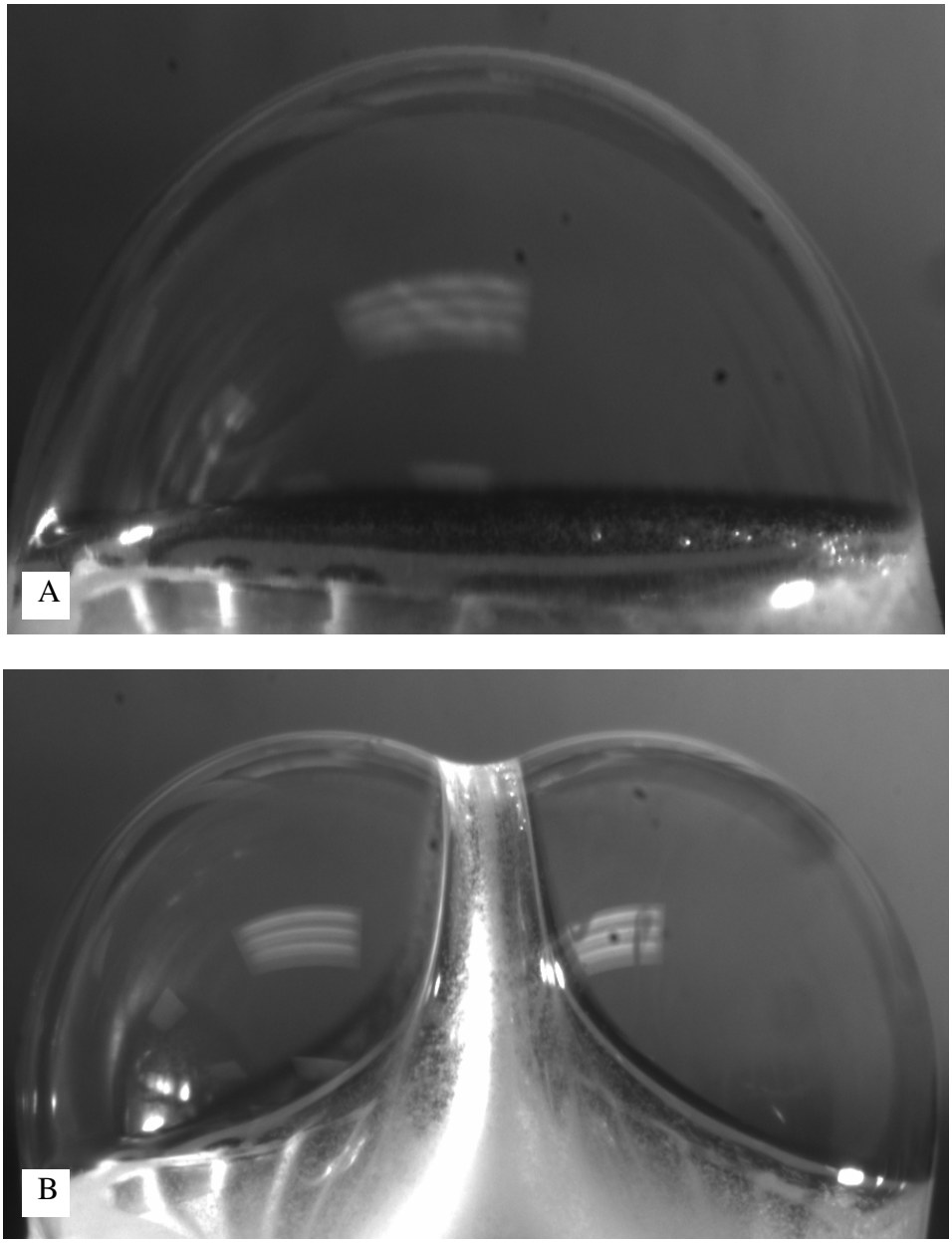

Figure 3.6. The effect of PF-68 on cell-bubble attachment A) single bubble; B) dual bubbles

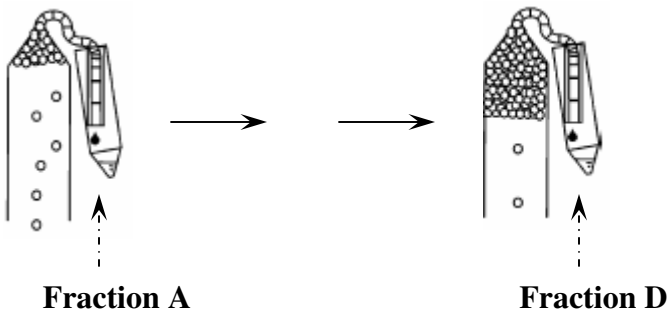

Figure 3.7. Illustration of bubble collector experiments

CHAPTER FOUR

THE SENSITIVITY OF *CRYPTHECODINIUM COHNII* TO LONG-TERM HYDRODYNAMIC FORCES

The content of this chapter has been prepared for publication: Hu W, Gladue R*, Hansen J*, Wojnar C*, Chalmers JJ, A case of mistaken blame: It was not shear sensitivity this time!

* Fermentation Sciences, Martek Biosciences Corporation, 555 Rolling Hills Lane, Winchester, KY 40391

4.1 SUMMARY

The economics of large scale, cell cultures are significantly enhanced when the product is a food additive, such as Docosahexaenoic acid (DHA) produced using the dinoflagellate algae, *Crypthecodinium cohnii*, compared to traditional pharmaceutical cultures. However, perceived sensitivity of *C. cohnii* cells to hydrodynamic forces has historically limited the agitation and aeration applied. In this study, we will demonstrate how, what first appeared to be a problem with shear sensitivity was in fact, a mass transfer limitation. Then we go on to demonstrate the limit of chronic, rapid energy

dissipation rate (EDR) that *C. cohnii* cells can experience. A scale-down model consisting of a microfluidic device and a stirred tank bioreactor was used to expose the cells to this EDR and understand the relationship between hydrodynamic forces and cell culture performance. Inhibition of cell growth was observed when *C. cohnii* cells were subjected to an energy dissipation rate, EDR, of 5.9×10^{6} W/m^{3} with an average frequency of 0.2 min^{-1} or more. This level of EDR is sufficiently high that *C. cohnii* can withstand typically encountered hydrodynamic forces.

4.2 INTRODUCTION

Long chain polyunsaturated fatty acids (PUFAs) with more than 18 carbon atoms have been of increasing interest in human nutritional supplements for more than two decades. Docosahexaenoic acid (DHA, 22:6) belongs to omega-3 PUFAs present in human brain and eye tissue. Because of the rapid development of newly-born babies, large quantities of DHA have to be supplied at least in the first two years of life through breast feeding or infant formula (Innis, 1994). In addition, DHA are being increasingly recognized for their benefits against cardiovascular disease (Kang and Leaf, 1996). Their activity against a variety of other conditions including Alzheimer's disease, diabetes, depression, and inflammation are also being investigated (Horrocks and Yeo, 1999).

Although oily fish are the most widely known source of DHA, they only acquire it through the food chain, predominately from the consumption of DHA in microalgae. DHA extracted from fish oil is problematic in some applications such as infant formula and pharmaceutics because it may contain environmental pollutants and other PUFAs

which have unknown or negative effects on human health (Ratledge, 2004). The purification of DHA from complex mixture of fatty acids in fish oil is also expensive.

In contrast to the challenge of purification from fish, it has been found that the dinoflagellate *Crypthecodinium cohnii* makes triglyceride oils, which are particularly rich in DHA (30~50% of the total fatty acids) (Behrens and Kyle, 1996). DHA is the major PUFA of *C. cohnii* cell oil along with a small percentage of oleic acid (18:1), while the content of other PUFAs are less than 1%. Therefore, microaglae cell culture using *C. cohnii* strain is considered a promising way to produce high quality DHA (Kyle, 1996), which has already been marketed worldwide for infant formula applications.

C. cohnii belongs to heterotrophic algal specie, making use of organic carbon substances for cell growth and DHA production. Traditional fermentation technology can be applied directly since there is no requirement for light, a bottleneck for large-scale photobioreactors. However, one of the biggest challenges faced by microalgae cell culture industry is economics; the products have relative low value compared to pharmaceuticals. It was this economic reality that resulted in the early failure of large scale algal cultures (Neenan et al, 1986). Despite this challenge, commercial manufacture of DHA has been successfully achieved by Martek Biosciences Corporation. as an additive to infant formula and other foods. However, it is this extraordinary success of large scale food additive manufacture that has lead to interest in further fundamental studies of large scale microalgal cultures to increase productivity.

Microalgea culture is an interesting mixture of mammalian and bacteria culture characteristics. The reported doubling times, on the order of 10 hours (de Swaaf et al., 1999), while somewhat faster than most animal cells, is substantially less than bacteria

cultures. On the other hand, even though the oxygen consumption rates of heterotrophic microalgae are rarely reported, it was believed to be significantly higher than typical animal cell cultures (de Swaaf et al., 2003a; Jorjani and Ozturk, 1999). It was also believed that oxygen dependent enzymes play an important role in desaturation and elongation of PUFAs (Higashiyama et al., 1999). Therefore, high oxygen demands, obviously, require higher mass transfer.

Unlike animal cell culture, the effect of hydrodynamic forces on algal cultures is less well studied. *Dunaliella* was found to be susceptible to damage by shear stress and it was suggested that was the result of the lack of a rigid cell wall (Silva et al., 1987). Barbosa et al. (2003) studied cell damage of *Dunaliella tertiolecta* and *Chlamydomonas reinhardtii* in bubble column bioreactors. They suggested that the gas entrance velocity at the sparger, in contrast to the typically assumed bubble rupture, was the most important parameter influencing cell death. With this assumption, they determined the critical gas-entrance velocity for *D. tertiolecta* and *D. salina* in the design of the nozzle sparger (Barbosa, et al., 2004).

In contrast, bubble rupture as well as high-intensity mechanical agitation were found to be predominant reasons for cell damage of *Porphyridium cruentum* in aerated and stirred bioreactors (Camacho et al., 2000). Sobczuk et al. (2006) demonstrated the sensitivity of *P. cruentum* and *Phaeodactylum tricornutum* to the rupture of small bubbles generated by mechanical agitation as well as the protective effect of the addition of Pluronic F68. As with animal cell culture, carboxymethyl cellulose was also demonstrated to provide protection to *P. triconutum* from aeration-associate cell damage in outdoor bubble columns (Camacho et al., 2001).

However, the effect of hydrodynamic force on *C. cohnii* cells has not been systematically investigated. Most of published studies have focused on the optimization of the cultivation process. Factors studied include: effect of oxygen and temperature on lipid composition (Beach and Holz, 1973); medium optimization (Tuttle and Loeblich, 1975), strain screening (Jiang et al. 1999); and a variety of carbon source on batch and fed-batch cultivations (de Swaaf et al., 2003a; 2003b; and 2003c).

In our previous study, we have used a well-defined microfluidic channel to study the effect of transient hydrodynamic forces on *C. cohnii* cells, where the loss of flagella was observed and which can be later regenerated. In the present work, we first demonstrate that what appears to be "shear sensitivity" in shake flask cultures is in reality oxygen limitations. We then proceeded to quantify the long-term effect of hydrodynamic forces on *C. cohnii* cell cultivation using the same type of microfluidic channel as reported previously, this time operated in a recycle mode connected to a bioreactor so that the cells can be subjected to a chronic, sub-lethal level of well defined hydrodynamic force. It has been proposed that such a system can be used as a "scale-down" model to simulate larger scale vessels. *C. cohnii* cells were cultured in this bioreactor-microfluidic channel apparatus so that cells were subjected to a variety of different well-defined hydrodynamic forces, and the effects were documented.

4.3 MATERIALS AND METHODS

4.3.1 Culture Vessel

Cells were grown in a custom-made, small bioreactor with 250 ml of total volume, 150 ml working volume in which a water jacket was used to maintain temperature control.

This vessel has a diameter of 63 mm, a liquid height of 50 mm, and agitated with a plastic rod of 45 mm in diameter positioned 20 mm from the bottom and controlled magnetically. All the experiments were performed at an impeller speed of 200 rpm. The temperature was controlled at 27 ºC and dissolved oxygen was kept at 60% of air-water saturation by a control system from a Bioflo® 3000 (New Brunswick Scientific, Edison, NJ) and on-line measured by a DO probe (Mettler Toledo, Columbus, OH). The rate of aeration using an 18 gauge needle as a sparger was fixed at 200ml/min and produced bubbles between 5 and 10 mm in diameter. Specific oxygen uptake rate (sOUR) was determined by the DO change after terminating aeration. The initial pH was adjusted to 6.5, which was not controlled during cultivation since it only varied within a small range (pH 6.5~7.0) and followed the same pattern for all experiments (data no shown).

Samples were taken every 12 hours for cell counting using a hemocytometer and glucose concentration using YSI 2700 SELECT (YSI Inc., Yellow Springs, Ohio). Since the cells can be significantly motile, a 0.1% (w/v) SDS solution was added during hemocytometer counting at a ratio of 1:10 (v/v) in order to stop the movement of swimming cells. The motility was defined as the percentage of motile cells to total cells.

4.3.2 Flow Contraction Device

The flow contraction device used in this study has been previously described (Ma et al., 2004). All the objects associated with the flow contraction device that contact the cell suspension during cultivation was autoclaved at 121 ºC for 30 min. The flow contraction device was connected to the bioreactor described above by way of tubing and the fluid was removed from the bioreactor and pumped through the flow contraction

device using a syringe pump (Model 33, Harvard Apparatus, Holliston, Massachusetts). Silicone sealing was applied to prevent any possible leakage in the recycle loop. Figure 4.1 presents a diagram of the recycle system.

The circulation rate between the bioreactor and the flow contraction device was set to 10, 30, and 50 ml/min. Table 4.1 presents the corresponding EDR for each of these flow rates, as well as the mean circulation time and how much times the cells went through the flow contraction device during the whole cultivation, i.e. average passes. In addition, an "energy dissipation/circulation function" EDCF, is reported which is defined as the product of EDR and inverse mean circulation time. Control experiments were performed under the same conditions except without the presence of the flow contraction device in the recycle loop. The rheology property of broth before and after fermentation was determined by ARES Rheometer (TA Instruments, New Castle, DE).

C. Cohnii (ATCC 30772) was maintained by sub-cultivation every four days at room temperature in 250ml Erlenmeyer flasks containing 50 ml. Two-day old static cultures were used to inoculate the bioreactor. The initial filter-sterilized medium contained 20g/L glucose (Sigma, St. Louis, MO), 5g/L yeast extract (Fisher Scientific, Hampton, NH), and 12.5g/L sea salt (Sigma, St. Louis, MO) (de Swaaf, et al., 1999). The inoculation density in the bioreactor was approximately 0.5 million cells/ml.

4.3.3 Static and Shake Flask Experiment

The effect of mechanical agitation on cell growth was also investigated by comparing static culture with shaking culture environments. In these experiments, *C. cohnii* cells were grown in Erlenmeyer flask (250ml volume) with 50 ml, 100 ml, and

150 ml medium, respectively, with or without continuous orbital shaking at 100 rpm or 200 rpm. These Erlenmeyer flasks were agitated in an Environ shaker with an orbit of 2.5 cm (Lab-line Instruments, Melrose Park, IL). Since the cells were not homogeneously distributed in static flasks (discussed later), sufficient mixing was applied by hand before sampling in order to obtain average cell concentrations.

4.4 RESULTS

4.4.1 Shake Flask Studies

The initial shake flask studies can be summarized as: two volumes of culture, 100 or 150 ml, which were either left as static cultures, or mechanically shaken. Figure 4.2a presents the average cell concentration (10^6 cells/ml) and 4.2b presents the glucose concentration (g/L) for these four conditions. Visual inspections of Figures 4.2a and 4.2b give consistent results indicating that the unshaken, low culture volume culture grew the best (and consumed the most glucose), while the high culture volume, shaken culture grew the worst. The other two conditions were consistently between these two extremes. The glucose yields were 2.4 and 2.2 $\times 10^5$ cells/ g glucose for 100 ml and 150 ml static culture, respectively, while the yields were 3.1 and 2.9 $\times 10^5$ cells/ g glucose for 100 ml and 150 ml shaking culture.

4.4.2 Chronic EDR Exposure Studies

The results of the shake flask studies appear to indicate that the microalgae are sensitive to mechanical agitation. This leaded to the following studies, in which the cells were cultivated in the bioreactor with the contraction flow device so that chronic levels of

well defined EDR could subject to the culture. The circulation between the bioreactor and the flow contraction device for each experiment was initiated one hour after inoculation, and did not stop until the end of the 48 hour cultivation. Figure 4.3a presents the cell growth under different flow rate and circulation times. In order to eliminate any variability as a result of inoculation variation, the cell growth was normalized by dividing by the initial cell density. At a flow rate of 10ml/min (maximum EDR of 6.4×10^5 W/m^3) and a corresponding mean circulation time of 15 min, no significant difference relative to the control could be observed. However, as the flow rate through the contractional flow device was increased to 30 ml/min and 50 ml/min, corresponding to maximum EDR of 5.9×10^6 W/m^3 and 1.6×10^7 W/m^3, respectively, the cell growth was inhibited, with the average double time was 12.0 hours and 13.0 hours, respectively, in comparison to 10.9 hours at control. In terms of EDCF, these three flow rates correspond to 4.3×10^4, 1.2×10^6 and 5.3×10^6 (W/m^3 • min). Figure 4.3b presents the glucose concentration as a function of time for these same four experiments. Consistent with the decrease in growth rate, there was a decrease in glucose consumption rate. However, the yield of glucose to cell was quite similar for each of the four experiments, with a range of $3.9\sim4.0\times10^5$ cells/ g glucose.

While it is a well established fact that the rupture of bubbles at the gas medium interface can be damaging to cells, it was also calculated and simulated by two research groups that the rupture of large bubbles creates significantly less EDR than small bubbles. Specifically, Boulton and Blake (1993) and Garicia-Briones et al. (1994) calculated that the EDR for bubble rupture of the size in this study is on the order of 10^4- 10^5 W/m^3 for

Newtonian fluid with 1 cP viscosity if bubble. This range of values is considerably smaller than the maximum EDR generated in the flow contraction device at 30 ml/min and 50 ml/min flow rates. In addition, the rupture of similar size and number of bubbles also occurred in the control experiments and no foam was observed in the bioreactor during cultivation. While it is quite common for *C. cohnii* cultures in a fed-batch mode of operation to achieve densities on the order of 100 g/L dry biomass with a subsequent significant increase in viscosity due to extracellular polysaccharide production (de Swaaf et al. 2003a). Analysis of several samples indicated that viscosity of the broth had a minor shear thinning characteristic, with no further change in viscosity above 100 s^{-1}.

The change of specific oxygen uptake rate, sOUR, and motility as a function of time and level of EDR is presented in Figures 4.4a and 4.4b, respectively. The initial, sOURs of cells from static culture was high, approximately 1.0×10^{-7} mg O_2/cell/hour, and, subsequently dropped for all four conditions during the batch cultivation. However, the sOUR was consistently lower for the higher levels of EDR. The initial motilities at inoculation were similar (75~80%), and while fluctuating, all of the cultures ended at an equal (within experimental error), or higher percentage of motility. It should be noted that a significant number of cells subjected to the 50 ml/min flow rate were found to spin slowly in one direction, which as mentioned in the previous chapter is a sign of partial deflagellation.

4.4.3 Potential Explanation for Apparent "Shear Sensitivity"

The experiments in the bioreactor-contraction flow device indicate that *C. Cohnii* can withstand EDR that are typically created in typical animal cell bioreactors, and an effect

of EDR only begins to be observed at EDR values that have been shown to damage animal cells (Mollet et al. 2004). However, the shake flask experiments appear to contradict this observation, both in this study and reported by others (Yeung and Wong, 2003; Zirbel, 2000). Consequently, this apparent contraction was further investigated.

Closer, visual inspections of the static cultures indicated that a significant layer of *C. cohnii* cells was found at the top liquid surface. This was quantitatively demonstrated by carefully measuring the concentration of cells in the bulk of the static culture without disturbing the flask and measuring the bulk concentration immediately after a transient shaking. By slightly inclining the previously static flasks, samples were carefully taken through a gap between the cell mass on the surface and the wall of the flask. Figure 4.5 presents the undisturbed, bulk concentration and the bulk concentration after transient shaking. This sampling process was conducted during eight hours after the first transient shaking. At the eight hour time point (Figure 4.5), a six fold increase in concentration in the bulk resulted from the second transient shaking. Figure 4.6 qualitatively showed the distribution of cells in the flasks.

de Silva et al. (2006) has reported that dissolved oxygen is a critical parameter for the growth of *C. cohnii* cells. The sOUR of *C. cohnii* cells that we measured, and reported in Figure 4.4a, supports this observation. However, unique to these organisms, compared to most other cells cultured commercially, is the cells motility. Figure 4.7 clearly indicates this motility. Figure 4.7a is a photograph of an air bubble trapped between a hemocytometer and the cover slip, the bubble being surrounded by motile *C. cohnii* cells. Figure 4.7b is a photograph of the same system, 1 minute later. Clearly, a large number of cells have migrated to the air bubble.

These observations led us to perform two more shake flask experiments. For the first experiment, the culture volume was decreased to 50ml in order to have better mass transfer (Büchs, et al., 2000; Zhang, et al., 2005). Figure 4.8, presents the results of this study of a static culture and a shaken culture, both using 50 ml. No difference in growth and minor differences in glucose consumption can be observed. The motility was also monitored, and did not show significant difference except that at the end of cultivation the motility of all static cultures dropped to 50% while that in the shaken culture was maintained above 65%. Figure 4.9 shows the distribution of cell size. The decrease of working volume from 150 ml to 50 ml in shake culture can significantly decrease cell size of *C. cohnii*, potentially indicating changes in the cell cycle (Yeung and Wong, 2003).

A second experiment consisted of increasing the shaking speed from 100 rpm to 200 rpm for 50 ml media in 250ml flasks. Cell growth was significantly enhanced in the shaken culture relative to the static culture (Figure 4.10a). The maximum cell concentration in the latter is only 65% of that in the former. The increase of glucose concentration to 40g/L increased the maximum cell concentration by 28% and 33% for static and shaken culture, respectively. The glucose consumption was similar (Figure 4.9b); consequently, the glucose yield in the shaken culture was significantly higher, 4.0×10^5 cells/ g glucose vs. 2.5×10^5 cells/ g glucose.

4.5 DISCUSSIONS

It is well documented that "turbulence" has negative effects on the growth of dinoflagellate in the ocean (Pollingher and Zemel, 1981) and in laboratory devices

(Zirbel et al., 2000). It has also been reported that dinoflagellate blooms, such as red tides, have high probability to happen in calm sea environment, and it was suggested by Yeung and Wong (2003) that the lack of fluidic mechanical forces was considered as a factor. Yeung and Wong (2003) also reported the detrimental effect of mechanical shaking on *C. cohnii* cells in 125 ml Pyrex flasks with loading volume of 60 ml. By using synchronized cells, the authors found transient cell cycle arrested at G1 phase as well as the increase in cell size was induced by shaking. The cell cycle rest was reversibly demonstrated by the resume of cell cycle progression after the termination of agitation. Furthermore, Yeung et al. (2006) demonstrated that both mechanical shaking and caffeine treatment can induce elevation of cytosolic calcium along with the increase in cell size and cell cycle arrest for *C. cohnii* cells. It was suggested that mobilization or depletion of caffeine-sensitive calcium stores, rather than the activation of the spindle checkpoint, was involved in the induction of cell cycle arrest by mechanical stimulation.

However, despite these reports, one must be careful in initially interpreting data. The first set of shake flask studies could have been incorrectly interpreted to imply that *C cohnii* is highly susceptible to hydrodynamic forces. However, as was demonstrated by the second set of shake flask experiments, and the studies in the bioreactor-contractional flow recycle system, *C. cohnii*, while susceptible to hydrodynamic damage, the level at which damage is observed is comparable to typical animal cells subjected to chronic levels of EDR, 6×10^6 W/m^3 (Chalmers et al., 2006).

In addition, Jüsten et al. (1998) found that the mean projected area of *Penicillium chrysogenum* and specific penicillin production rate had a negative correlation with

EDCF above 4.2×10^5 (W/m^3 • min), where the specific EDR in the impeller swept volume and the circulation frequency through that volume was concerned.

4.6 CONCLUSIONS

The results of this study indicates that while chronic exposure of *C. cohnii* to EDR of a level of 6 x 10^6 W/m^3 can result in a inhibition of cell growth, this level of EDR is high enough such that *C. cohnii* can withstand typical shake flask and bioreactor conditions. However, the inhibition of cell growth at levels of 6 x 10^6 W/m^3 and higher does indicate that care should be taken in the culture of these organisms. These levels, while high, can be attained at high levels of rpm in bioreactors as well as the EDR created by the rupture of small bubbles (Mollet et al. 2004).

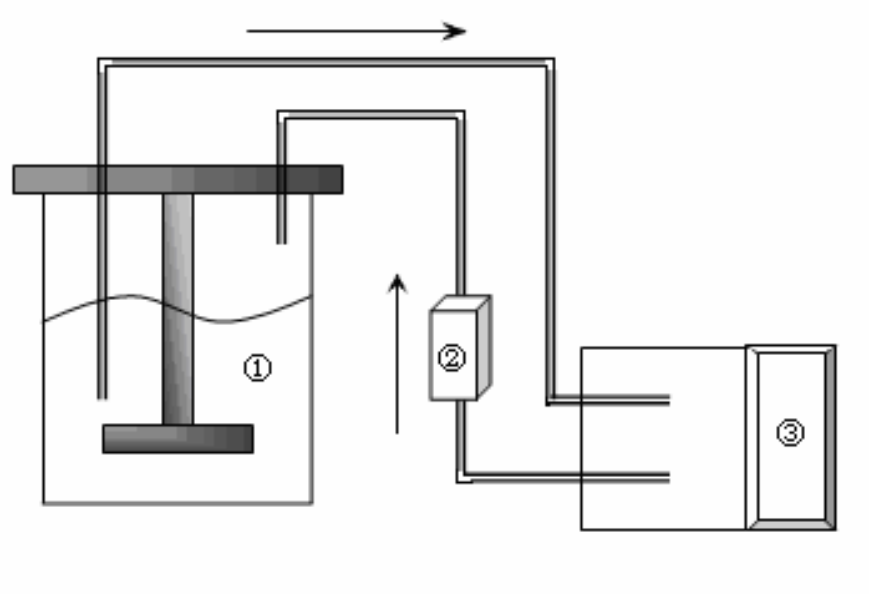

Figure 4.1. Schematic diagram of the scale-down model for hydrodynamic forces; (1) bioreactor; (2) flow contraction device; (3) continuous syringe pump system; Arrows indicate the direction of fluid flow

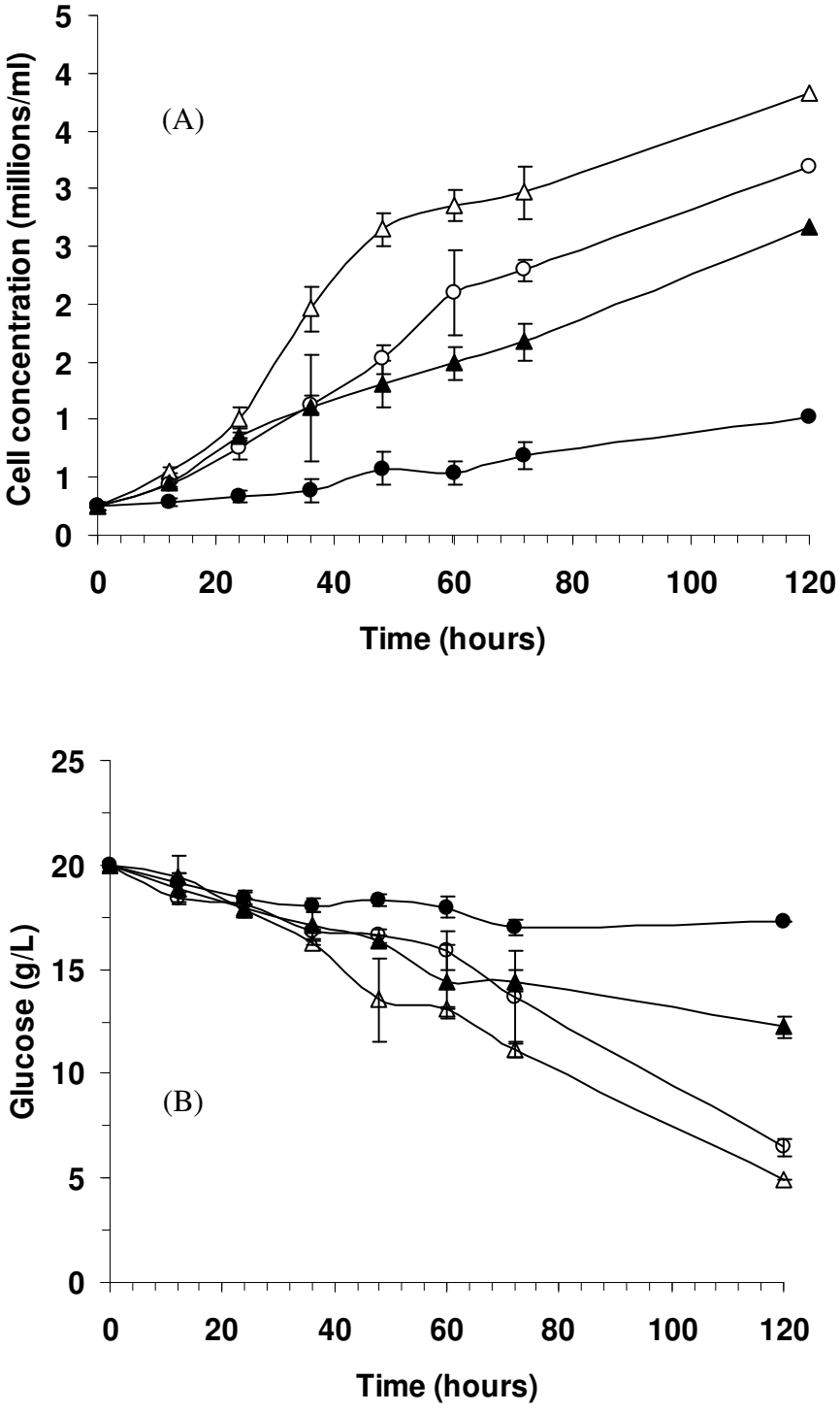

Figure 4.2. The comparison of cell growth (A) and glucose concentration (B) in static culture (open symbols) and shake culture at 100 rpm (filled symbols) with the loading volume of 100 ml (triangle symbols) and 150 ml (circle symbols) in 250 ml Erlenmeyer flasks

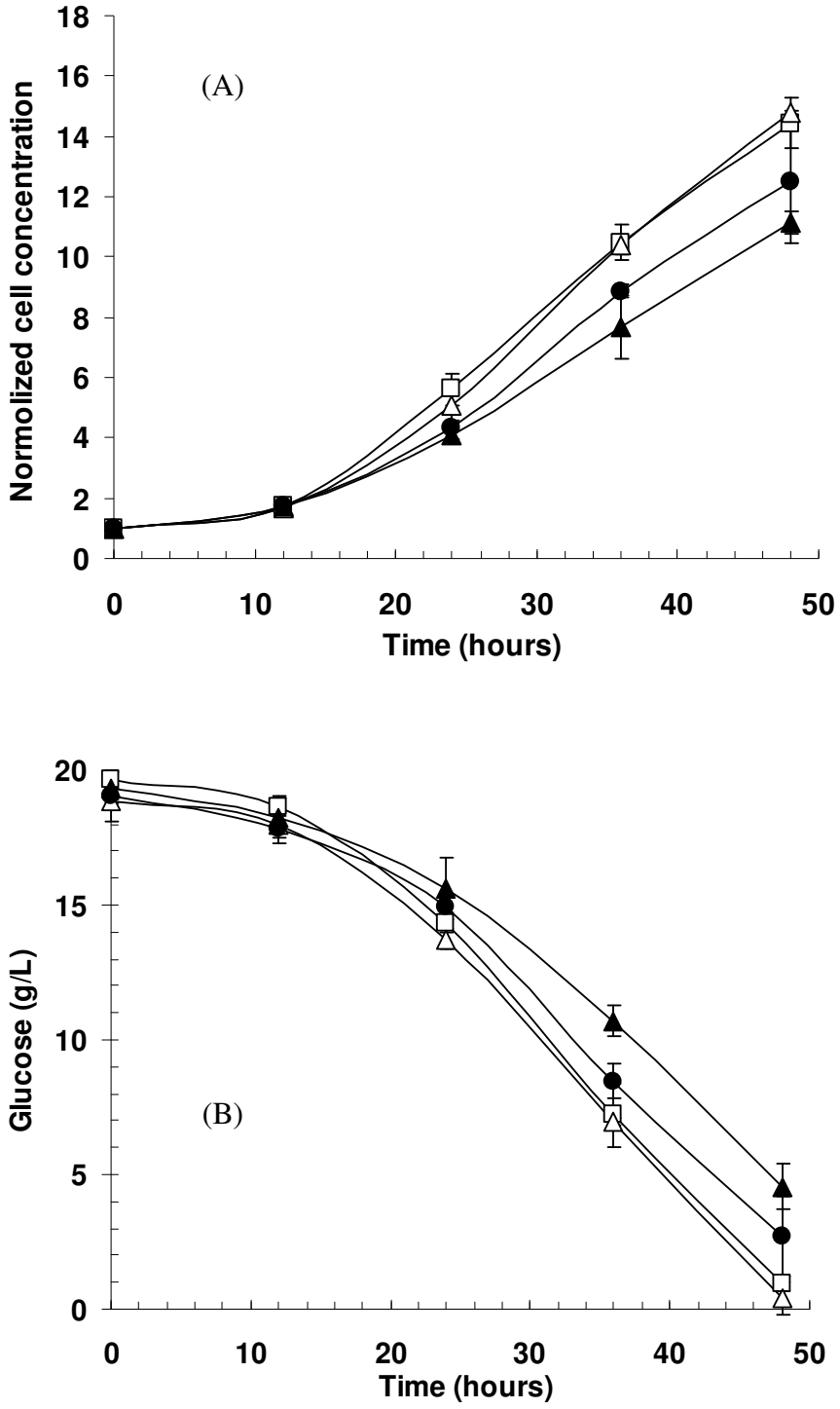

Figure 4.3. Cell growth (A) and glucose consumption (B) under different flow rate; (□) control; (△) 10 ml/min; (■) 30 ml/min; (▲) 50 ml/min

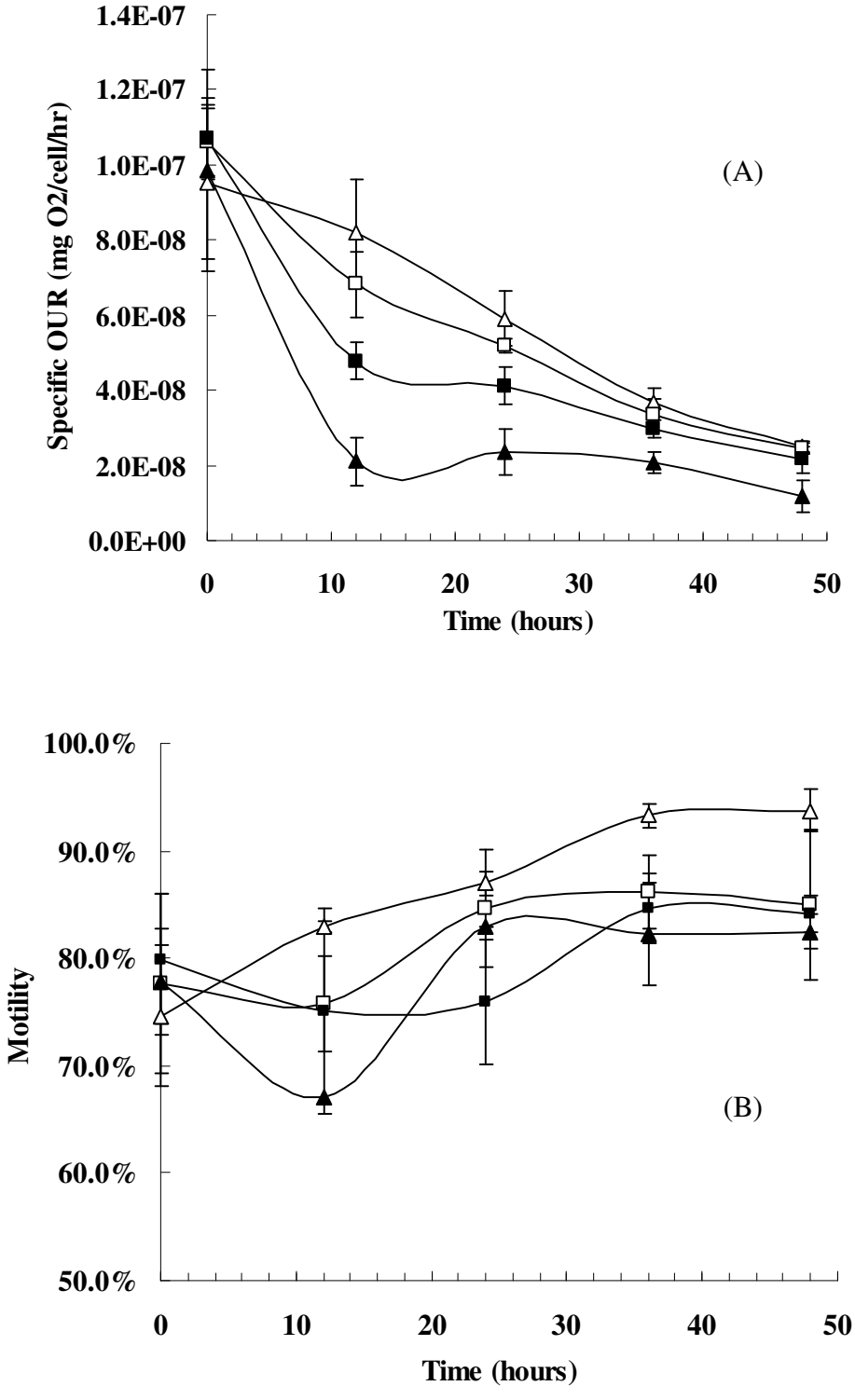

Figure 4.4. The change of specific OUR (A) and motility (B) under different flow rate; (□) control; (△) 10 ml/min; (■) 30 ml/min; (▲) 50 ml/min

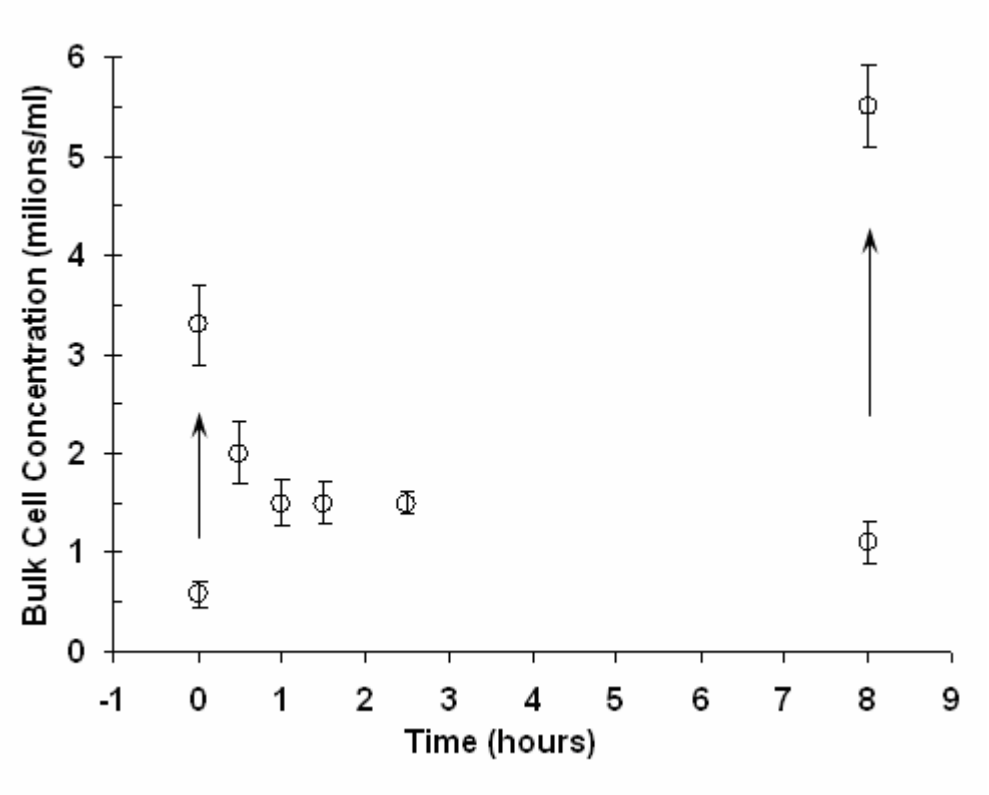

Figure 4.5. The change of bulk cell concentration in static culture resulted from transient shaking (indicated by arrows)

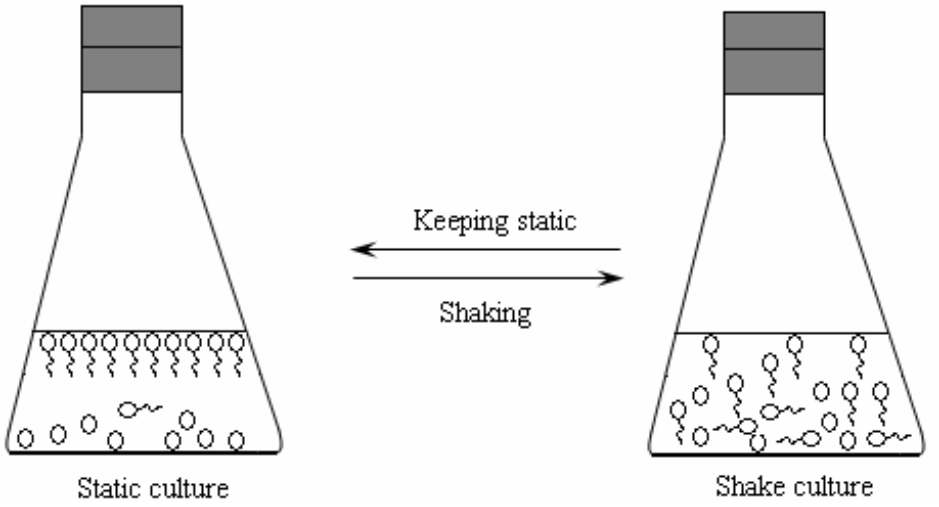

Figure 4.6. Illustration of cell distribution at static culture (left) and shake culture (right)

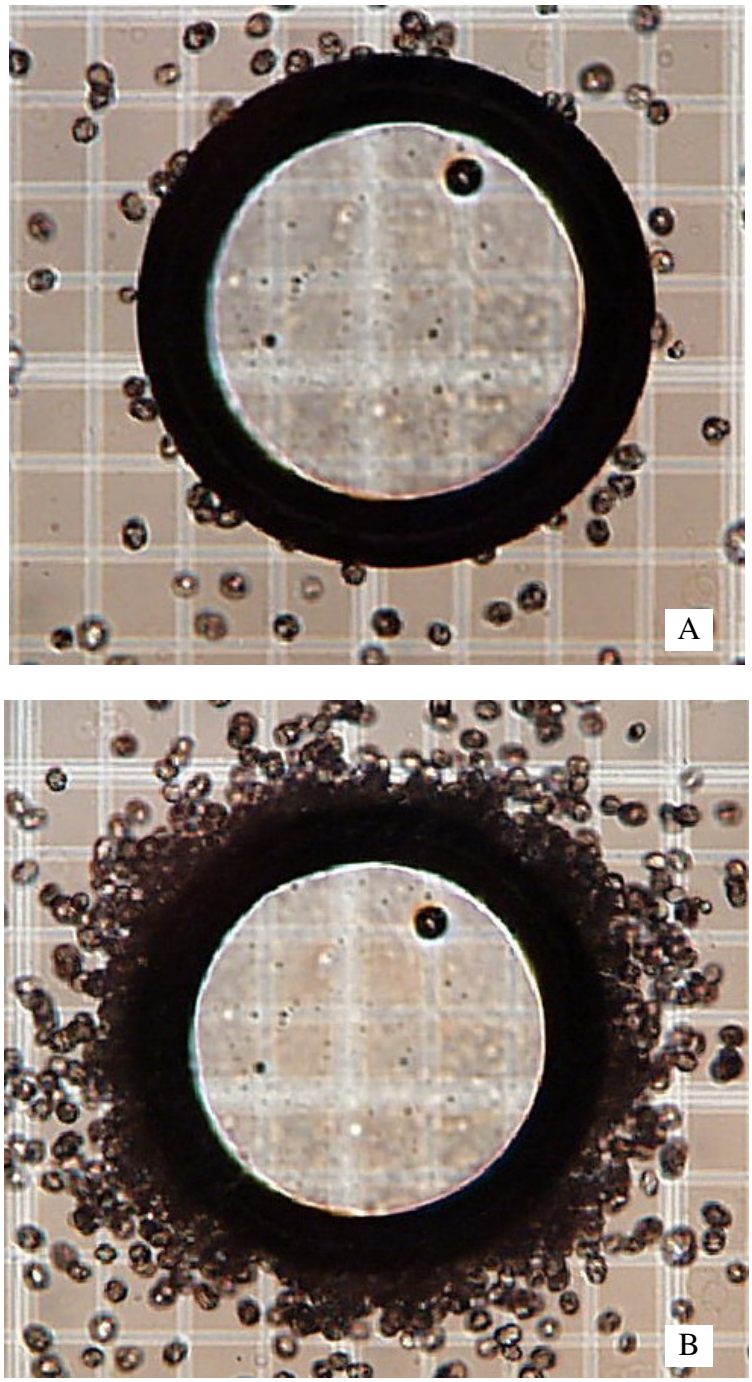

Figure 4.7. Microscopical pictures of a bubble in a hemocytometer before (A) and after (B) *C. cohnii* cell accumulation at the surface

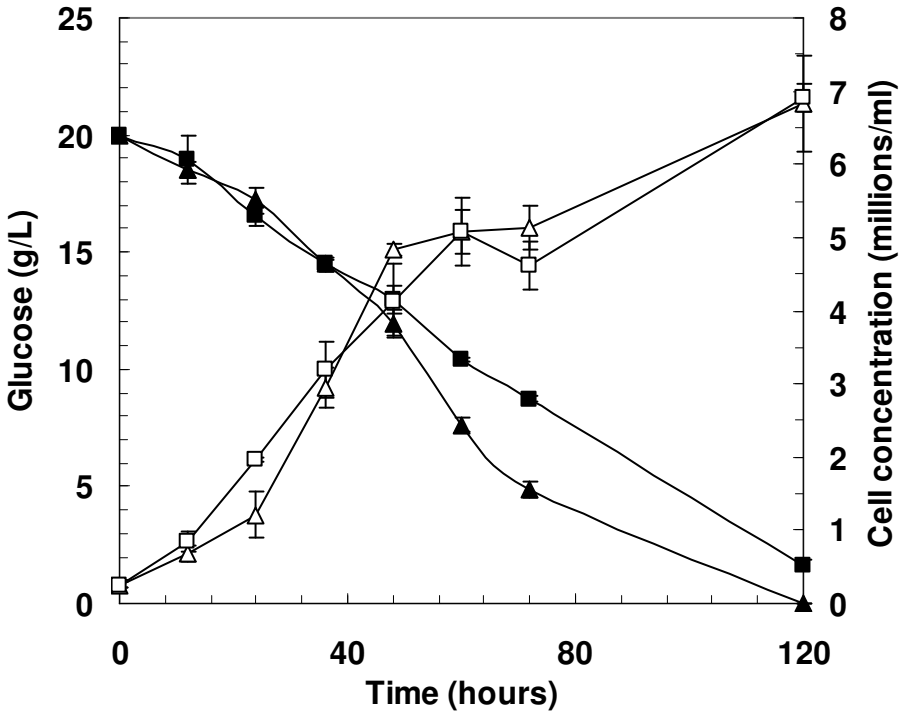

Figure 4.8. Cell growth (open symbols) and glucose consumption (filled symbols) in static culture (triangle symbols) and shake culture (rectangle symbols) at 100 rpm with 50 ml loading volume in 250 Erlenmeyer flasks

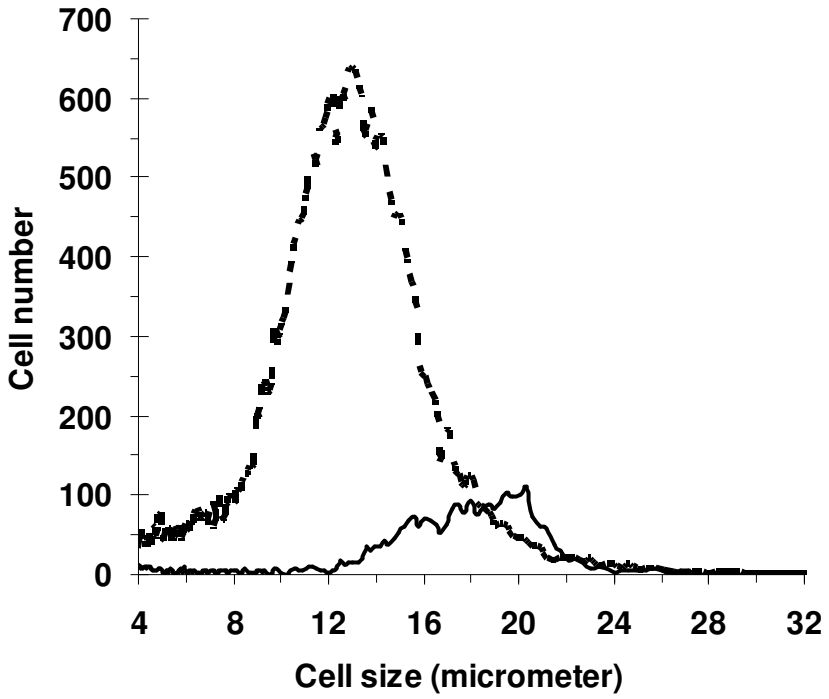

Figure 4.9. The distribution of *C. cohnii* cell size in 250 ml Erlenmeyer flasks shaken at 100 rpm with the loading volume of 50 ml (---) or 150 ml (—)

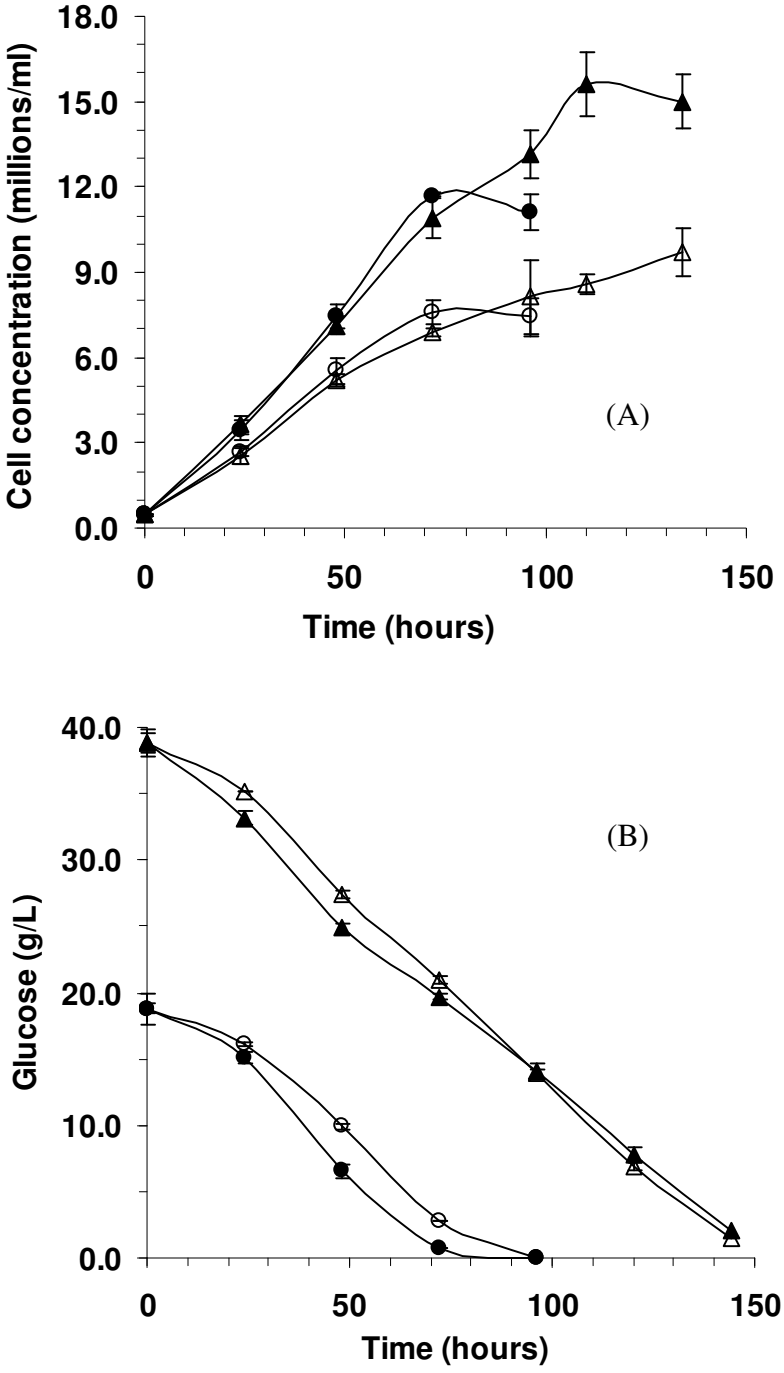

Figure 4.10. Cell growth (A) and glucose consumption (B) in static culture (open symbols) and shake culture at 200 rpm (filled symbols) with 20 g/L glucose (circle symbols) or 40 g/L glucose (triangle symbols)

Flow rate (ml/min)	10	30	50
Mean circulation time (min)	15	5	3
Average passes	192	576	960
Maximum EDR (W/m^3)	6.4×10^5	5.9×10^6	1.6×10^7
EDCF ($W/m^3 \cdot min$)	4.3×10^4	1.2×10^6	5.3×10^6

Table 4.1 Hydrodynamic conditions under different flow rates in the scale-down model

CHAPTER FIVE

MASS SCREENING SURFACTANT ADDITIVES FOR MAMMALIAN CELL CULTURE

The content of this chapter has been prepared for publication: Hu W, Rathman, JF, Chalmers JJ, An investigation of small molecule surfactants for alleviating bubble-associated cell damage

5.1 SUMMARY

It is well known that bubble rupture has a detrimental effect on mammalian cells. As a result, Pluronic F-68 (PF-68), a nonionic surfactant, is commonly used to alleviate bubble-associated cell damage in sparged bioreactors. While Pluronic F-68 is currently effective, there is a concern with respect to its decrease in effectiveness as cell concentrations increase. Given the empirical nature in which Pluronic F-68 was initially discovered as cell culture additive, a structure-performance study of small molecule surfactants, a distinct group from previously investigated additives, was performed to attempt to find a replacement for PF-68. In this study, a generic platform was established to evaluate various surfactants based on their cytotoxicity and dynamic surface tension behavior. Subsequently, their protective effect was compared with PF-68 in a term of

preventing cell-bubble attachment. Finally, some promising small-molecule surfactants and their concentration, such as 1.0 g/L nonyl-maltopyranoside (NM), was identified, which can alleviate cell-bubble attachment efficiently without being harmful to cells.

5.2 INTRODUCTION

Mammalian cell culture has emerged as an indispensable technology for the production of recombinant therapeutic proteins requiring post-translational modifications. The high demand of more than 100 kg per year for some of these proteins, such as monoclonal antibodies, inevitably leads to the requirement of more efficient manufacture processes, particularly high productivity and high cell density. However, mammalian cells are sensitive to the surrounding environment, including the concentration of ammonia, lactate (Ryll et al., 1994; Zhou et al., 1995), dissolved carbon dioxide and osmolality (deZengotita et al., 2002; Zhu et al., 2005), and pH (Osman et al., 2001). By considering these factors, as well as a number of other specific cellular needs, industrial fed-batch or perfusion cell culture processes have been able to increase product titers, from typically around 50 mg/L to over 5 g/L over a two decade period (Ozturk, 2006).

Along with a better understanding of cell metabolism from a biological perspective, significant effort have been made to explore physical challenges in mammalian cell culture, including mixing, mass transfer, and cellular sensitivity to hydrodynamic forces (Ozturk, 1996; Nienow, 2006). While a number of designs have been proposed for large scale culture, the stirred tank bioreactor with sparger aeration is the commercial system of choice. Such a system, while simpler to implement and

operate than other more complex systems, creates gas-liquid-solid multiphase environments within the vessel containing various interfaces.

The presence of surface-active compounds, including surfactants and proteins, makes these interfaces highly complex; however, these interfaces are fundamental to gas-liquid mass transfer (O_2 supplement and CO_2 removal), cell-to-bubble adhesion, foam formation, and protein/lipid adhesion to gas/solid surfaces. Unfortunately, our current understanding of interfacial phenomena in cell culture processes are predominately based on empirical studies since fundamental understandings is severely limited. A number of these empirical studies are investigated or summarized separately by Ma and Hsu (1997); Fazilet (1998); Langheinrich et al. (2002); and Wu (1995).

A number of additives have been examined for their protective effect on bubble-associated cell damage, such as fetal bovine serum (Kunas and Papoutasakis, 1989), Pluronic® (Murhammer and Goochee, 1990); methyl cellulose (Goldblum et al., 1990), Dextran (van der Pol et al., 1995), polyethylene glycol (Michaels and Papoutsakis, 1991) and polyvinyl alcohol (Michaels et al., 1992). Among them, Pluronic F-68 (PF-68), first advocated in the 1960s is still the most commonly used additive (Swim and Parker, 1960; Runyan and Geyer, 1963; Kilburn and Webb, 1968). There is no doubt that PF-68 contributes significantly to the success of industrial mammalian cell culture in bioreactors.

PF-68 is a nonionic surfactant with triblock structure consisting of hydrophobic poly(propylene oxide) center and two hydrophilic poly(ethylene oxide) tails, which does not have distinct critical micelle concentration (CMC). It has an average molecular weight of 8400. Even though a number of protective mechanisms of PF-68 have been proposed (Chisti, 2000; Wu, 1995), the ability of PF-68 to inhibit cell-bubble attachment

is considered the primary mechanism. Chattopadhyay et al. (1995b) suggested that this inhibition is the result of the PF-68 significantly decreasing the surface tension of the gas-liquid interface such that adhesion to the gas-liquid interface is thermodynamically unfavorable. Recently, Ma et al. (2004) quantitatively studied the interactions among cells, bubbles, and PF-68 over a broad range of PF-68 and PER.C6® cell concentrations. As previously reported the cell concentration in the foam liquid decreased dramatically with the increase of PF-68 concentration; however, as the cell concentration increased (on the order of 10^7 cells/ml, or higher) even at high PF-68 concentration of greater than 1 g/L, over 1000 PER.C6® per bubble become trapped in the foam layer.

In addition to their intended function at a gas-liquid interface, surfactant additives can have a significant effect on the cell membrane. The mammalian cell membrane is a thermodynamically-controlled and self-assembled bilayer consisting of phospholipids, triglycerides, cholesterol, and trans-membrane proteins. The membrane structure is dynamic with the lateral diffusion and flip-flop of lipid components. Surfactant additives can efficiently compete with the interactions within membrane lipids and proteins. Therefore, the most important criterion is that surfactant additives should not be harmful to mammalian cells. However, a significant number of surfactants have lytic effects on mammalian cells, many of which are intentionally used to extract membrane or intercellular compounds. Two mechanisms are proposed to explain the solubilization of cell membranes by surfactants, flip-flop or micellar attack (Maire et al., 2000). In the former, non-micellar surfactants penetrate the membrane and cause damage. In the latter, membrane compounds are transferred directly from outer side of membrane bilayer into surfactant micelles.

In spite of the importance of surfactants to protect, and alternatively, solubolize mammalian cells, the selection of surfactants, both with respect to type and concentration is still a "hit or miss" process. As the final cell concentration of commercial mammalian cell culture systems continue to increase, it is apparent that the effectiveness of PF-68 will diminish. While it can be argued that one can tolerate some loss of productivity of a relatively small number of cells in the foam, the lysis of this small number with the subsequent release of the intracellular components into the media is unwelcomed occurrence. In addition, it is highly desirable to have other, effective, alternatives than PF-68.

In this study, we present a systematic method to screen small molecule surfactants for cell culture purposes. First, a generic platform using 96-well plate and florescence dye was established to quickly assess the cytotoxicity of surfactant additives which allows general principles of surfactant structure and performance to be investigated. Secondly, the surface activity of promising candidates that has no negative effect on cells was determined, especially dynamic surface tension. Finally, an improved bubble collector was used to evaluate their protective effect in terms of alleviating cell-bubble attachment, and subsequent retention in a foam layer.

5.3 MATERIALS AND METHODS

5.3.1 Cytotoxicity Study

Chinese Hamster Ovary cells (CHO) cell line K1 (ATCC CCL-61) were used. The cells were initially cultured in Ham F-12 culture medium supplemented with 10% v/v fetal bovine serum (Sigma Aldrich Co., St. Louis, MO) in T-75 flasks. Then the cells

were gradually adapted to chemically-defined medium (CD CHO-A, Invitrogen, Carlsbad, CA), which contain no PF-68. The cells were subcultured every 3-4 days and maintained at 37°C incubator with 5% CO_2. All the cultures were anchorage-dependent.

A mass screening experiment was performed in order to quickly eliminate surfactants with high cytotoxicity. The surfactant additives used in the screening were listed at Table 1. SOS, SDeS, SDS, DDeAO, DDAO, DTAB, DDAO DTAB, CTAB, and PF-68 were purchased from Sigma Aldrich Company (St. Louis, MO). OG, OM, OT, DG, and DM were purchased from Anatace Inc. (Maumee, OH). Surfactants were experimentally compared at the same concentration relative to the specific surfactants critical micelle concentration, CMC, i.e. 0.01CMC or 0.1CMC. In order to minimize the effect of potential adsorption during filter sterilization, the concentrated surfactant solutions were applied, and then diluted to desired concentration later. The surface tensions before and after filtration did not show significant difference (data not shown).

Black clear-bottom 96-well plates (Fisher Scientific, Hampton, NH) were used in screening experiments. In each well, 150 µl cell suspensions with a total cell number of approximately 10^4 were inoculated along with surfactant additives and subsequently cultured at 37°C incubator with 5% CO_2. After 48 hours, the supernatant was carefully removed while the attached CHO cells remained at the bottom of the well. 100 µl of 4 µM calcein AM solution (Invitrogen, Carlsbad, CA), a fluorescence probe, was added to each well and incubated for one hour at 37°C in order to quickly assess cell growth (Yang et al., 2002). Calcein AM is an esterase substrate which can be converted into a polar, fluorescent product by intracellular enzymes, and which remains within the cells after enzyme treatment. The fluorescence density was read by Cytofluor 4000 (Applied

Biosystems, Foster City, CA). There were six replications for each condition (type of surfactant and concentration) and the positions on the 96 well plates were randomized.

Promising candidates were further investigated using T25 flasks. The concentration of surfactants was gradually increased beyond 0.1CMC until it reached a level which caused the inhibition of cell growth. Additional surfactants, nonyl-maltopyroniside (NM) and CYMAL®-4 (CM4), were purchased from Anatace Inc. (Maumee, OH). The inoculation was 3.0×10^5 cells/ml. After 48 hours, the cells were harvested by Accutase® (Innovative Cell Technologies Inc., San Diego, CA) and counted by a hemocytometer. Besides cell growth, the morphology of cells was also monitored by an inverted microscope (Nikon Ecllipse TE2000-U, Melville, NY).

5.3.2 Surface Tension Measurements

It is known that CMC depends on temperature and solution components. Therefore, the CMC of applied surfactants was determined at 37°C and in CD CHO-A medium using a SensaDyne bubble tensiometer PC500L (Chem-Dyne Research Corporation, Mesa, AZ), which uses the maximum bubble pressure method. The time between initial bubble formation and attainment of maximum bubble pressure, "surface age", can be varied by changing the gas flow rate. When the static surface tensions were measured, the surface age were adjusted to approximate 1 s, which was enough for small molecule surfactants to migrate to bubble surface and reach the equilibrium. The hydrodynamic headgroup areas of surfactants were calculated from the Gibb's surface excess. When the dynamic surface tensions were measured, the surface age was varied in the range of 0.1~3.0 s.

5.3.3 Bubble-Cell Interactions

An improved bubble collector device described at Ma et al. (2004) was used to quantitatively study cell entrapment in the foam. Specifically, this device can isolate bubble rupture events from foam formation as well as maintain a plug-flow of bubbles in the foam layer. The foam liquid only sustains a bubble rupture at the end of exit tube was collected and cell concentration determination by a lactate dehydrogenase (LDH) assay (CytoTox 96, Promega, Madision, WI). 9% (w/v) Triton X-100 solution was added into collected liquid with a ratio of 1 to 10, and subsequently inoculated at 37°C for 45 minutes in order to lyse all the cells. A standard curve between LDH absorption and cell concentration by hemocytometer measurement was made for each set of experiments. The foam liquid volume was also measured by weighing the collect tube before and after experiments, assuming a liquid density of 1.0 g/ml.

The CHO K1 cells, grown in CD-CHO medium, used in the bubble collector studies were harvested during exponential phase of growth in spinner flasks. Multiple cycles of centrifugation and re-suspension in PBS were performed in order to remove PF-68 originally presented in the medium. Finally, the cells were re-suspended in PBS solution with desired surfactant concentration and loaded into the bubble collector. The initial cell concentration was approximately 0.8×10^6 cells/ml with a high viability (>95%). A 1.0 ml foam layer was built up before bubbles coming out the exit tube and collected into the 15 ml centrifuge tubes. The gas flow rate was controlled at 2.5 ml/min by an automatic syringe pump (PHD 2000, Harvard Apparatus, Holliston, MA). No cell sedimentation was observed. Two spargers, a 22 gauge needle and a sintered glass (ACE

glass, Vineland, NJ) provided bubbles. It resulted in different bubble sizes, which was determined by a SCIMAX CCD digital camera (MVIA, Monaca, PA) with infinity lens (ISCO Precision Optics GMBH, Germany) in a glass square column. The cell enrichment factor can be defined as the ratio of total LDH concentration in the foam liquid to that in the bulk liquid after lysing all the cells.

5. 4 RESULTS

5.4.1 Effect of surfactants on cell growth

A total of twelve surfactants were investigated in screening experiments including sodium alkylsulfate, amino oxide, quats, and alkylglycosides. For the same hydrophilic head group, the surfactants with two or three different alkyl lengths were compared, which varied from 8 to 16. The molecule weight of surfactants was in the range of 200 to 500. CMC was in the range of 1-100 mM, which increased with the decrease of alkyl chain length as expected (Table 5.1). The salt components in medium resulted in the decrease of the CMC of ionic surfactants in comparison to water system. However, it did not affect the CMC of nonionic surfactants significantly, which were consistent with published data (Söderlind et al., 2003; Söderlind and Karlsson, 2006).

A reasonable linear relationship between cell number (less than 5×10^5 per well) and fluorescence density was confirmed before screening experiments; however, a control was created with each specific experiment. Figures 5.1 and 5.2 present the screening results of surfactants at 0.01CMC and 0.1 CMC, respectively. A number of observations can be made by comparing these two Figures. First, CTAB and DTAB are clearly the most toxic to cells. Microscopic observations confirm that these two

surfactants, at this concentration completely lysised the cells. Second, a commonly assumed strong detergent, SDS, had no effect on the cells at this concentration. Third, as the concentration approaches the CMC, all but two, DM and OM, become toxic. Fourth, both DM and OM share the same hydrophilic head group, maltose (Figure 5.3), while OG and DG, which have a glucose head group, and which are toxic at the higher concentration, share the same alkyl chain length as OM and DM, respectively. Clearly, the glucose head is more toxic than the maltose head group.

Figure 5.4 presents the surface tension of DG, OG, DM, OM, and NM as function of concentration in cell culture medium at 37°C. These five surfactants chosen for this further study because of toxicity study results presented previously. Both of the surfactants with glucose head groups lowered the surface tension the most, and to the same level, while the maltose head group surfactants lowered the surface tension to the same level, but not as low as the glucose head groups. Also, interesetingly, for both family of head groups, the surfactants with the longer chain lengths lowered the surface tension at a lower concentration of surfactant. It is speculated that the ultimate lowering of the surface tension is a function of hydrodynamic head group size (Table 5.2).

Therefore, all three maltopyranosides (OM, NM, and DM) were considered as promising candidates and tested further using T-25 flasks. Figure 5.5 presents the results of these studies which, effectively, demonstrated no toxic effects until concentration of 3.5, 1.0, and 0.28 g/L were reached for OM, NM, and DM, respectively. Beyond these concentration, cell growth was inhibited; yet high cell viability (>90%) was still maintained. Note that this trend of concentration is consistent with the increasing need of surfactant to achieve a given lowering of surface tension (Figure 5.4). It was found that

PF-68 also had a negative effect on cell growth at 2g/L and 3g/L, which was consistent with the results of Honda-Corrigan et al. (1997). The cell morphology was monitored during the cultivation, which did not show significant differences.

5.4.2 Dynamic Surface Tension

As presented previously, one of the suggested mechanisms of protection of surfactants, such as PF-68, is to lower the gas-liquid interfacial tension. However, such lowering is not an instantaneously process. A freshly formed bubble has a surface tension very close to that of culture medium without surfactants. The lowering by the surfactant molecules requires the diffusion, and subsequent adsorption of the surfactant to the gas-liquid interface. Depending on the type and concentration of surfactants, this time frame of can vary from milliseconds to days. The resident time of bubbles in bioreactor is normally in the range of seconds. Therefore, the second criterion for protective surfactants is reducing the surface tension rapidly (Chattopadhyay et al., 1995a; Dey and Emery, 1999).

Figure 5.6 presents the dynamic surface tension of the maltopyronosides discussed above and PF-68. As previously reported (Chattopadhyay et al., 1995a; Dey and Emery, 1999) 1.0 g/L PF-68 can rapidly decrease surface tension from 72 dyn/cm to around 55 dyn/cm within 0.1 second, followed by a slow decrease to the equilibrium surface tension reported by Chattopadhyay et al. (1995b) to be 45 dyn/cm, as determined by the Wilhelmy plate method. In contrast, both the OM and NM rapidly (less than 0.1 s) lowered the surface tension with very little change after the initial drop. It took approximately 0.5 second for 0.28 g/L DM to lower surface tension to reach equilibrium.

Figure 5.7 shows the effect of surfactant concentration on dynamic surface tension. The decrease of NM concentration from 1.0 g/L to 0.6 g/L resulted in a slow decrease of dynamic surface tension. Tetradecyl-maltopyranoside (TDM) has been used to enhance bioavailability of peptide drug in nasal distraction, which has no negative effect on cells even above its CMC (0.01g/L) (Arnold, 2004; Söderlind and Karlsson, 2006). The equilibrium surface tension of TDM above CMC was around 35 dyn/cm (Ericsson et al., 1995). At the first glance, this surfactant could be very promising in cell culture area. However, it was found that 0.01 g/L TDM can not lower the surface tension rapidly, which only achieved a surface tension of 67 dyn/cm after 2 seconds.

It has shown that high concentration benefits surfactants adsorption to interface. However, applicable concentration in mammalian cell culture is limited by cytotoxicity, which is determined by their structures. For example, CYLMAL®-4 has a similar molecular formula as DM but a different cyclic structure of hydrophobic tail in stead of straight alkyl chain, which resulted in an increase of CMC from 1.0mM to 4.0mM and head group size from 42 $Å^2$ to 57 $Å^2$ (Figure 5.8a). As expected, CYLMAL®-4 has no negative effect on cell growth as well as cell morphology within 1.5 g/L. Figure 5.8b shows that 1.5 g/L CYLMAL®-4 can lower the surface tension more quickly than 0.28 g/L DM.

5.4.3 Cell-Bubble Interactions.

In stead of trying to capture the image of rising bubbles, static bubbles at the bottom of foam layer were analyzed. It was a convenient and reliable way to measure

bubble size even though it may slightly differ from that of rising bubble. Table 5.3 presents the diameter of bubbles generated using a stintered glass sparger and a 22 guage needle and two different concentrations of PF-68 and NM. Table 5.3 presents the results of this study and, as can be observed, for a given sparger type, the only effect of surfactants was the change in PF-68 concentration from 0.03 g/L to 1.0 g/L.

Figure 5.9 presents the results of studies measuring the cell enrichment in the foam as a function of the two different spargers and different types and concentration of surfactants. Consistent with conventional understanding (Ma et al. 2004), a significant decrease in cell-bubble interactions (measured in this case by a decrease in the enrichment factor) is observed when the concentration of PF-68 is increased from 0.03 to 1.0 g/L. A second observation is that 0.6 g/L NM can achieve the similar effect as 1.0 g/L PF-68 and increasing NM to 1.0 g/L slightly decreases the enrichments factor. The effect of 0.28 g/L DM on the decrease of the enrichment factor was less than PF-68 and NM. A third observation that the effect of all of the surfactants on the enrichment factor was less for microbubbles than large bubbles.

Finally, the potential of a surfactant to create a foam layer was compared for PF-68, DM, and NM surfactants. Specifically, a parameter, called the foam liquid, which was the ratio of liquid volume collected in the centrifuge tube to the air pumped into the column (measured in standard cubic centimeter, sccm) was measured as a function of different surfactant concentrations. The results of this study are presented in Figure 5.10. Interestingly, very little difference in the parameter foam liquid was observed between surfactants, but a uniform, significant difference was observed between large bubbles and microbubbles.

5.5 DISCUSSION

Despite there importance to commercial, and research focused, cell culture, few systematic studies of surfactant additives in mammalian cell culture have been conducted, and the most relevant studies were conducted more than one decade previous to this study. (Wu et al., 1995). Murhammer and Goochee (1990) investigated the relationship between molecular structures of polyglycol polymers and their protective effects. They found that Pluronic and reverse Pluronic polyols with tri-block structure had protective effects if their hydrophilic-lipophilic balance (HLB) was larger than 18. However, this principle was not applicable for Plurafacs with di-block structure.

In this study, a generic platform for screening surfactants was established based on the surfactant cytotoxicity. Small molecule surfactants were only considered because 1) Most of investigated surfactants were large molecules (i.e. greater than 1000 molecular weight), 2) small molecules have a potential advantage in downstream purification, which can be easily separated by dialysis. PF-68 may induce the precipitation of concentrated recombinant proteins (van der Pol and Tramper, 1998).

In our screening experiments, maltopyranoside, a group of non-ionic surfactants consisting of a maltose moiety linked with cyclic or straight alkyl chains, showed the least cytotoxicity to CHO cells adapted to serum-free medium. It is a non-crystalline material with high water solubility and which is used in cosmetic products and as food emulsifiers (Claesson and Kjellin, 2002). It was also interesting to find that maltopyranoside, which is readily biodegradable, get more attention recently for solubilization of hydrophobic compounds in parenteral formulation.

In studies related to this current one, Söderlind et al. (2003) investigated the potential haemolytic activities of glucopyranoside and maltopyranoside with alkyl chains ranging from C_8 to $C_{12.}$ OM has shown less toxicity to red blood cells than OG. In addition, Söderlind and Karlsson (2006) reported that OM and DM did not induce haemolysis until 0.2~0.3 CMC, which is consistent with the result reported in this study. In these studies it was also suggested that ionic surfactants were more toxic than nonionic surfactants. It was hypothesized that the electrostatic interaction between head group of the ionic surfactants and zwitterionic hydrophilic moiety of membrane lipid contributes to their cytotoxicity. In addition, CMC values of ionic surfactants, a critical parameter regarding to their surface behaviors, changes dramatically with salt concentration in the suspending fluid.

In this study, all small molecule surfactants have negative effects on cells at concentration blow their CMCs, the penetration of surfactants into plasma membrane is a critical factor, which increases significantly with increasing of alkyl chain length (de la Maza et al., 1998). Larger and more flexible head group can alleviate the penetration, such as maltose vs. glucose. On the other hand, PF-68 will form an "inverted U" at interface with two tails extended toward hydrophilic bulk due to its unique structure. It has a very flexible hydrophobic head with a size around 140 $Å^2$ (Yang et al., 2001). Nigam (2006) verified that the penetration of PF-68 into a lipid monolayer at similar surface pressures of cell membrane was not significant, while that of SDS was noticeable.

Besides that, the degree of penetration also depends on the membrane components. Under the same surface pressure, the incorporation of surfactants into Dipalmitoyl-*sn*-glycero-3-phosphtidylcholine (DPPC; 16:0, 16:0) and palmitoyloleoyl-*sn*-glycero-3-

phosphtidylcholine (POPC; 16:0, 18:1c9), tow major membrane phospholipids, were different (Nigam, 2006). In addition, the presence of cholesterol can reduce the extent of penetration (Nigam, 2006). Therefore, the cytotoxicty of surfactants to cells could be changed if the cell membrane components were different. It may explain why 0.01 CMC OM and DM were found to be toxic to the cells isolated from cultures with 10% serum (data not shown). In addition, the cells cultured with high surfactant concentration than critical values maintained high viability larger than 90% even the cell growth was inhibited as in Figure 5.5. It implied that some cells can survive and grow. All of these can help us turn around perceived concept that small molecule surfactants were toxic to mammalian cells, especially for selected, robust industrial cell lines.

The importance of dynamic surface tension has been emphasized by Chattopadhyay et al. (1995a). The authors found that 0.1% (w/v) PVA, 0.1% (w/v) PEG 4000, and 5.0% (w/v) Dextran can not prevent cell adhesion to bubble surface even though they had equilibrium static surface tension at 45~50 dyn/cm. However, the dynamic surface tension was as high as 66-72 dyn/cm. Jordon et al. (1994) also demonstrated that bubble partially covered by surfactants still adsorbed the cells. The process of surfactant adsorption to new surface can be divided into following steps: 1) diffusion to sub-surface; 2) adsorption from sub-surface to the surface; 3) reorientation of surfactants at the surface. Diffusion controlled and the mixed kinetic-diffusion models have been proposed. In the former, the diffusion process is only rate-controlling step. In the later, surfactants have to overcome any potential energy barrier or correct orientation to strike “empty sites” in the interface after diffuse to sub-surface (Eastoe and Dalton, 2000). The adsorption process of sugar surfactants can be described by the first model,

while that of PF-68 fits the second model. Due to its flexible structure and large molecular weight, the migration of PF-68 from sub-surface to surface is difficult, especially for pre-occupied surface, corresponding to a slow decrease in surface tension in Figure 6. Base on both mechanisms, the concentration of surfactants should be sufficiently high in order to lower the surface tension rapidly. However, the highest applicable concentration of certain surfactant was limited by the cytotoxicity, which can be changed by modifying its hydrophobic moiety, such as CM4 vs. DM.

Subsequently, this study verified that the surfactants, which can reduce the surface tension rapidly and sufficiently, alleviated cell-bubble attachment and used as protective additives in cell culture medium. Regarding to different bubble size, Meier et al. (1999) reported that the cell-bubble attachment played an important role in cell damage in microbubble case, even with the presence of PF-68. It resulted from the larger resident time of microbubble in bioreactor than induction time of PF-68 proposed at Michael et al. (1995). Consistently, this study also demonstrated high cell enrichment in the liquid of foam layer generated by microbubbles, in which most of bubbles were still spherical. It was confirmed by foam liquid close to 0.20 (Pugh, 1996). However, the bubbles in foam layer generated by 22 gauge needle were polyhedral due to the rapid drainage. The surfactant can alleviate cell attachment to bubble film but not prevent cells stay at liquid phase, which will has similar concentration as in the bioreactor bulk. It can help us understand that PF-68 can not reduce cell enrichment in microbubble case since most of cells stay at liquid phase in the foam. It also can explain why the cell enrichment was low in microbubble case with little surfactant, even though cell-bubble attachment was significant. Therefore, the foam structure should be considered when analyze

bubble-associated cell damage in bioreactor using aeration strategy with different bubble size. Finally, the effect of promising surfactants on mass transfer coefficient, k_La, is still not clear even though they had no significant effect on bubble size, which need further investigation.

5.6 CONCLUSIONS

A systematic study of small molecule surfactants regarding their protective effects on bubble-associated damage was conducted. The criteria for applying surfactant additives in mammalian cell culture are strict. They should reduce the surface tension efficiently within a time frame of seconds, while have no negative effect on cells within a time fame of ten days. Fortunately this study resulted in several promising candidates, which was comparable to PF-68. In addition, the relationship between cytotoxicitiy and structure was explored, which suggested to use sugar surfactants with large hydrophilic head group. The concentration of surfactants should also be carefully selected based on the considerations of dynamic surface tension and economics. In the future, synthesis of novel surfactants, potentially to be more efficiency then PF-68, will be performed. An attempt to combine cell-protecting function with anti-foam capability into one “super” surfactant will be made, since some small molecule surfactants can lower the surface viscosity and elasticity that help liquid drain out of bubble film.

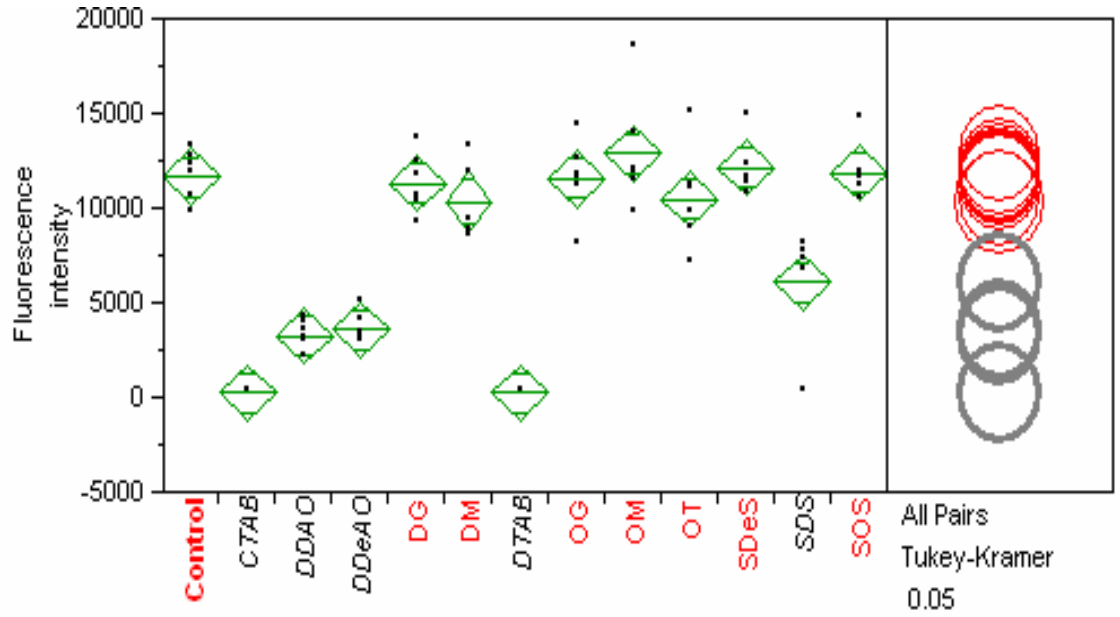

Figure 5.1. Comparison of surfactant cytotoxicity at 0.01 CMC, red color represents the surfactants with no significant difference with control

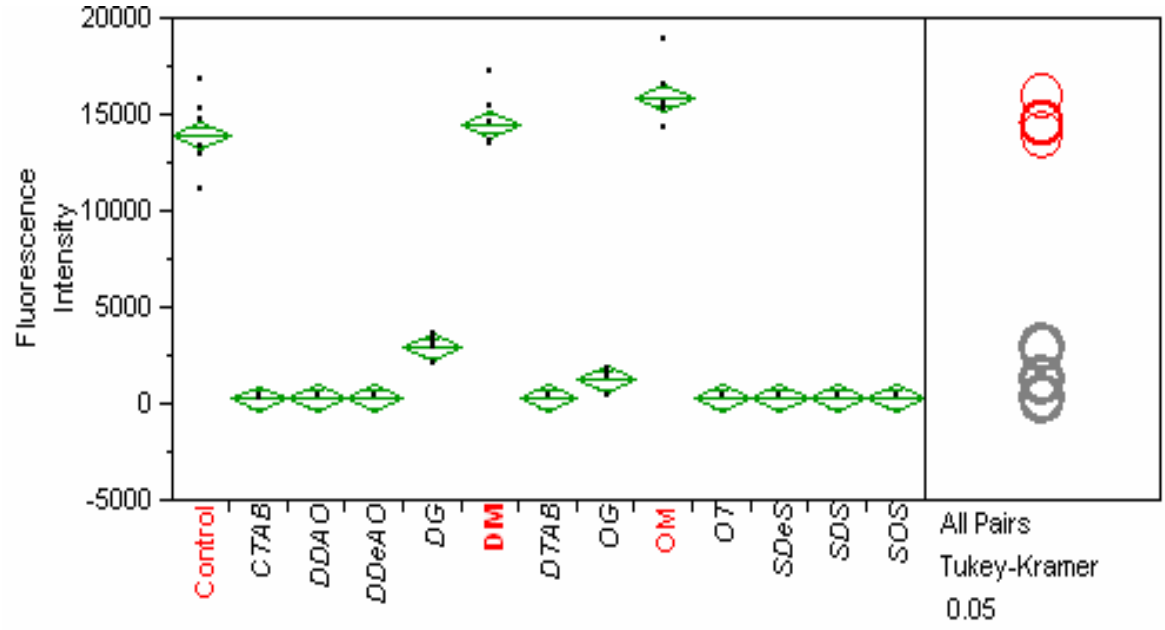

Figure 5.2. Comparison of surfactant cytotoxicity at 0.1 CMC, red color represents the surfactants with no significant difference with control

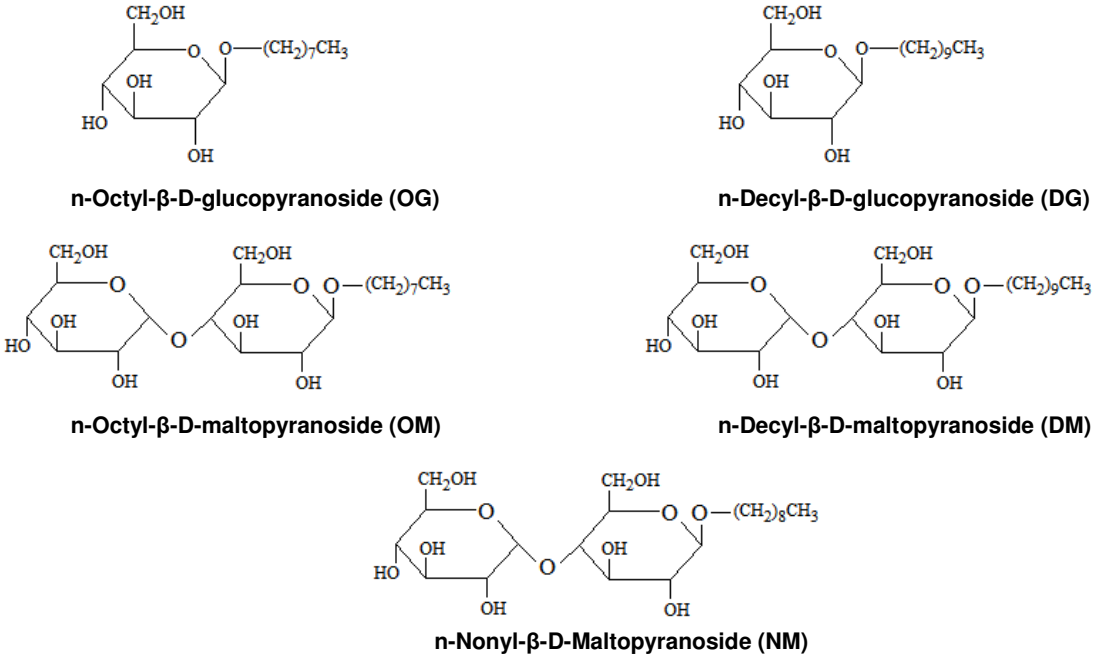

Figure 5.3. Molecular structure of alkylglycoside surfactants

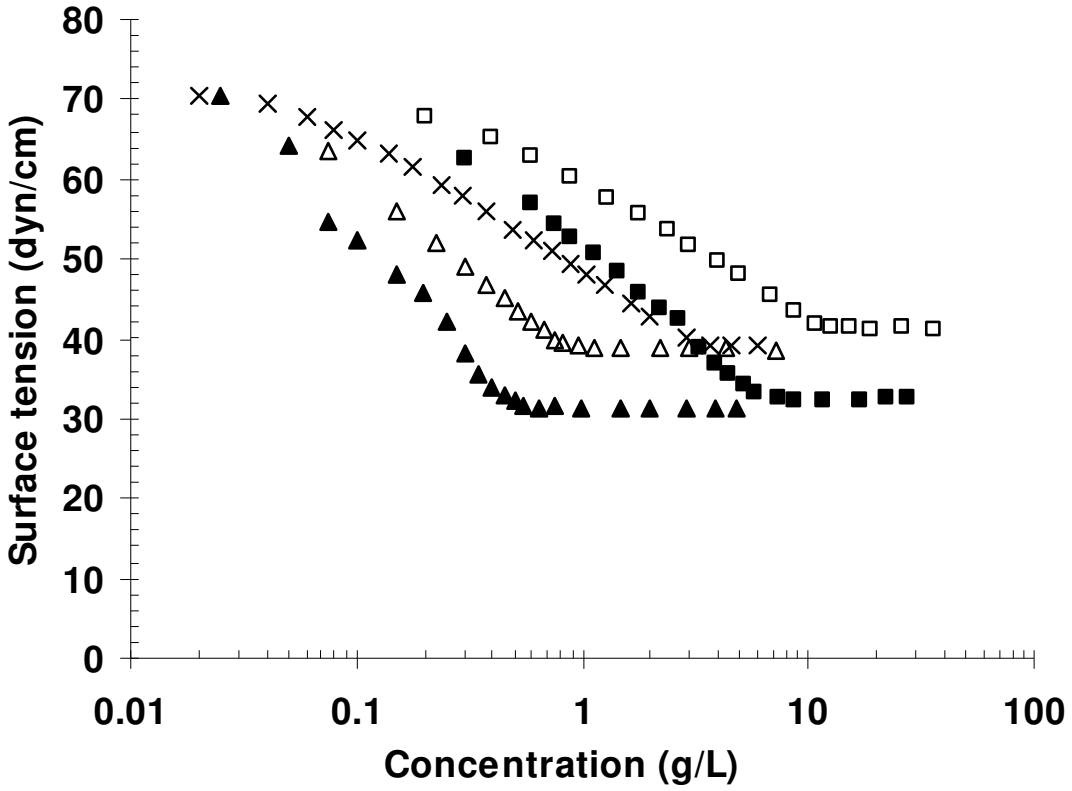

Figure 5.4. Surface tension of alkylglycoside surfactants in cell culture medium at 37ºC. ▲) DG; ■) OG; Δ) DM; □) OM; ×) NM

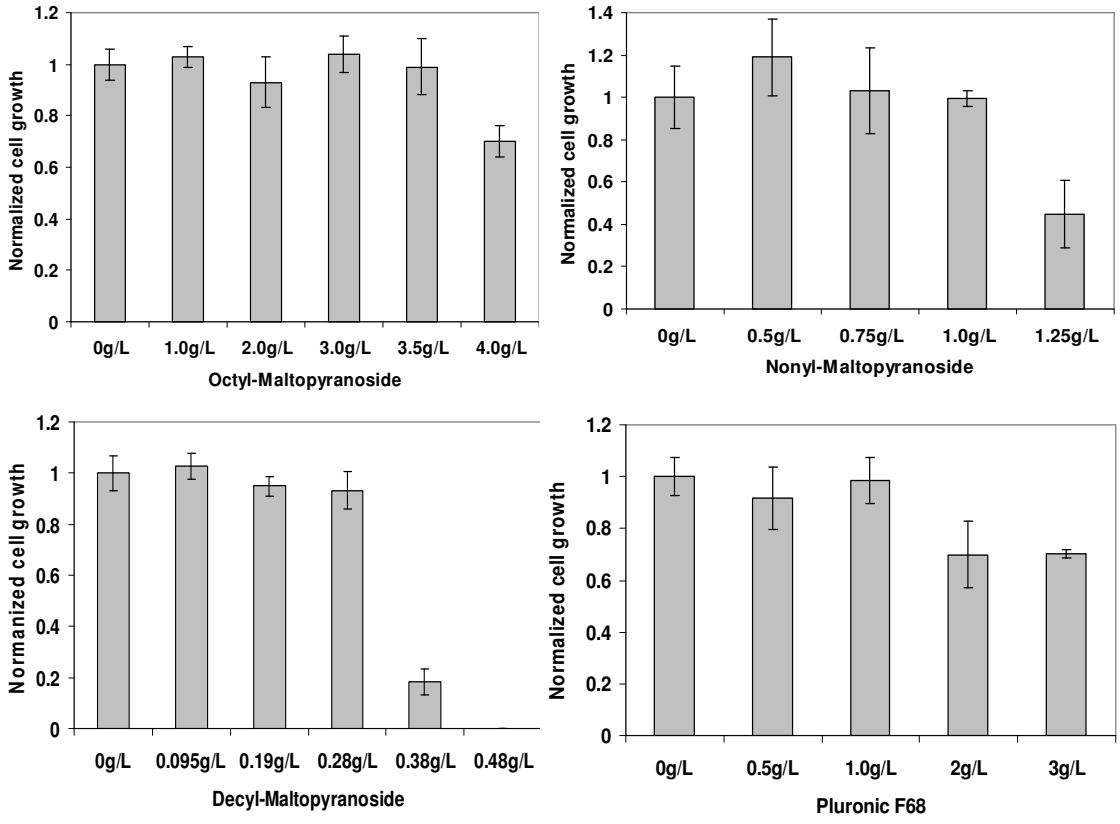

Figure 5.5. Cytotoxicity of promising surfactants (OM, NM, and DM) and PF-68 in T25 flasks

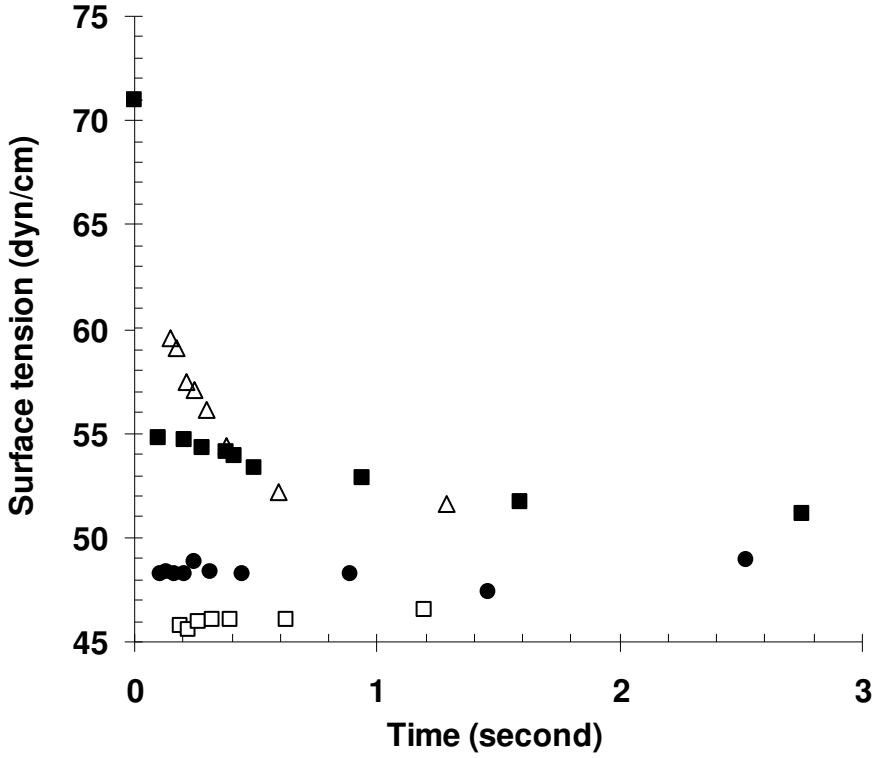

Figure 5.6. Dynamic surface tension of surfactants in cell culture medium at 37ºC, ■) 1.0 g/L PF-68; Δ) 0.28 g/L DM; □) 3.5 g/L OM; ●) 1.0 g/L NM

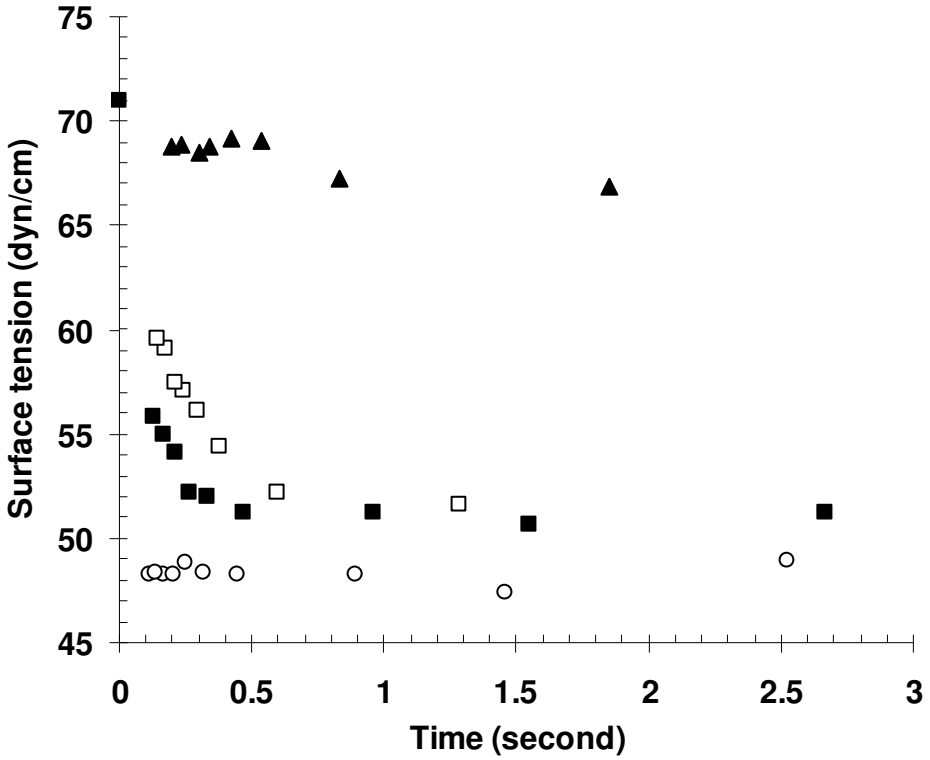

Figure 5.7. The effect of surfactant concentration on dynamic surface tension in cell culture medium at 37ºC, ■) 0.6 g/L NM; ▲) 0.01 g/L TM; □) 0.28 g/L DM; ○) 1.0 g/L NM

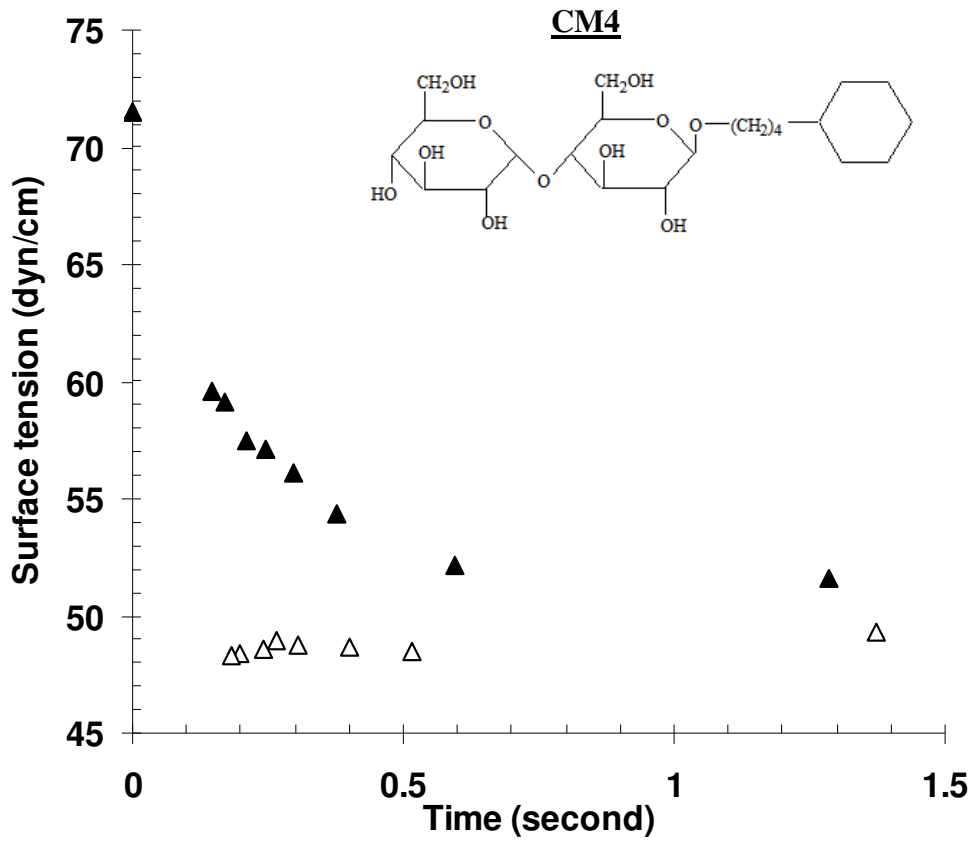

Figure 5.8. The dynamic surface tension of Δ) 1.5 g/L CM4; ▲) 0.28 g/L DM

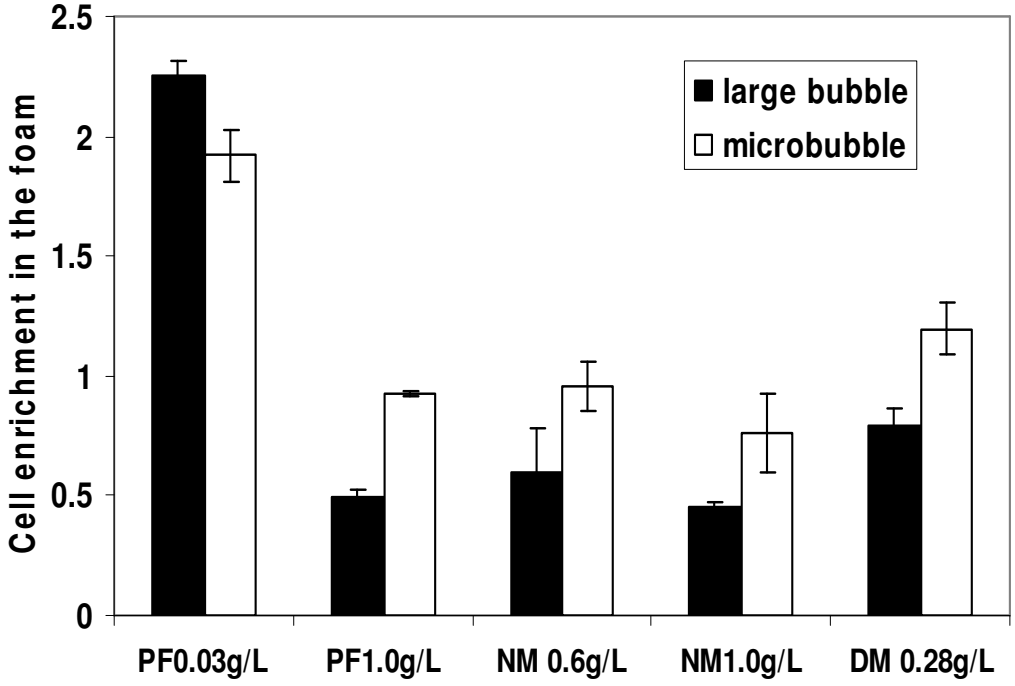

Figure 5.9. Comparison of cell-bubble interaction under different surfactant conditions

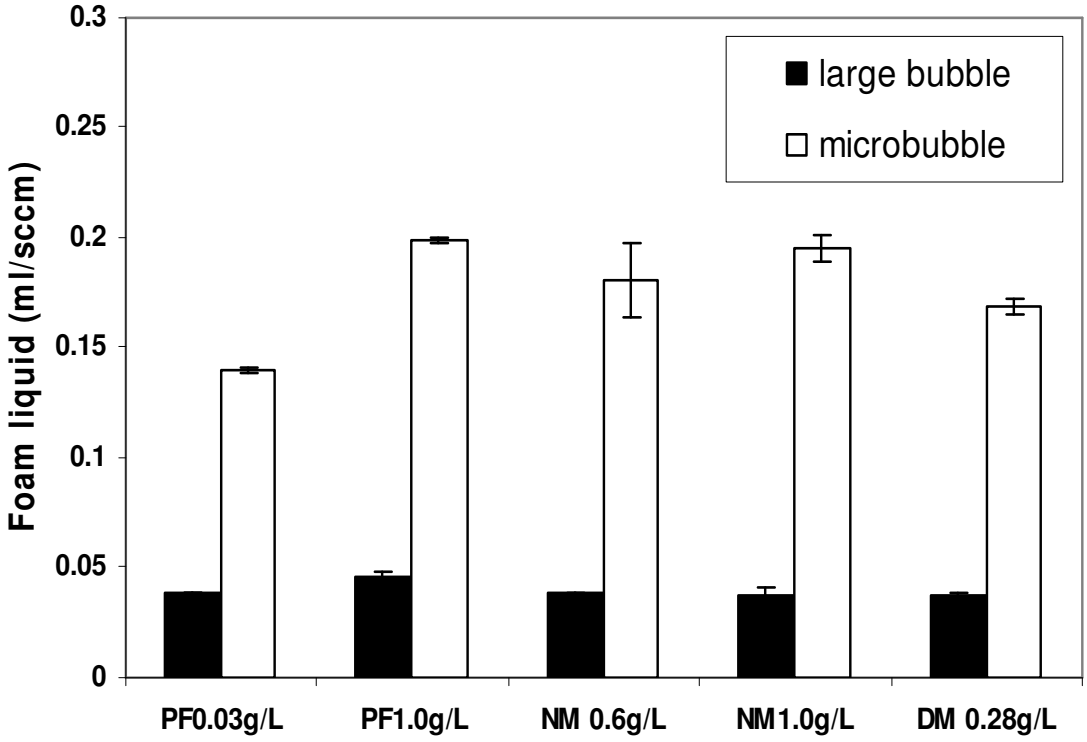

Figure 5.10. Comparison of foam capability under different surfactant conditions

	Name	MW	CMC (mM)	Alkyl Chain Length	Type
Sodium octyl sulfate	SOS	232	85.6	8	anionic
Sodium decyl sulfate	SDeS	260	12.2	10	anionic
Sodium dodecyl sulfate	SDS	288	2.3	12	anionic
N, N-Dimethyldecylamine N-oxide	DDeAO	201	16.4	10	nonionic
N, N-Dimethyldodecylamine N-oxide	DDAO	229	2.0	12	nonionic
Dodecyltrimethyl ammonium bromide	DTAB	308	7.0	12	cationic
Hexadecyltrimethyl ammonium bromide	CTAB	364	1.3	16	cationic
n-Octyl-β-D-glucopyranoside	OG	292	27.1	8	nonionic
n-Octyl-β-D-maltopyranoside	OM	455	24.5	8	nonionic
n-Octyl-β-D-thioglucopyranoside	OT	308	11.0	8	nonionic
n-Decyl-β-D-glucopyranoside	DG	320	2.3	10	nonionic
n-Detyl-β-D-maltopyranoside	DM	483	1.8	10	nonionic

Table 5.1. The properties of small molecule surfactants

	Head Group Size ($Å^2$)	Surface tension above CMC (dyn/cm)
OG	40	32.5
DG	32	31.3
OM	61	41.5
NM	59	40.1
DM	42	38.9

Table 5.2. Comparison of maltopyranoside with glucopyranoside

	Median Diameter	
Surfactants	Sintered glass (microbubble)	22 gauge needle (large bubble)
0.03 g/L PF-68	346μm	2.8 mm
1.0 g/L PF-68	147μm	2.7 mm
0.6 g/L NM	159μm	2.7 mm
1.0 g/L NM	157μm	2.5 mm

Table 5.3. The effect of surfactants on bubble size

CHAPTER SIX

AN INVESTIGATION OF AERATION STRATEGY IN MAMMALIAN CELL CULTURE

The content of this chapter has been prepared for publication: Hu W, Chalmers JJ, Should oxygen addition and carbon dioxide removal be uncoupled? A theoretical analysis

6.1 SUMMARY

Gas sparging has been the method of first choice to provide gas-liquid mass transfer to large-scale animal cell cultures. However, despite significant experience with sparging, bubble-associated cell damage and foaming are significant challenges if appropriate additives are not used. In addition, as animal cell concentrations increase, cells become increasing trapped (and presumably die) in the foam layer, even with the use of protective surfactants such as Pluronic F-68. In this study, we present theoretical calculations, based on experimentally determined constants, on the practicality of using two different gas sparging systems, to control dissolved O_2 and CO_2 separately. Since the solubility of each gas is significantly different, and the direction of mass transfer opposite, such an operating strategy potentially provides the minimum amount of gas sparging to a animal cell culture system at large-scale bioreactors, thereby maintaining the relative

simplicity of gas sparging for mass transfer; yet minimizing the foam forming gas sparging. The effect of bubble size on dissolved CO_2 removal was discussed as well.

6.2 INTRODUCTION

Large scale animal cell culture in bioreactors of 20,000 L, or greater, is routinely conducted by biopharmaceutical companies for the mass production of therapeutic proteins (Nienow, 2006). Almost all these industrial processes utilize anchorage-independent cell lines, which are cultured in stirred tank bioreactors, typically operated in a fed-batch mode. While animal cell cultures grow very well in bench scales, additional problems including some engineering challenges emerge as the scale of bioreactors increase (Ozturk, 1996). Recent work indicates that mass transfer, especially dissolved CO_2 removal, should be cautiously considered in order to achieve high product titer in large scale bioreactors (Meier, 2005).

The importance of mass transfer emerges, paradoxically, from the both the relatively limited solubility of oxygen and the relatively high solubility of carbon dioxide in the medium. While other methods have been proposed and used, commercial practioners typically return to sparging aeration due to its simplicity and extensive, practical experience. Even though the oxygen demand of mammalian cells is normally two orders of magnitude lower than that of bacteria or yeasts, the perceived "shear sensitivity" has historically restricted applicable agitation speed and aeration rates, consequently this limits the maximum mass transfer coefficient ($k_L a$). It is well known that hydrodynamic forces induced by bubble rupture causes cell damage and that the damage from these forces can be reduced by the addition of Pluronic F-68 (PF-68).

However, there is also a concern about the effectiveness of PF-68 at high cell concentrations. In these situations, even with PF-68 present, cells become entrapped in the foam layer (Ma et al., 2004).

In contrast to the low oxygen demand, CO_2 is produced by mammalian cells through several metabolic pathways, such as tri-carboxylic acid cycle and lipid synthesis. The detrimental effects of elevated dissolved CO_2 on cell growth, product titer, and product quality have been extensively reported (Aunins, et al., 1993; Kimura and Miller, 1996 & 1997). Besides its potential effect on intracellular pH after diffusion across cell membrane, elevated dissolved CO_2 also increases the hydrogen and bicarbonate ion concentration outside of the cells. Since pH is normally controlled in cell culture, the addition of base leaves more cations in the medium resulting in the increase of osmolality, which can also negatively impact the performance of cell cultures. For example, it was found that elevated osmalality induced apoptosis of hybridoma cells and affected glutamine metabolism; while the elevated dissolved CO_2 only inhibited glycolysis (deZengotita et al., 1998). Obviously, dissolved CO_2 should be removed from cell culture system efficiently.

In sparged bioreactors, dissolved CO_2 transfers from the liquid medium to rising bubbles and subsequently is released to the exhaust gas when bubbles rupture at the liquid surface. However, dissolved CO_2 accumulation as well as the increase of osmolarlity has been frequently reported in large scale bioreactors; consequently, maintaining a proper CO_2 concentration is considered one of the significant challenges in large scale operation. For example, it has been reported that pCO_2, the partial pressure of CO_2 gas in equilibrium with dissolved CO_2, can reach a level of 0.15 atm (~114 mmHg)

in a 150 L bioreactor (Garnier et al. (1996). Mostafa and Gu (2003) reported levels of pCO_2 70 mmHg and 170 mmHg at bench scale of 1.5 L and pilot plant scale of 1000 L, respectively. Zhu et al. (2005) also observed a high level of pCO_2 and osmolality up to 150 mmHg and 440 mOsm/kg in production-scale bioreactors, respectively.

In summary, a number of processes are involved during scale-up, some of which at times can be in opposition to each other. These processes are: 1) provide sufficient mass transfer to add sufficient oxygen, 2) provide sufficient mass transfer to remove dissolved CO_2, 3) minimize cell entrapment in the surface foam layer, 4) provide sufficient mixing to prevent gradients in concentrations. In addition, achievable cell concentrations keep increasing because of the state-of-art medium and mode of bioreactor operations which exacerbates the challenges discussed above. In this study, a dual-sparger system is proposed, which uncouples O_2 supplement and dissolved CO_2 removal, by employing microbubbles of pure oxygen and large bubbles of air in independent control loops. This mode of operation is then compared to ordinary one-sparger system regarding required aeration rates based on theoretical calculations. In addition, the capability to remove dissolved CO_2 was elaborated from a perspective of bubble carrying capacity.

6.3 MATHEMATICAL MODEL

Mammalian cell cultures are typically aerated by a mixture of air, oxygen, nitrogen, and CO_2. The percentage of various gas components is adjusted according to dissolved O_2 and pH level. Typically, CO_2 gas is only used at the very early period of cultivation with sodium bicarbonate buffer presented in the medium for pH control. It is

excluded gradually when acidic metabolites (lactic acid and CO_2) are accumulated. Therefore, the inlet gas only contains oxygen and/or nitrogen in the proposed mathematical model. In addition, most of animal cell cultures are operated at separate bubble formation regime. Because of the low agitation speed applied, gas dispersion is generally in the impeller-flooding regime, where the circulation of gas phase in the bioreactor is extremely limited with most of bubbles rising directly from bottom to top (Verley and Birth, 1999). Since the aeration rate is low, the liquid height does not change much after sparging.

It needs to be emphasized that the empirical correlations of $k_L a$ available in the literature for large scale animal cell culture system are extremely rare, and the values that are present also depend on the configurations and operation conditions of various bioreactors. Particularly, they are closely related to the type of sparger used. Therefore, a more generic mathematical model was used for theoretical calculations, which focused on the mass transfer of rising, single bubble. In this model, the liquid phase is assumed to be well mixed and homogeneous, while the gas phase changes as a plug flow from the bottom to the top.

The bioreactor (several different sizes was considered) was divided into 20,000 theoretical sections along the liquid height. The size, components, pressure, mass transfer coefficient and rise velocity of the bubble remain constant in each section. The gas-liquid mass transfer for O_2 or CO_2 was calculated on one bubble when it reached next section by the following equation (Gray et al., 1996).

$$dN = -k_L \times A \times \Delta C \times dt \qquad (6.1)$$

where N is the mass of gas, k_L is liquid-side mass transfer coefficient, A is interfacial area of one bubble, and ΔC is the difference of dissolved gas concentration between the interface and the bulk.

This study focused on two different bubble sizes, an initial bubble diameter out of the sparger, $d_{initial}$, of either 150 μm or 5 mm, referred to a microbubble and a large bubble, respectively. Since microbubbles have a rigid interface, the mass transfer coefficient k_L can be calculated from laminar boundary layer theory (Frössling, 1938),

$$k_L = 0.6 \times \sqrt{\frac{u_s}{d}} \times D^{2/3} \times \nu^{-1/6} \tag{6.2}$$

where u_s is the bubble-liquid relative velocity, d is the diameter of bubble, D is the diffusion coefficient, ν is the kinematic viscosity of the liquid. u_s is assumed to be equal to terminal velocity of ascending mircobubbles, which follows Stroke's theory (Fan and Tsuchiya, 1990),

$$u_s = \frac{g \times d^2}{18\nu} \tag{6.3}$$

Large bubbles normally have mobile interfaces. Their mass transfer coefficient k_L follows Higbie's penetration theory (Higbie, 1935),

$$k_L = 1.13 \times \sqrt{\frac{u_s}{d}} \times D^{1/2} \tag{6.4}$$

The terminal velocity of large bubble with a diameter in the range of 4 to 10 mm is similar, around 0.22 m/s (Fan and Tsuchiya, 1990). Since k_L, bubble diameter, and driving force (ΔC) for O_2 and CO_2 mass transfer varied during bubble rising process, time-average values were calculated. The mass balance of CO_2 is complex since it can

react with water. However, a steady state of dissolved O_2 and CO_2 was assumed in this study for simplification. Therefore, the number of bubbles required to be present in the bioreactor simultaneously (N_{bubble}) was calculated according to the oxygen uptake rate (OUR) and carbon dioxide evolution rate (CER), respectively. Then the required aeration rate (Q) for the overall mass transfer was calculated using the larger one of N_{bubble}.

$$Q = \frac{N_{bubble} \times (\frac{1}{6}\pi d_{initial}^3)}{V_r \times t_r} \tag{6.5}$$

where V_r is the volume of bioreactor, t_r is bubble resident time, which is assumed to be the sum of time a rising bubble stays at each theoretical section. The diagram of theoretical calculation is illustrated in Figure 6.1. The parameters used in calculation are listed in Table 6.1.

6.4 RESULTS AND DISCUSSION

Available k_La values from the literature in mammalian cell culture system are listed in Table 6.2. These values range from 1 ~ 20 h^{-1} except for the case of microbubbles. The calculated k_La from the model for large scale bioreactors from 100 to 10,000 L was consistent with published data, which stayed in the range of 2 ~ 7 h^{-1} for large bubbles with an initial diameter of 5 mm (data not shown). For microbubbles, k_La values around 200 h^{-1} was obtained from theoretical calculations, which was higher than the experimental data of 50-80 h^{-1} reported in the literature (Zhang et al., 1992). The variation could result from different bubble sizes or long response time of DO probe regarding to high oxygen transfer capability of microbubbles (Jorjani and Ozturk, 1999).

Figure 6.2 illustrates the change of driving force for CO_2 removal with the position of a bubble, relative to the point of injection, in a 10,000 L bioreactor. It can be clearly observed that the driving force decreased to zero quickly within 4 cm from the bottom for the microbubble case, which means that a microbubble rapidly saturates with CO_2 and will not remove any more CO_2 from the liquid (Figure 6.2a). This theoretical observation is supported by Park (2003) who reported that there was equilibrium between dissolved CO_2 concentration in the medium and CO_2 fraction in the exit gas in a 10 L bioreactor using microsparge oxygenation without headspace ventilation. In contrast, even 3.5 meters above the injection point, the driving force for CO_2 removal by the large bubble is non-zero (Figure 6.2b). Here, a key observation is that the equilibrium situation obtained with small bubbles indicates the higher k_La with smaller bubbles. However, larger bubbles are more effective at removing CO_2 with the same aeration rate, especially at large scale bioreactor (Mostafa and Gu, 2003).

Figure 6.3 demonstrates the change of microbubble size with the vertical position in bioreactors. It was found that the shrinkage of microbubble was significant when it contains pure oxygen, and will totally dissolved approximately 0.5 m before it reached the top liquid surface. As a result, no dissolved CO_2 can be removed from the system. The dissolution of microbubbles can be interpreted as following steps: First, microbubble was rapidly saturated by dissolved CO_2. Then, O_2 was continuously delivered to liquid medium from bubble side causing the over-saturation of CO_2. Finally, CO_2 inside of microbubble transferred back to liquid again. Therefore, both mass transfer directions of O_2 and CO_2 were from gas bubble to liquid at this moment. Due to the high specific surface area of microbubble and driving forces of oxygen transfer, the decrease of bubble

size was dramatically. The increase of nitrogen percentage in bubbles can alleviate the shrinkage since it is inert gas which can not be consumed by cells and remains in the bubble, which was also shown in Figure 6.3. The quick decrease of bubble size to certain extent depending on the nitrogen percentage was observed at the very beginning. Then the bubble size turned to increase mainly because of the reduction of hydrostatic pressure when bubble raise.

On the other hand, the shrinkage of bubble with a large size was not significant, even with pure oxygen (Figure 6.4). The reason is that the relative size of the gas volume to the mass transfer rate is sufficiently higher for the large bubbles. The benefit of nitrogen for CO_2 removal lies on maintaining the bubble size and exhaust gas flow rate. However, current control loop based on DO normally results in high oxygen percentage in bubbles at high cell density. Qi (2001) developed a novel cascade method to control dissolved CO_2 by adjusting the total microsparging rate, which should be below a critical value in order to prevent significant cell damage. In addition, Li et al. (2006) also reported that adjusting the overall sparge rate along with a fixed ratio of air to oxygen, instead of changing gas components, was applied for the cultures at 2,000 L scale in order to avoid high dissolved CO_2 accumulation.

The comparison of O_2 and CO_2 mass transfer properties was made in Table 6.3. They have opposite mass transfer directions. CO_2 have high solubility due to the low Henry's constant. The mass transfer coefficient of CO_2 is slightly smaller than that of O_2 resulting from relative large molecule size. The difference between inlet gas partial pressure and saturated value for CO_2 is only about 1.0×10^4 Pa, which also implies the easy saturation of CO_2. Due to the dissimilarity of two processes, it is relative difficult to

find an optimized condition for one sparger to fulfill those tasks. Gray et al. (1996) suggested using pure oxygen bubbles of 2-3 mm diameter to achieve both mass transfer requirements simultaneously. However, it was specifically suitable for a 500 L bioreactor with a certain value of respiratory quote for cells.

Therefore, an aeration strategy using dual-sparger system targeting on O_2 and CO_2 mass transfer separately was proposed. Particularly, microbubbles of pure oxygen and large bubbles of air were used. It was found that dual-sparger system required smaller aeration rates compared to one-sparger system using microbubbles with a gas composition of air to oxygen ratio at 1:1, which is a normal condition at the end of cultivation based on the current four-gas control system (Mostafa and Gu, 2003). For example, the novel aeration system required only half the aeration rate at a 10,000 L scale (Table 6.4). In comparison to microbubbles of air, the required aeration rates for the dual-sparger system was in a similar range for bioreactor of more than 1,000 L. In addition, more than 90 % of aerated gas was used for CO_2 removal by large bubbles in dual-sparger system.

The aeration rate is not the only standard to evaluate different aeration strategies. Cell damage and foaming problem should also be considered. It is well know that the rupture of small bubble, especially mcirobubbles, will generate large hydrodynamic forces causing cell damage. Dual-sparger system mainly used large bubbles, which are less damaging to cells. In addition, microbubbles will result in significant foaming problems. It was reported that the foam level was almost 10-fold lower even when the rate of aeration by an open pipe was 5-fold higher than that by a stone sparger (Mostafa

and Gu, 2003). Finally, it is convenient for dual-sparger system to control DO and dCO_2 levels purposely and separately.

6.5 CONCLUSIONS

Although there is an increasing awareness on the detrimental effect of elevated dissolved CO_2, the study of aeration strategy regarding CO_2 removal was still rare. This study pointed out the impact of microbubble dissolution on its limited capability to remove dissolved CO_2. A novel dual-sparger system uncoupling O_2 supplement and CO_2 removal was proposed. It has the potential to decrease the aeration rates as well as minimize cell damage and foam problem based on theoretical calculation. Even though a simplified model was applied in this study, it provides meaningful information for further development of aeration strategy. Future, experimental tests should be performed to confirm it.

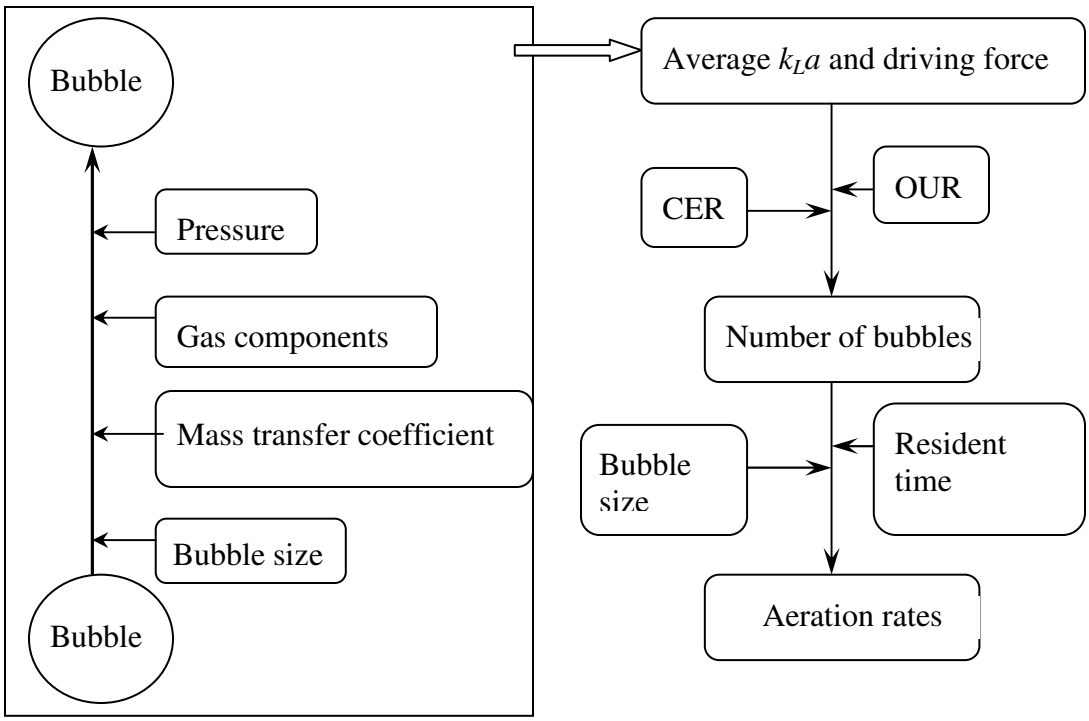

Figure 6.1. The flowchart of theoretical calculation

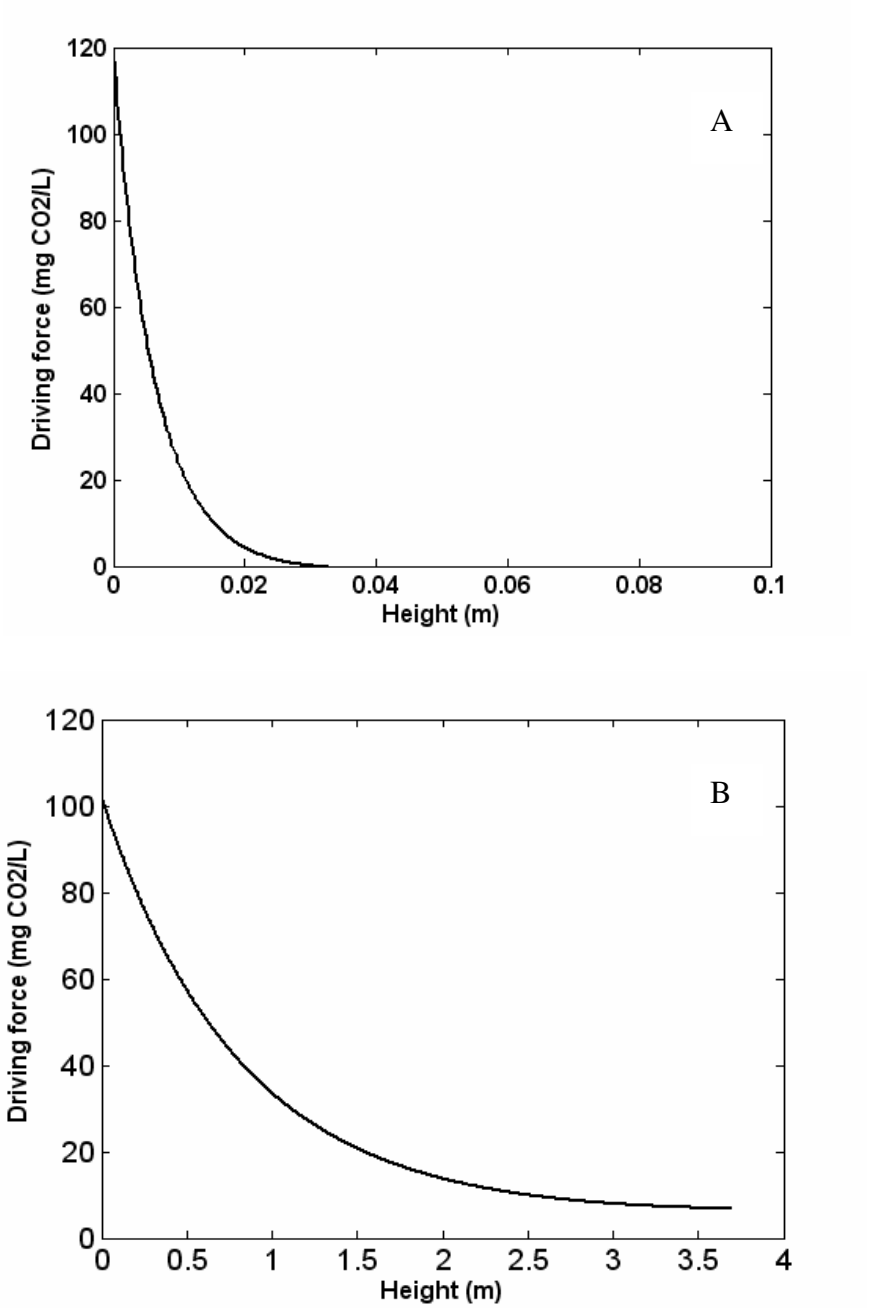

Figure 6.2 The driving for dissolved CO_2 removal by A) microbubble; B) large bubble

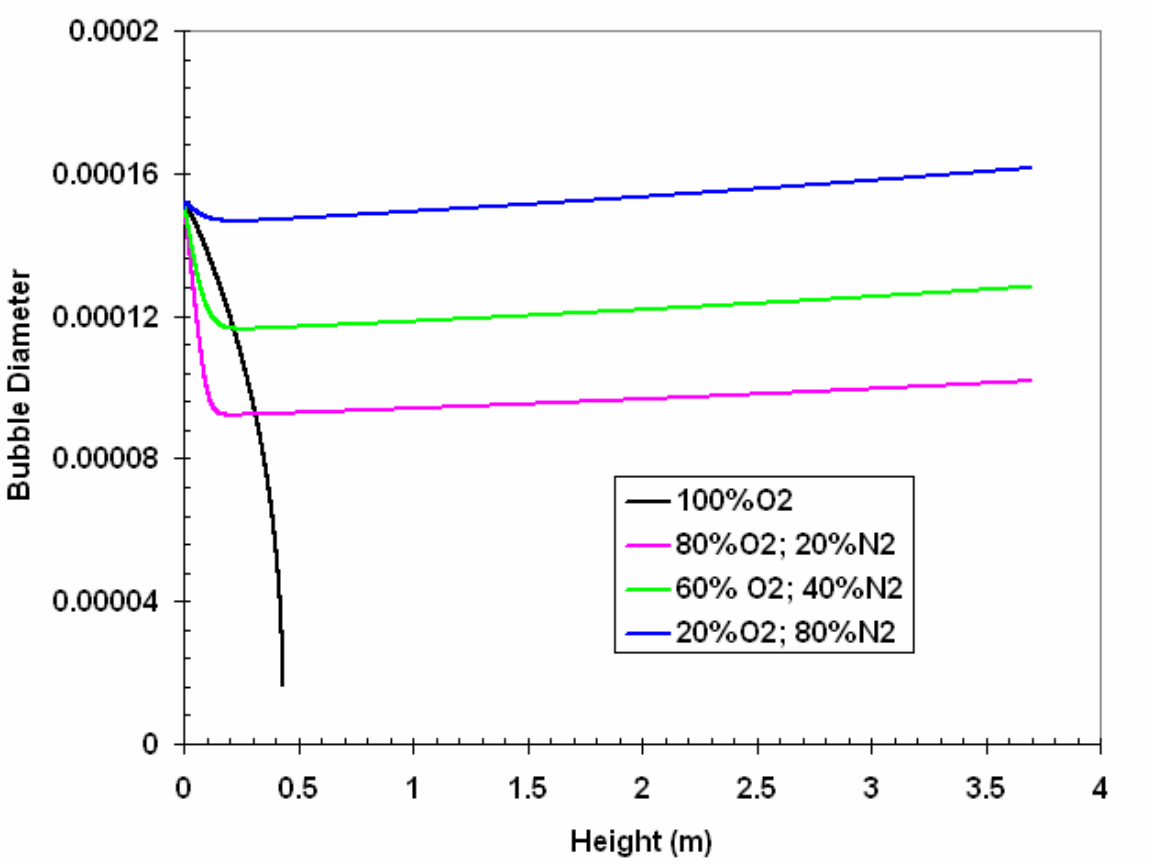

Figure 6.3 The change of bubble size at 10, 000 L bioreactor: microbubble case

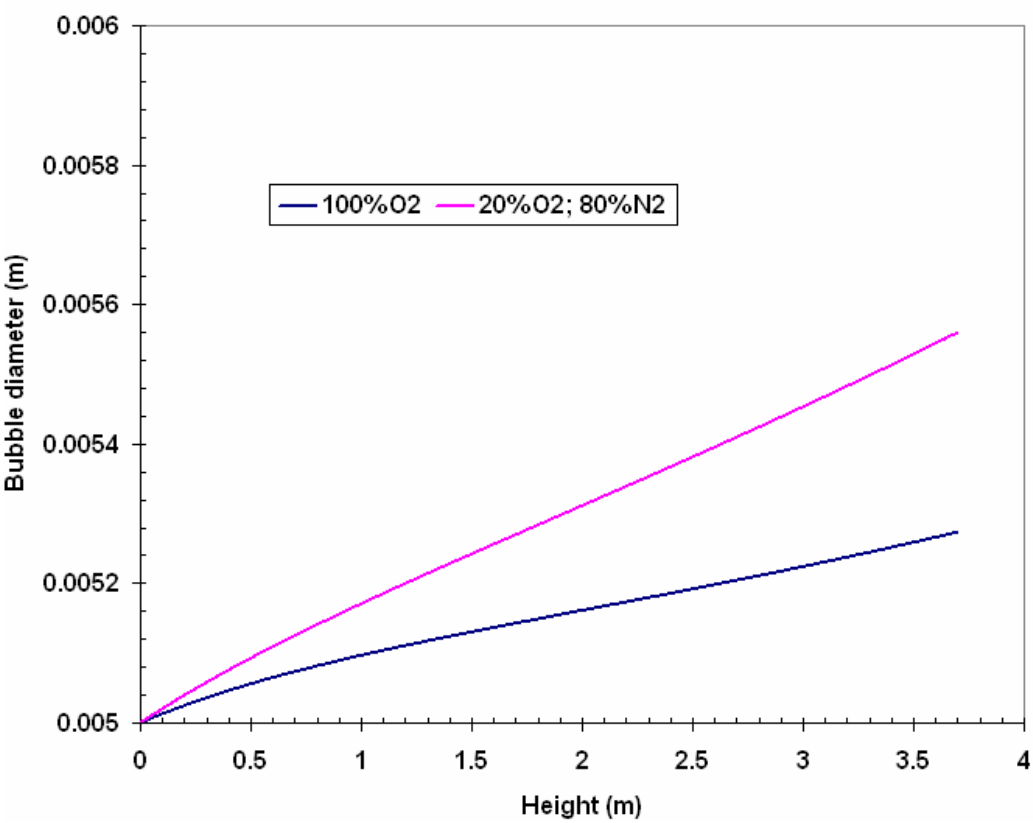

Figure 6.4 The change of bubble size at 10, 000 L bioreactor: large bubble case

dissolved CO_2	70 mmHg (102 mg/L)	Diffusivity	2.50×10^{-9} m^2/s (O_2) 2.08×10^{-9} m^2/s (CO_2)
dissolved O_2	50% air saturation (3.6 mg/L)	Reactor volume	100, 500, 1000, 8000, & 10,000 L
Specific OUR	1.0×10^{-8} mgO_2/cell/hr	Aspect ratio	2
Cell density	10^7 cells/ml	Kinematic viscosity	7×10^{-7} m^2/s
Initial bubble size	150 µm (microbubble) 5 mm (large bubble)	Henry's constant	93771 $Pa\cdot m^3/mol$ (O_2), 4015 $Pa\cdot m^3/mol$ (CO_2)
Respiration quote	1.0	Temperature	37ºC
Headspace pressure	3 psig	Medium density	1.03 kg/L

Table 6.1 Important parameters used in theoretical calculation

Bioreactor volume (L)	1.5	1.5	3.0	2.0	1.5		8000
Superficial gas velocity (cm/min)	0.45	0.93-10.6	n/a	0.09-0.36	0.9-5.3		1.2
Aeration rates (vvm)	0.067	0.07-0.8	n/a	0.01-0.04	0.067-0.4		0.0047
Agitation (rpm)	100-300	150-350	40-120	50-350	60		50-140
Medium	RPMI with serum and antifoam	Self-prepared medium with PF-68	MEM Hank's medium with serum	DMEM with serum	DMEM/RPMI with serum, antifoam and PF-68		In-house medium from Wellcome Inc
k_La (h^{-1})	1.2-3.2	4-22	0.8-2.0	1.5-15.5	2-6	50-80*	1-10
Ref.	Lavery and Nienow, 1987	Murhammer and Pfalzgraf, 1992	Dorresteijn et al., 1994	Moreira et al., 1995	Zhang et al., 1992		Nienow et al., 1996

* microbubble case

Table 6.2 k_La value of mammalian cell culture in the literatures

	O_2	CO_2
Mass transfer direction	Gas to liquid	Liquid to gas
Desired concentration in liquid (g/L)	3.6	102
Henry's constant ($Pa \cdot m^3/mol$)	93771	4015
$(k_L^{CO2}) / (k_L^{O2})$	0.89 (microbubbles); 0.91 (large bubbles)	
Inlet gas partial pressure (Pa)	32890*	0
Saturated partial pressure of the gas with desired liquid concentration (Pa)	10550	9335

* 20 % oxygen

Table 6.3 Comparison of O_2 and CO_2 mass transfer

Bioreactor volume (L)	One sparger (O_2: 60%; N_2: 40%)	One sparger (O_2: 20%; N_2: 80%)	Dual-sparger		
			Large bubble (air)	Microbubble (pure O_2)	Total
100	0.032	0.014	0.022	0.0012	0.0232
500	0.027	0.014	0.016	0.0010	0.0170
1000	0.026	0.013	0.015	0.0008	0.0158
8000	0.024	0.012	0.012	0.0008	0.0128
10000	0.023	0.012	0.012	0.0008	0.0128

Table 6.4 Comparison of required aeration rates (vvm) from different sparger system

CHAPTER SEVEN

CONCLUSIONS AND RECOMMANDATIONS

There are a number of trade-offs in sparged bioreactor for cell culture processes, which potentially limit further improving the productivity of process. The culture conditions have to be carefully selected in order to reach a compromising status. Currently, most of selection processes are based on experiences, especially for large scale bioreactor, which may not be optimized. This study particularly focused on the engineering dilemmas regarding hydrodynamic forces and gas-liquid mass transfer in bioreactors. Even though microalgae cell culture and mammalian cell culture were used separately as models, the methodologies can be applied to each other as well.

The first goal of this research was to evaluate the sensitivity of *Crypthecodinium cohnii*, a marine dinoflagellate for DHA production, to hydrodynamic forces. Even though the microfluidic channel device has already been developed in our laboratory, this study focused on the non-Newtonian fluid for the first time, which was considered in the computational fluid dynamics (CFD) using FLUENT and calculation of energy dissipation rate (EDR). In addition, the EDR in the channel was weighted by the flow velocity for a close representation of hydrodynamic conditions, which have not done before. The existence of sub-lethal effect of hydrodynamic forces has been disputed for a

long time. It was clearly demonstrated in our study of *C. cohnii* cells with transient and high EDR exposure that the loss of flagellate was found when an EDR of 1.6×10^7 W/m^3 was experienced. It is also found after the rupture of small bubble around 1-2 mm in diameter since *C. cohnii* cells were verified to be present in bubble film and foam layer. From another perspective, this sub-lethal effect can be applied to assess the level of hydrodynamic forces in future. In addition, the response of transverse and longitudinal flagellum may be different, which resulted in interesting spinning of *C. cohnii* cells in stead of normal straight moving. The flagellate can be regenerated after exposure.

Furthermore, the repeated exposure of *C. cohnii* cells to high hydrodynamic forces was studied by recycling the culture between the microfluidic channel and a small stirred tank bioreactor. Such a system can be considered as a scale-down model to simulate the circulation between impeller and bulk zone at large scale bioreactors. The results indicated that the growth of *C. cohnii* cells was not inhibited until the cells were repeatedly exposed to an EDR level of 6×10^6 W/m^3, which is normally beyond that created by impeller agitation but reachable by the rupture of small bubbles. This high critical level may due to the protective effect of their surrounding cellulosic plates compared to mammalian cells. The shear sensitivity is the most commonly used word to explain the negative effect on cells, which was also claimed to be an issue in shaken flask culture of *C. cohnii* cells by a number of publications. However, it was illustrated that the limited oxygen transfer capability of shaken flask in comparison to high respiration requirement of cells plays an important role other than share stress. In static culture, the motile dinoflagellate can concentrated in gas-liquid interface which facilitate they obtain oxygen. Here is a clear example to show how data can be miss-interrupted. In addition,

this finding has great impact on the research in oceanology area, which focuses on environmentally important dinoflagellate. Future works of this part will involve further development of the circulation model in order to comply with FDA regulations for broad industrial applications. The mechanism underneath the sub-lethal effect should also be explored at the level of gene/protein expression. Therefore, the sensitivity of cells to hydrodynamic forces can be enhanced by genetic methods in future.

According to above experiments, the upper limit of hydrodynamic forces that the cells can tolerate was obtained. Therefore, the maximum agitation speed for a certain impeller can be calculated, which ensures sufficient mixing without damaging cells. However, the bubble rupture still could be dangerous since they normally generate high hydrodynamic forces, which leads to another research of interfacial phenomena in bioreactors. This is a complicated area has not been systematically investigated. The second goal of this research is to find a better way to balance the necessary mass transfer function of bubble and its unnecessary or detrimental effect on cells in mammalian cell culture. On one hand, the number of bubbles introduced into culture system should be reduced when the mass transfer requirement has been met. A novel dual-sparger aeration strategy was proposed. Based on the dissimilar properties of oxygen and dissolved carbon dioxide mass transfer, microbubbles of oxygen and large bubbles of air were applied simultaneously to uncouple them. It has the potential to minimize the required aeration rates in large scale bioreactor and also foam layer. Due to the lack of experimental conditions, it was only performed by theoretical calculation at this moment even though it was somehow consistent with published data. Collaboration with industrial partner will be made in future in order to verify this idea.

On the other hand, the detrimental effect of bubble is closely related to the cell-bubble interaction, which can be regulated by the addition of surfactants. Currently, Pluronic F-68 is the only available one to alleviate cell-bubble attachment and consequent cell damage during bubble rupture. In this study, a set of methods were established for screening more surfactant additives as well as exploring their structure-performance relationship. Small molecule surfactants were particularly investigated, which are generally considered to be toxic to mammalian cells. However, we did find some promising candidates, such as nonyl-maltopyranoside, which can not only reduce cell enrichment in the foam layer to similar level of Pluronic F-68 but also have no negative effect on cell growth. In addition, it was found that the concentration of applied surfactants should be sufficiently high to ensure quick migrating to gas-liquid interface and lowering the surface tension.

In the future, the novel surfactants can be synthesized according to the findings from this research, which may have higher efficiency than Pluronic F-68. More importantly, efforts will be made to combine the protective effect of small molecule surfactants with antifoam function since the cells entrapped into foam layer have high probability to die. For example, Calik et al. (2005) reported a novel water-soluble fluorocarbon-hydrocarbon hybrid unsymmetrical bolaform surfactant had antifoam function in *E. coli* fermentation while it can also lower the surface tension to less then 55 dyn/cm within one second. However, its anti-foam mechanism is still being investigated. Finally, the toxicity of surfactants to mammalian cells may be adjustable by changing cell membrane components, such as cholesterol content, through genetic methods or adaptation processes, which can bring more surfactants into consideration.

BIBLIOGRAPHY

Alberts, B., Bray, D., Lewis, J., Raff, M., Roberts, K, Watson, J.D. 1989. *Molecular Biology of the Cell*, Garland, New York.

Aloi, L.E., Cherry, R.S. 1996. Cellular response to agitation characterized by energy dissipation at the impeller tip. *Chem. Eng. Sci.* **51**: 1523-1529.

Al-Rubeai, M., Emery, A. N., Chalder, S., Goldman, M. H. 1993. A flow cytometric study of hydrodynamic damage to mammalian cells. *J. Biotechnol.* **31**: 161-177.

Amanullah, A., McFarlane, C.M., Emery, A.N., Nienow, A.W. 2001. Scale-down model to simulate spatial pH variation in large-scale bioreactors. *Biotechnol. Bioeng*. **73**: 390-399.

Amanullah, A., Buckland, B.C., Nienow, A.W. 2004. Mixing in the fermentation and cell culture industries, In: *Handbook of industry mixing*, (Paul, E., Atiemo-Obeng, V.A., Kresta, S.M. eds), John Wiley & Sons, New Jersey.

Arnold, J. J., Ahsan, F., Meezan, E., Pillion, D. J. 2004. Correlation of tetradecyl maltoside induced increases in nasal peptide drug delivery with morphological changes in nasal epithelial cells. *J. Pharm. Sci*. **93**: 2205-2213.

Aunins, J.G., Glazomitsky, K., Buckland, B.C. 1993. Cell culture reactor design: known and unknown. In: *Proc. 3rd int. conf. on bioreactor and bioprocess fluid dynamics* (Nienow A.W., ed). Mechanical Engineering Publication Ltd., London.

Arakawa, T., Kita, Y. 2000. Protection of bovine serum albumin from aggregation by Tween 80. *J. Pharm. Sci*. **89**: 646-651.

Bailey, J. E. Ollis, D.F. 1986. *Biochemical Engineering Fundamentals*, 2nd ed., McGraw-Hill, New York.

Bam, N.B., Cleland, J.L., Yang, J., Manning, M. C., Carpenter, J.F., Kelley, R.F, Randolph, T.W. 1998. Tween protects recombinant human growth hormone against agitation-induced damage via hydrophobic interaction. *J. Pharm. Sci.* **87**: 1554-1559

Barbosa, M.J., Albrecht, M., Wijffels, R.H. 2003. Hydrodynamic stress and lethal events in sparged microalgae cultures. *Biotechnol. Bioeng.* **83**: 112-120.

Barbosa, M.J., Hadiyanto, Wijffels, R.H. 2004. Overcoming shear stress of microalgae cultures in sparged photobioreactors. *Biotechnol. Bioeng.* **85**: 78-85.

Bavarian, F., Fan, S.L., Chalmers, J.J. 1991. Microscopic visualization of insect cell-bubble interactions. I: rising bubbles, air-medium interface, and the foam layer. Biotechnol. Prog. 7: 140-150.

Beach, D.H., Holz, Jr, G.G. Environmental influences on the docosahexaenoate content of the triacylglycerols and phosphatidylcholine of a hetetrotrophic marine dinoflagellate, *Crypthecodinium cohnii*. *Biochim. Biophys. Acta.* **316**: 56-65.

Behrens, P.W., Kyle, D.J. 1996. Microalgae as a source of fatty acids. *J. Food Lipids*, **3**: 259-272.

Bhakta, A., Ruckenstein, E. 1996. Modeling of the generation and collapse of aqueous foams. *Langmuir*, **12**: 3089-3099.

Bilgen, B., Chang-Mateu,J.M., Barabino, G.A. 2005. Characterization of mixing in a novel wavy-walled bioreactor for tissue engineering. *Biotechnol. Bioeng.* **92**:907-919.

Bombac, A., Zun, I., Filipic, B., Zumer, M. 1997. Gas-filled cavity structures and local void fraction distribution in aerated stirred vessel. *AICHE J.* **43**: 2921-2931.

Boulton-Stone, J.M., Black, J.R. 1993. Gas bubbles bursting at a free surface. *J. Fluid Mech.* **254**: 466-473.

Braun, A., Kwee, L., Labow, M.A., Alsenz, J. 1997. Protein aggregates seem to play a key role among the parameters influencing the antigenicity of interferon alpha (IFN-alpha) in normal and transgenic mice. *Pharm Res.* **14**: 1472-1478.

Broekhuizen, N. 1999. Simulating motile algae using a mixed Eulerian-Lagrangian approach: does motility promote dinoflagellate persistence or co-existence with diatoms? *J. Plank. Res*. **21**: 1191-1216.

Büchs, J., Maier, U., Milbradt, C., Zoels, B. 2000. Power consumption in shaking flasks on rotary shaking machines: I. Power consumption measurement in unbaffled flasks at low liquid viscosity. *Biotechnol. Bioeng*. **68**: 589-593.

Bujalshi, J.M., Jaworshi, Z., Bujalshi, W., Nienow, A.W. 2002. The influence of the addition position of a tracer on CFD simulated mixing tiems in a vessel agitated by a Rushton turbine. *Trans. IchemE.* **80**:824-831.

Byun, T.G., Zeng, A.P., Deckwer, W.D. 1994. Reactor comparison and scale-up for the microaerobic production of 2,3-butanediol by of *Enterobacter aerogenes* at constant oxygen transfer rate. *Bioprocess Eng.* **11**: 167-175.

Camacho, F. G., Cómez, A. C., Sobczuk, T.M., Grima, E.M. 2000. Effects of mechanical and hydrodynamic stress in agitated, sparged cultures of *Porphyridium cruentum*. *Process Biochem*. **35**:1045-1050.

Camacho, F. G., Grima, E.M., Mirón, A.S., Pascual, V.G., Chisti, Y. 2001. Carboxymethyl cellulose protects algal cells against hydrodynamic stress. *Enzyme Microbial Technol.* **29**: 602-610.

Calik, P., Ileri, N., Erdinc, B.I. 2005. Novel antifoam for fermentation processes: fluorocarbon-hydrocarbon hybrid unsymmetrical bolaform surfactant. *Langmuir*, **21**: 8613-8619.

Chalmers, J.J., Bavarian, F. 1991a. Microscopic visualization of insect cell-bubble interactions. I: rising bubbles, air-medium interface, and foam layer. *Biotechnol.Prog*. **7**: 140-150.

Chalmers, J.J., Bavarian, F. 1991b. Microscopic visualization of insect cell-bubble interactions. II: the bubble film and bubble rupture. *Biotechnol. Prog*. **7**: 151-158.

Chalmers, J.J. 2000. Animal cell culture, effect of agitation and aeration on cell adaptation, In: *Encyclopedia of cell technology*, (Spier, R., Griffins, J.B., Scragg, A.H. eds), Wiley, New York.

Chalmers, J.J., Godoy, R., Berdugo, C. 2006. The use of energy dissipation rate as a parameter to assist in the evaluation, scale-up, and scale-down of bioprocesses. 232nd ACS annual meeting, San Francisco, CA, September 10-14.

Chang, B.S., Kendrick, B.S., Carpenter, J.F. 1996. Surface-induced denaturation of proteins during freezing and its inhibition by surfactants. *J. Pharm. Sci*. **85**: 1325-1330.

Chattopadhyay, D., Rathman, J., Chalmers, J.J. 1995a. A thermodynamic explanation for cell adhesion to gas-liquid interfaces. *Biotechnol. Bioeng.* **48**: 649-658.

Chattopadhyay, D., Rathman, J.F., Chalmers, J.J. 1995b. The protective effect of specific medium additives with respect to bubble rupture. *Biotechnol. Bioeng.* **45**: 473-80.

Chen, A.K., Latz, M.I., Frangos, J.A. 2003. The use of dinoflagellate bioluminescence to characterize cell stimulation in bioreactors. *Biotechnol. Bioeng*. **83**: 93-103.

Chi, E.Y., Krishnan, S., Randolph, T.W., Carpenter, J.F. 2003. Physical stability of proteins in aqueous solution: mechanism and driving forces in nonnative protein aggregation. *Pharm. Res.* **20**: 1325-1336.

Chisti, Y. 2000. Animal-cell damage n sparged bioractors. *Trends Biotechnol.* **18**: 420-432.

Chu. L., Robinson, D.K. 2001. Industrial choices for protein production by large-scale cell culture. *Curr. Opinion Biotechnol.* **12**: 180-187.

Claesson, P.M., Kjellin, U.R.M. 2002. Sugar surfactants. In: Encyclopedia of surface and colloid science. (Hubbard, A.T. ed.) Marcel Dekker, New York.

Craig-Schmidt, M. C., Huang, M. C. 1998. Interaction of n-6 and n-3 fatty acid: implications for supplementation of infant formula with long-chain polyunsaturated fatty acids. 63-84. In: *Lipids in Infant Nutrition* (Huang, Y. S., Sinclair, A. J. eds.), American Oil Chemists' Society, Champaign, IL, USA.

Davidson, K.M., Sushil, S., Eggleton, C.D., Marten, M.R. 2003. Using computational fluid dynamics software to estimate circulation time distributions in bioreactors. *Biotechnol. Prog.* **19**:1480-1486.

de la Maza, A., Coderch, L., Gonzalez, P., Parra, J.L. 1998. Subsolubilizing alterations caused by alkyl glucoside in phosphatidylcholine liposomes. *J. Control. Release* **52**: 159-168.

Denkov, N.D., Cooper, P., Martin, J.Y. 1999. Mechanisms of action of mixed solid-liquid antifoams. 1. Dynamics of foam film rupture. *Langmuir*, **15**: 8514-8529

de Silva, T.L., Mendes, A., Mendes, R.L., Calado, V., Alves, S.S., Vasconcelos, J.M.T., Reis, A. 2006. Effect of *n*-dodecane on *Crypthecodinium cohnii* fermentations and DHA production. *J. Ind. Microbiol. Biotechnol*. **33**: 408-416.

de Swaaf, M.E., de Rijk, T.C. Eggink, G., Sijtsma, L. 1999. Optimization of docosahexaenoic acid production in batch cultivation by *Crypthecodinium cohnii*. *J. Biotechnol.* **70**: 185-192.

de Swaaf, M.E., Grobben, G. J., Eggink, G., de Rijk, T.C. van der Meer, P., Sijtsma, L. 2001. Characterisation of extracellular polysaccharides produced by Crypthecodium cohnii. *Appl. Micro. Biotechnol.* **57**: 395-400.

de Swaaf, M.E., Sijtsma, L., Pronk, J.T. 2003a. High-cell-density fed-batch cultivation of the docosahexaenoic acid producing marine alga *Crypthecodinium cohnii*. *Biotechnol. Bioeng.* **81**: 666-672.

de Swaaf, M.E., Pronk, J.T., Sijtsma, L. 2003b. Fed-batch cultivation of the docosahexaenoic-acid-producing marine alga *Crypthecodinium cohnii* on ethanol. *Appl. Microbiol. Biotechnol.* **61**: 40-43.

de Swaaf, M.E., de Rijk, T.C., van der Meer, P., Eggink, G., Sijtsma, L. 2003c. Analysis of docosahexaenoic acid biosynthesis in alga *Crypthecodinium cohnii* by ^{13}C labeling and desaturase inhibitor experiments. *J. Biotechnol.* **103**: 21-29.

de Swaaf, M. E. 2003. Docosahexaenoic acid production by marine alga Crythecodinium cohnii. Ph.D. dissertation, Delft University, The Netherlands.

Dey, D., Emery, A. N. 1999. Problems in predicting cell damage from bubble bursting. *Biotechnol. Bioeng.* **65**: 240-245.

deZengotita, V., Kimura, R., Miller, M. 1998. Effects of CO_2 and osmolality on hybridoma cells: growth, metabolism and monoclonal antibody production. *Cytotechnol.* **28**: 213-227.

deZengotita, V.M., Schmelzer, A.E., Miller, W.M. 2002. Characterization of hybridoma cell responses to elevated pCO2 and osmolality: intracellular pH, cell size, apoptosis, and metabolism. *Biotechnol. Bioeng.* **77**: 369-380.

Dhanasekharan, K.M., Sanyal, J., Jain, A., Haidari, A. 2005. A generalized approach to model oxygen transfer in bioreactors using population balances and computational fluid dynamics. *Chem. Eng. Sci.* **60**: 213-218.

Dong, A.C., Prestrelshi, S.J., Allison, S.D., Carpenter, J.F. 1995. Infrared spectroscopic studies of lyophiization-induced and temperature-induced protein aggregation. *J. Pharm.Sci.* **84**: 415-424.

Dorresteijn, R. C., de Gooijer, C.D., Tramper, J., Beuvery, E.C. 1994. A simple dynamic method for on-line and off-line determination of k_La during cultivation of animal cells. *Biotech. Techniques.* **8**, 675-680.

Eastoe, J., Dalton, J.S. 2000. Dynamic surface tension and adsorption mechanisms of surfactants at the air-water interface. *Adv. Colloid Interface Sci.* **85**:103-144.

Einsele, A. 1978. Scaling up bioreactors, *Proc. Biochem.* **13**:13-14.

Ericsson, C. A., Soederman, O., Garamus, V.M., Bergstroem, M., Ulvenlund, S. 2005. Effects of temperature, salt, and deuterium oxide on the self-aggregation of alkyl-glycosides in dilute solution. 2. n-tetradecyl-β-D-maltoside. *Langmuir,* **21**:1507-1515.

Fan, L.S., Tsuchiya, K. 1990. *Bubble Wake Dynamics in Liquids and Liquid-Solid Suspensions*. Stoneham: Butterworth-Heinemann.

Fazilet, V.S. 1998. Foaming: consequences, prevention and destruction. *Biotechnology Advances*, **16**:913-948.

Fife, J.P., Derksen, R.C., Ozkan, H.E., Grewal, P.S., Chalmers, J.J., Krause, C.R. 2004. Evaluation of a contraction flow field on hydrodynamic damage to entomopathgenic nematodes-a biological pest control agent. *Biotechnol. Bioeng.* **86**: 96-107.

Frössling, N. J 1938. Übber die verdünstung fallenden tropfen (Evaporation of f alling drops). *Gerlands Beitage zur Geophysik*. **52**:170-216.

Frye, G.C., Berg, J. 1989. Antifoam action by solid particles. *J. Colloid Interface Sci.* **127**: 222-238.

Garcia-Briones, M., Brodkey, R., Chalmers, J. 1994. Computer simulations of the rupture of a gas bubble at a gas-liquid interface and its implications in animal cell damage. *Chem. Eng. Sci*. **49**: 2301-2320.

Gargett, A.E. 1997. "Theories" and techniques for observing turbulence in the ocean euphotic zone. *Sci. Mar.* **61**: 25-45.

Garnier, A., Voyer, R., Tom, R., Perret, S., Jardin, B., Kamen, A. 1996. Dissolved carbon dioxide accumulation in a large scale and high density production of TGFβ receptor with baculovirus infected *Sf-9* cells. *Cytotechnol.* **22**: 53-63.

Goldblum, S., Bea, Y.K., Hink, W.F., Chalmers, J.J. 1990. Protective effect of methylcellulose and other polymers on insect cells subjected to laminar shear stress. *Biotechnol. Prog*. **6**: 383-390.

Gray, D., Chen, S., Howarth, W., Inlow, D., Maiorella, B. 1996. CO_2 in Large-Scale and High-Density CHO Cell Perfusion Culture. *Cytotechnol*. **22**: 65-78.

Green, R., Su, T., Joy, H., Lu, J.R. 2000. Interaction of lysozyme and sodium dodecyl sulfate at the air-liquid interface. *Langmuir* **16**: 5797-5805

Gregoriades, N., Clay, J., Ma, N., Koelling, K., Chalmers, J.J. 2000. Cell Damage of microcarrier culture as a function of local energy dissipation created by a rapid extensional flow. *Biotechnol. Bioeng.* **69**: 171-182.

Handa-Corrigan, A., Emery, A.N., Spier, R. E., 1989. Effect of gas-liquid interfaces on the growth of suspended mammalian Cells: mechanisms of cell damage by bubbles. *Enzyme Microb Technol.* **11**: 230-235.

Handa-Corrigan, A., Weeratunge, N.P., Braybrook, J.H., Mackay, G.A., Chescoe, D. 1997. animal cell technology, from vaccines to genetic medicine (Carrondo, M,J.T., Griffiths, B., Moreira, J.L.P. eds, pp. 121-126. Butterworth-Heinemann.

Henry, C.M. 2000. The next pharmaceutical century. *Chem. Eng. News*. 85-100.

Higashiyama, K., Murakami, K., Tsujimura, H., Matsumoto, N., Fujikawa, S. 1999. Effects of dissolved oxygen on the morphology of an arachidonic acid production by Mortierella alpine 1S-4. *Biotechnol. Bioeng*. **63**: 442-448.

Higbie, R. 1935. The rate of absorption of a pure gas into a still liquid during a short time of exposure. *Trans. AICHE.* **31**:365–389.

Horrocks, L.A., Yeo, Y.K. 1999. Health benefits of docosahexaenoic acid (DHA). *Pharmacol. Res.* **40**: 211-225.

Innis, S.M. 1994. Fatty acid requirements of the newborn. *Can. J. Physiol. Pharmacol.* **72**: 1483-1492.

Jaworshi, Z., Fyster, K.N., Nienow, A.W. 2001. The effect of size, location, and pumping direction of pitched blade turbine impellers on flow patterns: LDA measurement and CFD prediction. *Trans. IChemE*. **79**:887-894.

Jensen, G.S., Ginsberg, D.I., Drapeau, M.S. 2001. Blue-green algae as an immuno-enhancer and biomodulator. *J. Am. Nutraceutical Assoc.* **3**:24-30.

Jiang, Y., Chen, F., Liang, S. 1999. Production potential of docosahexaenoic acid by the heterotrophic marine dinoflagellate *Crypthecodinium cohnii*. *Process Biochem.* **34**:633-637.

Jordan, M., Sucker, H., Einsele, A., Widmer, F., Eppenberger, H.M. 1994. Interactions between animal cells and gas bubbles: the influence of serum and Pluronic F68 on the physical properties of the bubble surface. *Biotechnol. Bioeng.* **43**: 446-454.

Jorjani, P., Ozturk, S.S. 1999. Effects of cell density and temperature on oxygen consumption rate for different mammalian cell lines. Biotechnol. Bioeng. 64: 349-356.

Joshi, J.B., Elias, C.B., Patole, M.S. 1996. Role of hydrodynamic shear in the cultivation of animal, plant and microbial cells. *Chem. Eng. J.* **62**: 121–141.

Juhl, A.R., Velazquez V., Latz. M. 2000. Effect of growth conditions on flow-induced inhibition of population growth of a red-tide dinoflagellate. *Limnol. Oceanogr.* **45**: 905-915.

Juhl, A., Latz, M. 2002. Mechanisms of fluid-induced inhibition of population growth in a red-tide dinoflagellate. *J. Phycol.* **38**: 683-694.

Jüsten, P., Paul, G.C., Nienow, A.W., Thomas, C.R. 1998. Dependence of Penicillium chrysogenum growth, morphology, vacuolation, and productivity in fed-batch fermentations on impeller type and agitation intensity. *Biotechnol. Bioeng.* **59**: 762-775.

Kang, J.X., Leaf, A. 1996. The cardiac antiarrhythmic effects of polyunsaturated fatty acid. *Lipids*, **31**:S41-S44.

Katakam, M., Bell, L.N., Banga, A.K. 1995. Effect of surfactants on the physical stability of recombinant human growth hormone. *J. Pharm. Sci.* **84**: 713-716.

Kimura, R., Miller, W. 1996. Effect of elevated pCO_2 and /or osmolality on the growth and recombinant tPA production of CHO cells. *Biotechnol. Bioeng*. **52**: 152-160.

Kimura, R., Miller, W. 1997. Glycosylation of CHO-derived recombinant tPA produced under elevated pCO_2. *Biotechnol. Prog.* **13**: 311-317.

Kilburn, D.G., Webb, F.C. 1968. The cultivation of animal cells at controlled dissolved oxygen partial pressure. *Biotechnol. Bioeng*. **10**: 801-814.

Koehler, S.A., Hilgenfeldt, S., Stone, H.A. 2004a. Foam drainage on the microscale I. modeling flow through single Plateau borders. *J. Colloid Interface Sci.* **276**: 420-438.

Koehler, S.A., Hilgenfeldt, S., Weeks, E.R., Stone, H.A. 2004b. Foam drainage on the microscale II. Imaging flow through single Plateau borders. *J. Colloid Interface Sci.* **276**: 439-449.

Krzan, M., Lunkenheimer, K., Malysa, K. 2003. Pulsation and bouncing of a bubble prior to rupture and/or foam film formation. *Langmuir*, **19**; 6586-6589.

Kreilgaard, L., Jones, L.S., Randolph, T.W., Frokjaer, S., Flink, J.M., Manning, M.C., Carpenter, J.F.1998. Effect of Tween 20 on freeze-thawing and agitation-induced aggregation of recombinant human factor XIII. *J. Pharm. Sci*. **87**: 1597-1603.

Kunas, K.T., Papoutsakis, E.T. 1989. Increasing serum concentrations decrease cell death and allow growth of hybridoma cells at higher agitation rates. *Biotechnol. Lett*. **11**: 525-530.

Kwok Alvin C.M., Wong Joseph T.Y. 2003. Cellulose synthesis is coupled to cell cycle progression at G1 in the dinoflagellate *Crythecodinium cohnii.* Plant Physiology, **131**, 1681-1691.

Kyle D.J. 1996. Production and use of a single oil which is highly enriched in docosahexaenoic acid. *Lipid Technol.* **8**: 107-110.

Langheinrich, C., Nienow, A.W., Eddleston, T., Stevenson, N.C., Emery, A.N., Clayton, T.M., Slater, NKH. 2002. Oxygen transfer in stirred bioreactors under animal cell culture conditions. *Food Bioproduct Proc (Trans I Chem E, Part C)*. **80**: 38-44.

Larsson, G., Enfors, S.O. 1985. Influence of oxygen starvation on the respiratory capacity of *Penecillium chrysogenum*. *Appl. Microbiol. Biotechnol.* **21**: 228-233.

Larsson, G., Enfors, S. O. 1993. Kinetics of *Escherichia coli* hydrogen production during short term repeated aerobic-anaerobic fluctuations. *Bioprocess Eng.* **9**: 167-72.

Larsson, G., Tornkvist, M., Wernersson, S., Tragardh, C., Noorman, H., Enfors, S.O. 1996. Substrate gradients in bioreactors: origin and consequences. *Bioprocess Eng.* **14**: 281-289.

Latz, M.I., Rohr, J. 1999. Luminescent response of the red tide dinoflagellate *Lingulodinium polyedrum* to laminar and turbulent flow. *Limnol. Oceanogr.* **44**: 1423-1435.

Lavery M., Nienow, A.W. 1987. Oxygen transfer in animal cell culture medium. *Biotech. Bioeng.* **30**, 368-370.

Li, F., Hashimura, Y., Pendleton, R., Harms, J., Collins, E., Brain, L. 2006. A systematic approach for scale-down model development and characterization of commercial cell culture processes. *Biotechnol. Prog*. **22**: 696-703.

Ma, N., Koelling, K.W., Chalmers, J.J. 2002. Fabrication and use of a transient contractional flow device to quantify the sensitivity of mammalian and insect cells to hydrodynamic forces. *Biotechnol. Bioeng.* **80**: 428-437.

Ma, N., Chalmers, J., Aunins, J., Zhou, W., and Xie, L. 2004. Quantitative studies of cell-bubble interactions and cell damage at different Pluronic F-68 and cell concentrations. *Biotechnol. Prog*. **20**: 1183-1191.

Maa, Y., Hsu, C.C. 1996. Effect of high shear on proteins. *Biotechnol. Bioeng.* **51**: 458-465.

Maa, Y., Hsu, C.C. 1997. Protein denaturation by combined effect of shear and air-liquid interface. *Biotechnol. Bioeng.* **54**: 503-512.

Maa, Y., Nguyen, P.T., Hsu, S.W. 1998. Spray-drying of air-liquid interface sensitive recombinant human growth hormone. *J. Pharm. Sci.* **87**: 152-159.

Maa, Y., Hsu, C.C. 1998. Investigation on fouling mechanisms for recombinant human

growth hormone sterile filtration. *J. Pharm. Sci.* **87**: 808-812.

Margalef, R. 1978. Life-forms of phytoplankton as survival alternatives in an unstable environment. *Oceanologica Acta*, **1**, 493-509.

Marie, M.L., Champeil, P., Moller, J.V., 2000. Interaction of membrane proteins and lipids with solubilizing detergents. *Biochimica et Biophysica Acta.* **1508**: 86-111.

Maruyama, T., Katoh, S., Nakajima, M., Nabetani, H. 2001. Mechanisms of bovine serum albumin aggregation during ultrafiltraion. *Biotechnol. Bioeng.* **75**: 233-238.

McQueen, A. Bailey, J. E. 1989. Influence of serum level, cell-line, flow type and viscosity on flow-induced lysis of suspended mammalian-cells. *Biotechnol Lett* **11**:531–536.

Meier, S. J., Hatton, T. A., Wang, D. I. C. 1999. Cell death from bursting bubbles: role of cell attachment to rising bubbles in sparged reactors. *Biotechnol. Bioeng.* **62**: 468-478.

Meier, S.J. 2005. Cell culture scale-up: mixing, mass transfer, and use of appropriate scale-down models. Biochemical Engineering XIV. Harrison Hot Springs, Canada.

Metting, F.B. 1996. Biodiversity and application of microalgae. *J. Ind. Microbiol.* **17**: 477-489.

Michaels, J.D., Papoutsakis E.T. 1991. Polyvinyl alcohol and polyethylene glycol as protectants against fluid-mechanical injury of freely-suspended animal cells (CRL 8018). *J. Biotechnol*. **19**: 241-258.

Michaels, J.D., Kunas, K.T., Papoutsakis, E.T. 1992. Fluid-mechanical damage of freely-suspended animal cells in agitated bioreactors: effects of dextran, derivatized celluloses and polyvinyl alcohol. *Chem. Eng. Commun.* **118**: 341-360.

Michaels, J.D., Nowak, J.E., Mallik, A.K., Koczo, K., Wasan, D.T., Papoutskis, E.T. 1995. Analysis of cell-to- bubble attachment in sparged bioreactors in the present of cell-protecting additives. *Biotechnol. Bioeng.* **47**: 407-419.

Middelberg, A.P.J., Radke, C.J., Blanch, H.W. 2000. Peptide interfacial adsorption is kinetically limited by the thermodynamic stability of self association. *Proc. Nat. Acad. Sci. USA* **97**: 5054-5059.

Mollet, M., Ma, N., Zhao, Y., Brodkey, R., Taticek, R. Chalmers, J.J. 2004. Bioprocess equipment: characterization of energy dissipation rate and its potential to damage cells. *Biotechnol. Prog*. **20**: 1437-1448.

Mollet M., Godoy-Silva, R., Chalmers, J.J. 2006. Does acute hydrodynamic forces induce apoptosis in CHO cells? *Biotechnol. Bioeng.* Accepted.

Molowa, D.T., Shenouda, M.S., Meyers, A.P., Tublin, P.W., Fein, A.S. 2002. The state of biologics manufacturing: part 2, J.P. Morgan Securities Inc.

Moore R.E. 1996. Cyclic peptides and depsipeptides from cyanobacteria: a review. *J. Ind. Microbiol.* **16**:134-143.

Moreira, J. L., Cruz, P.E., Santana, P.C., Feliciano, A.S., Lehmann, J., Carrondo, M.J.T. 1995. Influence of power input and aeration method on mass transfer in a laboratory animal cell culture vessel. *J. Chem. Tech. Biotechnol.* **62**, 118-131.

Mostafa, S. S., Gu. X. 2003. Strategies for improved dCO2 removal in large-scale fed-batch cultures. *Biotechnol. Prog*. **19**: 45-51.

Murhammer, D.W., Goochee, C.F. 1990. Structural features of nonionic polyglycol polymer molecules responsible for the protective effect in sparged animal cell bioreactors. *Biotechnol. Prog*. **6**: 142-148.

Murhammer D.W., Pfalzgraf, E.C. 1992. Effects of pluronic F-68 on oxygen transport in an agitated, sparged bioreactor. *Biotech. Techniques.* **6**, 199-202.

Neenan, B., Feinberg, F., Hill, A., McIntoshm R., Terry, K. 1986. *Fuels from microalgae: technology, status, potential and research requirements.* Solar Energy Research Institute, Golden, Colorado.

Neubauer, P., Ahman, M., Toernkvist, M., Larsson, G., Enfors, S.O. 1995. Response of guanosine tetraphosphate to glucose fluctuations in fed-batch cultivations of *Escherichia coli*. *J. Biotechnol.* **43**:195-204.

Niagam, P. 2006. Interaction of water-soluble surfactants with self-assembled lipid monolayers at the vapor-liquid interface: equilibrium and dynamic phenomena. PhD thesis. The Ohio State University.

Nienow, A. W., Langheinrich, C., Stevenson, N.C., Emery, A.N., Clayton, T.M., Slater, N.K.H. 1996. Homogenisation and oxygen transfer rate in large agitated and sparged animal cell bioreactors: some implications for growth and production. *Cytotechnol.* **22**, 87-94.

Nienow, A.W. 2006. Reactor engineering in large scale animal cell culture. *Cytotechnology*. **50**: 9-33.

Norde, W., Giacomelli, C.E. 2000. BSA structural changes during homomolecular exchange between the adsorbed and dissolved states. *J. Biotechnol.* **79**: 259-268.

Oh, S.K.W., Nienow, A.W., Al-Rubeai, M., Emery, A.N. 1992. Further studies of the culture of mouse hybridomas in an agitated bioreactor with and without continuous sparging. *J. Biotechnol.* **22**: 245-270.

Oh, S.K.W., Nienow, A.W., Al-Rubeai, M., Emery, A.N. 1989. The effects of agitation intensity with and without continuous sparging on the growth and antibody production of hybridoma cells. *J. Biotechnol.* **12**: 45-62.

Oldshue, J. Y. 1966. Fermentation mixing scale-up techniques, *Biotechnol. Bioeng.* **8**:3-24.

Oldshue, J.Y. 1983. *Fluid Mixing Technology*, McGraw-Hill, New York, USA.

Oosterhuis, N.M.G., Kossen N.W.F., Olivier, A.P.C., Schenk, E.S. 1985. Scale-down and optimization studies of the gluconic acid fermentation by *Gluconobacter oxydans*. *Biotechnol. Bioeng.* **27**:711-720.

Osman, J.J., Birch, J., Varley, J. 2001. The response of GS-NS0 myeloma cells to pH shifts and pH perturbations. *Biotechnol. Bioeng.* **75**: 63-73.

Osman, J.J., Birch, J., Varley, J. 2002. The response of GS-NS0 myeloma cells to single and multiple pH perturbations. *Biotechnol. Bioeng.* **79**: 398-407

Ozturk, S.S., Palsson, B.O. 1991. Effect of medium osmolarity on hybridoma growth, metabolism, and antibody production. *Biotechnol. Bioeng.* **37**: 989-993.

Ozturk, S.S. 2006. Cell culture technology-an overview, *Biotechnol. Bioprocess.* **30**:1-13.

Park, S. 2003. Mammalian cell respiration and oxygen and carbon dioxide transfer in high-density perfusion culture with microsparge oxygenation and on-line mass spectrometry. Ph.D.dissertation. University of California, Davis.

Pashley, T.M., Karaman, M.E. 2004. Applied colloid and surface chemistry. John Wiley & Sons Ltd, West Sussex, England.

Pilon, L., Viskanta, R. 2004. Minimum superficial gas velocity for onset of foaming. *Chem. Eng. Proc*. **43**: 149-160.

Pilon, L, Feorov, A.G., Viskanta, R. 2002. Analysis of transient thickness of pneumatic foams. *Chem. Eng. Sci*. **57**: 577-590.

Pollingher, U., Zemel, E. 1981. In situ and experimental evidence of the influence of turbulence on cell division processes of *Peridinium cinctum* forma *westii* (Lemm.) Lefèvre. *Phycol. J.* **16**: 281-287.

Pugh, R.J. 1996. Foaming, foam films, antifoaming and defoaming. *Adv. Colloid Interface Sci*. **64**: 67-142

Qi, H.N. 2001. Membrane and micro-sparging aerations in long-term high-density perfusion cultures of animal cells. PhD thesis. Oregon State University.

Quarmby, L.M., Yueh, Y.G., Cheshire, J.L., Keller, L.R., Snell, W.J., Crain, R.C. 1992. Inositol phospholipids metabolism may trigger flagellar excision in *Chalmydomonas reinhardtii*. *J. Cell Biol.* **116**, 737-744.

Raikov, I.B. 1995. The dinoflagellate nucleus and chromosomes: The mesokaryote concept reconsidered. *Acta Prorozool.* **34**: 239-347.

Ratledage, C. 2004. Fatty acid biosynthesis in microorganisms being used for single cell oil production. *Biochimie*, **86**: 807-815.

Reuss, M., Schmalzriedt, S., Jenne, M. 2000. Application of computational fluid dynamics (CFD) to modeling stirred tank bioreactors. *Bioreaction Engineering*, 207-246.

Roth S., Murry, B., Dickinson, E. 2000. Interfacial shear rheology of aged and heat treated beta-lactoglobulin films: displacement by non-ionic surfactants. *J. Agri. Food Chem.* **48**: 1491-1497.

Running, J. A., Huss, R.J., Olson, P.T. 1994. Heterotrophic production of ascorbic acid by microalgae. *J. Appl. Phycol*. **6**:99-104.

Runyan, W.S., Geyer, R.P. 1963. Growth of L cell suspensions on a Warberg apparatus. *Proc. Soc. Biol. Med.* **112**: 1027-1030.

Ryll, T., Valley, U., Wagner, R. 1994. Biochemistry of growth inhibition by ammonium ions in mammalian cells. *Biotechnol. Bioeng.* **44**: 184-193.

Schmalzriedt, S., Jenne, M., Mauch, K., Reuss, M. 2003. Integration of physiology and fluid dynamics. *Advances in Biochemical Engineering/Biotechnology*, **80**: 19-68.

Schmelzer, A.E., Miller, W.M. 2002. Effects of osmoprotectant compounds on NCAM polysialytion under hyperosmotic stress and elevated pCO2. *Biotechnol. Bioeng.* **77**: 359-368.

Silva, H.J., Cortiñas, T., Ertola, R.J. 1987. Effect of hydrodynamic stress on *Dunaliella* growth. *J. Chem. Tech. Biotechnol.* **40**: 41-49.

Sobczuk, T.M., Gamacho, F.G., Grima, E.M., Chisti, Y. 2006. Effects of agitation on the microalgae *P. cruentum* and *Phaeodactylum tricornutum*. *Bioprocess Biosyst. Eng.* **28**: 243-250.

Söderlind, E., Karlsson, L. 2006. Haemolytic activity of maltopyranoside surfactants. *Eur. J. Pharm. Biopharm*, **62**: 254-259.

Söderlind, E., Wollbratt, M., von Gorswant, C. 2003. The usefulness of sugar surfactants as solubilizing agents in parenteral formulations. *Int. J. Pharm*. **252**: 61-71.

Soletto, D., Binaghi, L., Lodi, A., Carvalho, J.C.M., Converti, A. 2005. Batch and fed-batch cultivation of Spirulina platensis using ammonium sulphate and urea as nitrogen sources. *Aquaculture*, **243**:217-224.

Spolaore, P., Joannis-Cassan, C., Duran, E., Isambert, A. 2006. Commercial application of microalgae, *J. Biosci. Bioeng.* **101**:87-96.

Stolz, P., Obermayer, B. 2005. Manufacturing microalgae for skin care. *Cosmetics Toiletries*, **120**:99-106.

Sullivan, J.M., Swift, E. 2003a. Effects of small-scale turbulence on net growth rate and size of ten species of marine dinoflagellates. *J.Phycol.* **39**: 83-94.

Sullivan, J.M., Swift, E., Donaghay, P.L., Rines, J.E.B. 2003b. Small-scale turbulence affects the division rate and morphology of two red-tide dinoflagellates. *Harmful Algae*, **2**: 183-199.

Swim, H.E., Parker, R.F. 1960. Effect of Pluronic F68 on growth of fibroblasts in suspension on rotary shaker. *Proc. Soc. Exp. Biol. Med*. **103**: 252-254.

Takagi, M., Ohara, K., Yoshida, T. 1995. Effect of hydrostatic pressure on hybridoma cell metabolism. *J. Ferment. Bioeng.* **80**:619-621.

Terray, E.A., Donelan, M.A., Agrawal, Y.C., Drennan, W.M., Kahma, K.K., Williams, I.I., Hwang, P.A., Kitaigorodskii, S.A. 1996. Estimates of kinetic energy dissipation under breaking waves. *J. Phys. Oceanogr.* **26**: 792-807.

Thomas, W.H., Gibson, C.H. 1990a. Effects of small-scale turbulence on microalgae. *J. Appl. Phycol.* **2**. 71-77.

Thomas, W.H., Gibson, C.H. 1990b. Quantified small-scale turbulence inhibits a red tide dinoflagellate, *Gonyaulax polyedra* Stein. *Deep Sea Res.* **37**: 1583-1593.

Thomas, W.H., Gibson, C.H. 1992. Effects of quantified small-scale turbulence on the dinoflagellate, *Gymnodinium sanguineum* (splendens): contrast with *Gonyaulax (Lingulodinium) polyedra* and fishery implications. *Deep Sea Res.* **39**: 1429-1437.

Thomas, W.H, Vernet, M., Gibson C.H. 1995. Effects of small-scale turbulence on photosynthesis, pigmentation, cell division, and cell size in the marine dinoflagellate Gonyaulax Polyedra (Dinophyceae). *J. Phycol.* **31**:50-59.

Trample, J., Smith, J.D., Straatman, J., Valk, J.M. 1987. Bubble column design for growth of fragile insect cells. *Bioprocess Eng.* **2**: 37-41.

Tramper, J., 1995. Oxygen gradients in animal-cell bioreactors. *Cytotechnology*, **18**:27-34.

Trinh, K., Garcia-Briones, M., Hink, F., Chalmers, JJ. 1994. Quantification of damage to suspended insect cells as a result of bubble rupture. *Biotechnol. Bioeng.* **43**: 37-45.

Tuttle, R.C., Loeblich, A.R. 1975. An optimal growth medium for the dinoflagellate *Crypthecodinium cohnii*. *Phycologia*, **14**:1-8.

Van Barneveldt, J., Smit, W., Oosterhuis, N.M.G., Pragt, H.J. 1987. Measuring the liquid circulation ntime in a large gas-liquid contactor by means of a radio pill: 2. Circulation time distribution. *Ind. Eng. Chem. Process. Des. De*v. **26**: 2192-2195.

van der Pol, L.A., Paijens, I., Tramper, J. 1995. Dextran as protectant against damage caused by sparging for hybridoma cells in a bubble column. *J. Biotechnol*. **43**: 103-110.

van der Pol, L., Tramper, J. 1998. Shear sensitivity of animal cells from a culture-medium perspective. *TIBTECH*, **16**: 323-328.

Varley, J., Birth, J. 1999. Reactor design for large scale suspension animal cell culture. *Cytotechnol.* **29**:177-205.

Wang, D.I.C., Cooney, C.L., Demain, A.L., Funnill, P., Humphrey, A.E., Lilly, M.D. 1979. *Fermentation and Enzyme Technology*, Wiley, New York.

Warmoeskerken, M.M.C.G. 1986. *Gas-liquid dispersing characteristics of turbine agitators*, Ph.D. dissertation, University of Delft, The Netherlands.

Wu, J. 1995. Mechanisms of animal cell damage associated with gas bubbles and cell protection by medium additives. *J. Biotechnol.* **43**: 81-94.

Wu, J., Daugulis, A.J., Faulkner, P., Goosen, M.F.A. 1995, Protective effects of polymer additives on animal cells exposed to rapidly falling liquid film. *Biotechnol. Prog.* **11**: 127-132.

Wurm, F.M. 2004. Production of recombinant protein therapeutics in cultivated mammalian cells, *Nature Biotech*. **22**:1393-1398.

Yang, A., Cardona, D.L., Barile, F.A. 2002. In vitro cytotoxicity testing with fluorescence-based assays in cultured human lung and dermal cells. *Cell Biology Toxicology*, **18**:97-108.

Yang, C., Ansong, C., Bockrath, L., Chalmers, J.J., Lee, Y.S., O'neil, M., Rathman, J.F., Sakamoto, T. 2001. Mechanistic study of model monolayer membranes and their interactions with surfactants: correlation to effects on CHO cell cultures. *Studies in Surface Science and Catalysis*, **132**: 435-439.

Yap, C.Y., Chen, F. 2001. Polyunsaturated fatty acid: biological significance, biosynthesis, and production by microalgae and microalgae-like organisms. In: *Algae and their biotechnological potential*, (Chen, F., Jiang Y., eds), Kluwer Academic Publishers, the Netherlands.

Yeung, P.K.K., Wong, J.T.Y. 2003. Inhibition of cell proliferation by mechanical agitation involves transient cell cycle rest at G1 phase in dinoflagellates. *Protoplasma*, **220**: 173-178.

Yeung, P.K.K., Lam, C.M.C., Ma, Z.Y., Wong, Y.H., Wong, J.T.Y. 2006. Involvement of calcium mobilization from caffeine-sensitive stores in mechanically induced cell cycle arrest in the dinoflagellate *Crypthecodinium cohnii*. *Cell Calcium*. **39**: 259-274.

Zanghi, J., Schmelzer, A.E., Mendoza, T.P., Knop, R.H., Miller, W.M. 1999. Bicarbonate concentration and osmolality are key determinants in the inhibition of CHO cell polysialyation under elevated pCO_2 and pH. *Biotechnol. Bioeng.* **65**: 182-191.

Zaslavskaia, L.A., Lippmeier, J.C. Shih, C., Ehrhardt, D., Grossman, A.R., Apt, A.E. 2001. Trophic conversion of an obligate photoautotrophic organism through metabolic engineering, *Science*, **292**:2073-2075.

Zhang, H., Williams-Dalson, W., Keshavarz-Moore, E., Shamlou, P.A. 2005. Computational-fluid-dynamics (CFD) analysis of mixing and gas-liquid mass transfer in shake flasks. *Biotechnol. Appl. Biochem.* **41**: 1-8.

Zhang, M., Ferrari, M. 1997. Reduction of albumin adsorption onto silicon surfaces by Tween 20. *Biotechnol. Bioeng.* **56**: 618-625.

Zhang, S., Handa-Corrigan, A., Soier, R.E. 1992. Oxygen transfer properties of bubbles in animal cell culture media. *Biotech. Bioeng.* **40**, 252-259

Zhou, G., and Kresta, S.M. 1996a. Distribution of energy dissipation between convective and turbulent flow for three frequently used impellers. *Trans IChemE*, **74**: 379-389.

Zhou, G., and Kresta, S.M. 1996b. Impact of tank geometry on the maximum turbulence energy dissipation rate for impellers. *AIChE J.* **42**: 2476-2490.

Zhou, W., Rehm, J., Hu, W. 1995. High viable cell concentration fed-batch cultures of hybridoma cells through online nutrient feeding. *Biotechnol. Bioeng.* **46**: 579-587.

Zhu, M. M., Goyal, A., Rank, D.L., Gupta, S.K., Vanden Boom, T., Lee, S.S. 2005. Effect of elevated pCO2 and osmolality on growth of CHO cells and production of antibody-fusion protein B1: a case study. *Biotechnol. Prog*. **21**: 70-77.

Zirbel, M., Veron, F., Latz, M. 2000. The reversible effect of flow on the morphology of *Ceratocorys horrida* (Peridiniales, Dinophyta). *J. Phycol.* **36**:46-58.